1959

Strength in shear of prestressed concrete I-beams

David Alan VanHorn
Iowa State University

STRENGTH IN SHEAR OF PRESTRESSED CONCRETE I-BEAMS

by

David Alan VanHorn

A Dissertation Submitted to the
Graduate Faculty in Partial Fulfillment of
The Requirements for the Degree of
DOCTOR OF PHILOSOPHY

Major Subject: Structural Engineering

Approved:

Signature was redacted for privacy.
In Charge of Major Work

Signature was redacted for privacy.
Head of Major Department

Signature was redacted for privacy.
Dean of Graduate College

Iowa State University
Of Science and Technology
Ames, Iowa

1959

TABLE OF CONTENTS

INTRODUCTION

History

The basic principle of prestressing concrete has been used in construction for many years. The purpose of the prestressing operation is to reduce or eliminate tensile stresses produced in the concrete. In prestressed concrete beams the concrete is initially stressed by the action of forces applied in the end regions of the beam. The forces produce compressive stresses on the beam cross-sections which counteract the tensile stresses produced by loads on the beam. Thus, the entire cross-section of the prestressed beam is effective in resisting deformation. In comparison, cracking on the tension side of reinforced concrete (non-prestressed) beams results in the loss of resistance of approximately two-thirds of the cross-sectional area. Consequently, the proper use of prestressing permits extended use of concrete as a construction material.

The principle of prestressing was first applied to concrete arches in 1886 by P. H. Jackson, an American engineer. However, it was not until 1928 that Eugene Freyssinet, the French structural engineer, initiated the modern development of prestressed concrete. Freyssinet demonstrated the need for high quality concrete and high strength steel reinforcement to counteract the prestress losses due to elastic deformation, shrinkage, and creep.

Even though the principle of prestressing concrete had been demonstrated, practical application immediately became the major problem. Finally, in 1939, Freyssinet developed a system of prestressing which made it possible to produce prestressed beams for use in construction. Progress became more rapid as other systems of prestressing were developed.

Extended use of prestressed concrete first became evident in Europe near the end of World War II. Almost all prestressing done in Europe was of the linear type used for beams and slabs. In contrast, the first practical use of prestressed concrete in the United States began in the 1930's with circular prestressing used mainly in storage tank construction. In 1951, the first major prestressed concrete bridge in the United States was completed in Philadelphia. Since that time, the use of prestressed concrete has increased to the extent that, in many states, the number of new highway bridges built of prestressed concrete is greater than that of any other type.

In Iowa, the first prestressed concrete bridge was built in Butler County in 1953. It was a single span bridge, 30 feet in length, in which channel-shaped sections were utilized. In 1954, the first standard prestressed concrete bridge designs of the Iowa Highway Commission were approved by the Bureau of Public Roads for use on the secondary highway system. The designs were for bridges having spans of 30 and 42 1/2 feet. The first such bridge was built in Franklin County in 1954 and was composed of five equal spans, 42 1/2 feet in length. In 1956, prestressed concrete bridges were first used on the primary highway system when five bridges in Louisa County were widened by adding prestressed beams to the existing structures. In December, 1956, standard designs were approved for bridges on the primary system. Prestressed beams with spans of 30, 42 1/2, 55, and 67 1/2 feet were included in the designs. The first prestressed concrete bridges constructed on the primary system were completed in Warren County in 1957.

Use of prestressed concrete for highway bridges in Iowa has increased

rapidly since 1956. In 1957, 61 of the 109 bridges built on the primary system and 31 of the 86 built on the secondary system utilized prestressed concrete. As the number of producers of prestressed concrete has grown, this type of construction has become a valuable and much-used construction material in Iowa as well as in most other states.

The development of a method of construction which minimized the need for labor was necessary before prestressed concrete could become an economical construction material in the United States. One of the most common of the methods used in the United States is the long-line system developed in Germany by Ewald Hoyer. In this system, high strength wires or strands are stretched between two abutments, several hundred feet apart. Forms for the concrete are then placed around the prestressing steel. After the concrete has gained strength, the prestressing steel is released and the beams are separated by cutting the steel exposed between adjacent beam ends. This method, which is one of two general methods of prestressing concrete, is called pretensioning since the prestressing steel is stressed before the concrete is placed. In the pre-tensioning method, anchorage of the prestressing steel is completely dependent upon bond developed between the steel and the concrete at the ends of the beam. The other method is called post-tensioning because the prestressing steel is stressed after the concrete is placed. The prestressing steel is placed in tubes, coated with non-bonding material, or placed outside the concrete. After the concrete has gained strength, the steel is stressed and mechanically anchored at the ends of the beam.

Almost all of the prestressed concrete construction in Iowa utilizes

the pre-tensioning system. But, since post-tensioning can be done at the site of the structure, some post-tensioned beams have been used for span lengths greater than the maximum length which can be transported on Iowa highways.

Through the development of practical methods of prestressing concrete, design problems have arisen which are distinctive to this new method of construction. Research through the years has provided answers to some of the questions, but many of the problems are still unsolved. Some of the problems related to pre-tensioned beams are centered around the ends of the beam which make up the anchorage zones for the pre-stressing steel. Since the stresses produced in this anchorage zone are produced by both internal and external forces, the problems involved in a stress analysis are complex.

It has been common practice to provide end blocks as a method of eliminating critical stress conditions which might exist in the anchorage zone. The end block is normally a rectangular section having a length of from one to two times the depth of the beam. The problem of forming pre-tensioned beams in the long-line process is lessened measurably if the end blocks are not required. In 1956, Prestressed Concrete of Iowa, Inc., under the direction of J. H. Boehmler, constructed some building beams having no end blocks. The apparent success of the design suggested that the end block requirement for highway bridge beams might be eliminated. A design for bridge beams having no end blocks was developed by J. H. Boehmler and P. H. Barnard, bridge design engineer at the Iowa Highway Commission. This design was initially used in 1957 for

construction of the first prestressed bridges built on the primary system in Iowa.

The shear strength of beams having no end blocks has provoked much thought and discussion among engineers with the result that at the present time some states are using beams with no end blocks while others are still requiring end blocks. Thus, the controversy between engineers has created a definite need for research concerning the anchorage zone in pre-tensioned beams. One area of research which must, of necessity, be concerned with the anchorage zone is a study of shear strength, since shear strength is usually critical near the ends of the beams. Such a study would certainly shed some light on the end-block controversy, and yield shear strength information which, at present, is extremely limited.

The Problem

It is the purpose of this paper to present a method for evaluating the shear strength of pre-tensioned I-beams having no end blocks. The term shear strength, as used in this paper, refers to the resistance of the beams to failure by shear. A shear failure is defined as a failure which is initiated by an inclined tension crack resulting from the combined effects of cross shear and bending moment. Some writers refer to shear strength as the ultimate strength of the beam when the failure mechanism is started by the formation of inclined cracks. But, in this paper, shear strength will be defined as having been reached when a sudden, inclined tension crack completely traverses the web of the beam, and ultimate strength will be defined as having been reached when the beam will support no more applied load.

As will be shown in the literature review, the approach to the problem of determining shear strength has been through formulation of empirical equations which most nearly agree with experimental findings. However, it appears that because of the great number of variables which might influence the shear strength, it would be very difficult to include all pertinent variables in one general expression which could be applied to any prestressed beam. In contrast, a more general approach will be presented, involving the determination of principal stresses produced in the beam and a comparison of these stresses with limiting stresses dictated by a theory of failure for the concrete.

In beams, the effect of cross shear is normally the dominant factor in producing critical stress conditions in the end portions. Thus, shear strength of a beam depends mainly on its ability to withstand the effects of cross shear at or near the supports. Since the prestressing steel is anchored at the ends of prestressed concrete beams, the anchorage zone is subjected to the effect of the transmission of the prestressing force through bond between the steel and concrete, as well as the effects of the dead load and the applied load.

An element of the beam in the anchorage zone is subjected to shearing stress as well as normal stresses on both the vertical and horizontal planes. But, the exact manner in which each stress is determined has never been resolved. Probably the simplest effect to evaluate is the primary effect of cross shear and bending moment caused by the dead load and the applied load. But, there exists a secondary effect at or near points of application of concentrated loads. This secondary effect results mainly in compressive stresses on horizontal planes, but is also

responsible for normal stresses on vertical planes, and shearing stresses on both planes. The effects produced by the transmission of the prestress force are the most difficult to evaluate. Primarily, the prestress force produces compressive stresses on vertical planes. But, because of the inadequacies of completed research, the manner in which these compressive stresses are built up in the anchorage zone is known only for a few cases. In addition to the compressive stresses on vertical planes, normal stresses on the horizontal planes together with shearing stresses are the result of the transmission of the prestress force in the anchorage zone. Even though the prestress force undoubtedly causes stresses in three directions, it will be assumed that the stress condition is two-dimensional and that the stresses ignored are small in comparison to those recognized in the following analyses.

In this study, 33 pre-tensioned I-beams were tested to failure in such a manner that the failure mechanism was initiated by a sudden inclined tension crack which completely traversed the web. All of the beams had the same cross-section and were prestressed with 3/8-inch, seven wire steel strand. None of the beams had end blocks. The variables introduced in the study were (1) amount of web reinforcement, (2) prestress stress distribution, (3) length of shear span, (4) length of overhang at the supports, and (5) concrete strength at time of release of the prestressing steel. A method which utilizes a theory of combined stresses was used to evaluate the shear strength of the test beams.

LITERATURE REVIEW

The literature pertinent to a study of the shear strength of prestressed concrete beams can be divided into three general areas. The first area concerns previous studies of the shear strength of reinforced concrete beams, the second is comprised of similar studies of prestressed concrete beams, and the third presents the theories of failure which have been used in describing the failure of concrete. A comparison of the research completed on shear strength of reinforced beams with comparable studies of prestressed beams will indicate a definite similarity regarding variables considered and general approach to the problem. The discussion of the theories of failure will reveal the wide diversity of opinion concerning the mechanism of failure of concrete subjected to combined stresses.

Reinforced Concrete Beams

Studies of the strength in shear have always been an important aspect of research regarding concrete beams. The early research was concerned with reinforced concrete beams since the use of prestressing for beams had not yet been developed. According to Seiss (18), the most significant of the early research was done during the period between 1903 and 1908 by Talbot at the University of Illinois and by Moritz and Withey at the University of Wisconsin. The results of these studies indicated that the ultimate shear strength of the beams was dependent upon (1) the compressive strength of the concrete, (2) the amount of longitudinal reinforcement, and (3) the ratio of length to depth for a given type of loading. The effect of web reinforcement and the character

of the shear failure was recognized.

Later, in the 1920's, shear studies were aimed at determining the relationship between the nominal shear stress, $v = V/bjd$, and the stress in the web reinforcement. The recommendations for an expression for ultimate shear strength were of the form

$$v = 0.005f_y + rf_y$$

or $$v = C + rf_y$$

where f_y = yield point of the steel

and r = percentage of web reinforcement.

After 1940, research on shear strength was characterized by attempts to evaluate the contribution of the various elements of a beam to its strength in shear. In 1945, Moretto (16) tried to determine the relative contributions of the concrete and the web reinforcement. Tests were conducted in which the variables were concrete strength, amount of web reinforcement, inclination of web reinforcement, and amount of longitudinal reinforcement. The expressions presented were of the form

$$v = Krf_y + Cf'_c + 5000p$$

where α = inclination of web reinforcement

K = a function of α

C = a constant

f'_c = concrete strength

and p = percentage of longitudinal reinforcement.

Later tests of rectangular beams were reported by Clark (2) in 1951. The variables involved were concrete strength, amount of web

reinforcement, amount of longitudinal reinforcement, and the ratio of beam depth to shear span. The expression recommended by Clark was of the form

$$v = 2500r + (0.12f'_c)d/a + 7000p$$

where d/a = ratio of beam depth to shear span.

It should be noted that the d/a ratio is omitted in Moretto's expression, while α and f_y do not appear in Clark's expression. The test beams used by both Moretto and Clark were greatly over-reinforced against flexural failure.

In 1953, Ferguson and Thompson (6) reported on a series of tests performed on T-beams having no web reinforcement. It was pointed out that the effect of the end reaction was to strengthen the end portion of the beam, and that the apparent effect of the depth-shear span ratio was due mainly to this strengthening by the end reaction. It was further stated that general significance is attached to the local effect of the end reaction when shear strength is expressed as a continuous function of d/a. Hence, the T-beams tested were designed to produce failure outside this locally strengthened zone. The equation representing the shear strength of the test beams was

$$v = 145 + 0.02f'_c$$

In 1955, Laupa (12) presented a paper in which the object was to correlate the results of previous research regarding shear strength of reinforced beams, and to develop a general expression for the shear strength of beams subjected to different loading conditions. An empirical

equation, of a different form than the expressions reported in earlier studies, was derived for the shear strength of rectangular beams having no web reinforcement. The test beams were simply supported and subjected to one or two concentrated loads. The basic equation was of the form

$$\frac{M_s}{bd^2 f'_c} = (k + np')(0.57 - \frac{4.5f'_c}{10^5})$$

where M_s = shear-compression moment,

and p' = percentage of compression reinforcement.

Methods of modifying the basic equation were provided to extend use of the equation to include beams with web reinforcement, T-beams, restrained beams, and beams subjected to distributed loads.

In 1955, Moody and Viest (15) reported more tests in which the purpose was to evaluate the shear strength of reinforced beams. The failure of the test beams was found to occur in two phases. The first phase occurred when diagonal tension cracks formed, and the second when the compression zone in the concrete was destroyed. The equation which represented the first stage of failure was of the form

$$v = 0.12(1 + 0.1\frac{a}{d})f'_c(1 - \frac{f'_c}{10000}).$$

This equation represents the shear strength as defined in this paper. The second stage concerns the ultimate strength of the beams and will not be discussed.

Ferguson (5) recently summarized the previous work concerning shear strength of reinforced beams. The failure pattern of test beams is

emphasized. The failure is considered to take place in steps, each of which is rationalized or explained in terms of the standard theory of combined stresses. In conclusion, the author encourages use of a theory of combined stresses in determination of shear strength. All of the earlier approaches seem to emphasize an expression for the nominal shear stress, $v = V/bjd$, in terms of dimensions of the beam, the shear span, the strength of the concrete, and the strength and amount of the steel reinforcement. But, Ferguson appears to be one of the first to mention a theory of combined stresses.

Prestressed Concrete Beams

Research concerning the shear strength of prestressed concrete has been very limited to date. The scope of the problem is broad due to the many types of prestressing systems and the large variety of types of sections used.

In 1942, Evans and Wilson (4) reported the results of tests designed to investigate (1) the effect of horizontal prestressing on the load required to produce diagonal cracking in beams having no web reinforcement, and (2) the effect of prestressing vertical stirrups on the load required to produce diagonal cracking in beams having no horizontal prestress. The specimens tested were I-sections having a depth of 10 inches, a clear span of 58 inches, and a shear span of 25 inches. Both top and bottom flange widths were 4 inches, and the web thickness was 1 inch. The horizontal prestressing steel consisted of one 1-inch diameter high strength steel bar located in the bottom flange. The beams had end blocks at each end and a rectangular cross-section at the center under

the applied loads. Crack patterns were predicted in consideration of a theory of failure for concrete. The maximum-normal-stress theory was used, and it was assumed that the cracks would appear when the principal tensile stress reached the ultimate tensile strength of 450 psi. The experimental results agreed closely with predicted crack patterns, apparently confirming the conventional theory used.

By far the most extensive shear studies of prestressed beams have been conducted at the University of Illinois. A report by Sozen, Zwoyer, and Seiss, (20) published in 1959, describes the investigation of the behavior of prestressed beams with no web reinforcement, in resisting failure by shear. Tests of 43 rectangular beams and 56 I-beams are described and analyzed. The rectangular beams, some post-tensioned and some pre-tensioned, were 6 x 12-inches in cross-section. The overall measurements of the I-beams were 6 x 12-inches. Web thicknesses were either 3 or 1-3/4 inches. All of the I-beams were pre-tensioned and had end blocks. The prestressing steel consisted of single, high strength, steel wires. All but three of the I-beams had prestressed, external stirrups to prevent propagation of the cracks into the end block. Thus, the beam failures occurred in a zone which was relatively free from the effect of the end reaction.

On the basis of test results, an expression was developed to represent the load required to produce the inclined tension crack. The expression is of the form

$$\left(\frac{V_c}{f_t bd}\right)\left(\frac{1}{\sqrt{\frac{b}{b}}}\right)\left(\frac{a}{d}\right) = 1 + \frac{F_{se}}{A_c f_t}$$

where V_c = shear force required to provide an inclined crack,

F_{se} = the effective prestress force,

f_t = the assumed tensile strength of the concrete,

and A_c = gross area of the concrete.

A limitation is placed on the equation because of the nature of its derivation. It is to represent only the loads which produce cracks which start in the lower portion of the cross-section near the load. It is also limited by the fact that the end blocks were prestressed vertically.

Shear failures of the test specimens were placed in two categories, (1) shear-compression and (2) web distress, to describe the mode of ultimate failure. However, it is significant that the beams exhibited different characteristics of behavior only after the formation of inclined tension cracks. It was concluded that the useful ultimate shear strength of prestressed beams without web reinforcement should be limited to the load which produces inclined cracking, unless definite measures are taken to prevent web distress.

Because of the wide range of variables which might influence the shear strength of prestressed beams, the tests reported to date represent only a tiny portion of the work required to provide a knowledge of shear failure.

Theories of Failure

Theories of failure for structural materials have been developed as aids in determining the load capacities of structural members in which biaxial and triaxial conditions exist. Each of the theories is based on

the assumption that when a specific stress, strain, or combination of stresses and strains is reached, a limiting condition is attained.

The maximum-normal-stress theory is based on the assumption that the material will fail when the maximum normal stress at any point in the member reaches the value of the critical stress. The maximum-normal-strain theory is based on the assumption that the material will fail when the maximum principal strain at any point in the member reaches the critical strain. Likewise the maximum-shearing-stress theory is based on the assumption that the material will fail when the maximum shearing stress at any point in the member reaches the critical shearing stress.

The internal-friction theory advanced by Coulomb represents a different approach. This theory is based on the concept that failure occurs when a sliding action takes place within the material. The resistance to sliding is considered to be a combination of the shearing resistance and the frictional resistance of the material. It is assumed that failure occurs when the maximum shearing stress on any plane exceeds this combined resistance. The internal-friction theory is illustrated in in Figure 1b. As indicated, the theory assumes a straight-line relationship between the total shearing resistance and the normal stress. A generalization of the internal-friction theory was given by Mohr, whose concept did not limit the shape of the limiting curve to a straight line. The Mohr theory is illustrated in Figure 1a. It is assumed that failure occurs when a Mohr circle for stresses at any point touches or extends beyond the limiting curve. All circles shown represent stress

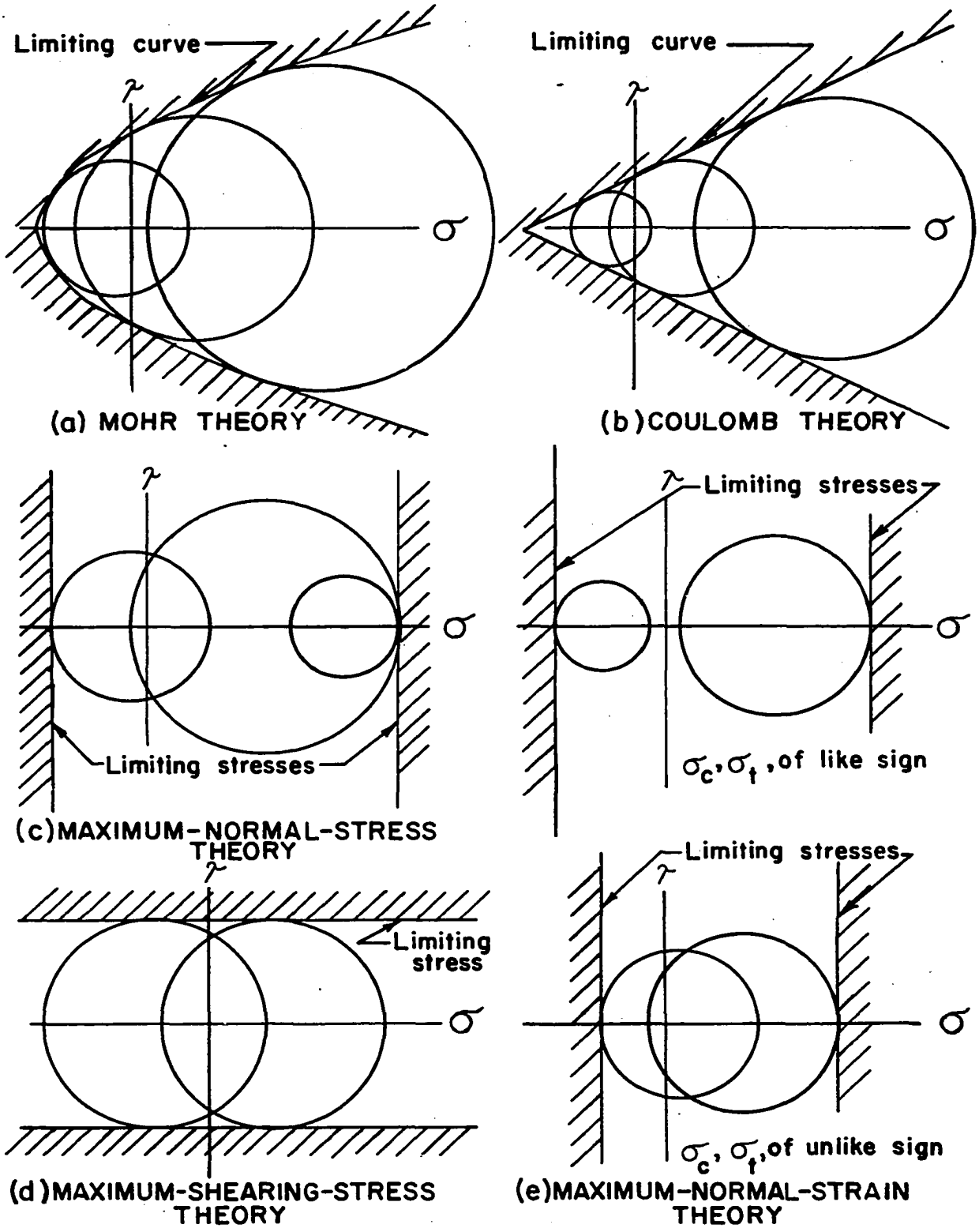

FIGURE 1. THEORIES OF FAILURE

conditions which would be critical.

The other theories of failure mentioned can also be illustrated graphically, since each of them is a special case of the Mohr theory. The maximum-normal-stress and maximum-normal-strain theories are shown in Figures 1c and 1e. In both theories, the limiting curves are represented by vertical straight lines, indicating that the shearing strength of the material is not critical. The maximum-shearing-stress theory is illustrated in Figure 1d. In this case the limiting curve is represented by horizontal straight lines, indicating that the normal stresses have no influence on the shearing resistance of the material. Therefore, these three theories represent the two extremes of the Mohr theory.

There are varying opinions as to which of the theories most nearly represents a theory of failure for concrete. Of the theories of failure mentioned, the maximum-normal-stress theory appears to give satisfactory results with brittle materials, while the maximum-normal-strain and maximum-shearing-stress theories indicate better agreement with the results of tests of ductile materials.

Kesler and Seiss (11) suggest the use of the Mohr theory for the interpretation of results of tests of concrete. Guyon (8) also recommends the Mohr theory and presents a method for obtaining the limiting curve. A report published by the Bureau of Reclamation (22) describes tests of 6 x 12-inch cylinders subjected to triaxial compressive stresses. A method of analysis is developed which leads to a curved envelope for the Mohr diagram. Data from these tests present evidence that a straight line does not define the relationship between the stresses nor accurately

describe the Mohr envelope in general. The experimental results support curvilinear analysis of this envelope.

Bresler and Pister (1) believe that the Mohr theory is not satisfactory when applied directly. As a result of experimental work in which the test specimens were plain concrete hollow cylinders, a theory was proposed which was similar to the Mohr theory but which included the effect of the third principal stress. It was stated that the maximum-normal-stress theory is unsatisfactory due to a lack of agreement with test results, and further that the maximum-normal-strain theory is not readily applicable.

Richart, Brandtzaeg, and Brown (17) published results of a study of the failure of concrete under combined compressive stresses. Experimental data indicated that the maximum-normal-stress theory was not representative of the failure of the specimens. But, the results of a number of the tests were in near agreement with the internal-friction theory. However, the large lateral deformations of the specimens did not follow the physical concept of failure which takes place through a sliding on plane surfaces continuous throughout the material. It was concluded that no theory based on the assumption of failure by sliding on continuous planes of least resistance could give a correct representation of failure of concrete in compression. The theory which seemed to give a reasonable picture of the process of failure was a concept advanced by Brandzaeg. This theory was developed considering the material to be made up of a number of non-isotropic elements which yield plastically through a sliding action in directions which vary arbitrarily throughout

the material. The concept involved consideration of the internal-friction theory applied to individual elements of the material rather than to the member as a whole. However, sliding failure was not considered to be the only type of failure possible. A splitting failure was assumed to occur whenever the principal tensile stress reached a limiting value.

Tests performed by Cowan and Armstrong (3) on a series of rectangular reinforced concrete beams resulted in another contribution to knowledge regarding failure of concrete. The proposed theory, which was in close agreement with experimental results, was a combination of the maximum-normal-stress theory and the internal-friction theory of Coulomb. The combination implies that the maximum-normal-stress theory is valid for a given range of ratios of normal stress to shearing stress while the Coulomb theory is valid for another range of ratios.

According to Cowan and Armstrong (3), Fisher performed a series of tests on plain concrete. The test results indicated satisfactory agreement with the maximum-normal-stress theory. Grassam (7) suggests use of the maximum-normal-stress theory with a modification to include the effect of plasticity. In tests made on plain concrete subjected to bending and torsion, results indicated that the material could be expected to fail when the maximum normal tensile stress reached a value equal to 1.2 times the measured tensile strength. Thus, the modification was introduced simply by extending the limiting curve in the maximum-normal-stress theory to a value of 1.2 times the tensile strength.

Smith (19) proposed a theory of failure in the form of a simple stress-ratio equation based upon the ultimate compressive strength and

the modulus of rupture of the material. The theory showed correlation with results of tests performed on plain concrete rectangular beams. It appears that no further material has been published favoring this approach.

In the review of literature presented, it can be seen that opinion is divided on the subject of a theory of failure for concrete. Two theories, the Mohr theory and the maximum-normal-stress theory, or modifications of these theories stand out as being favored by most researchers.

DEFINITIONS, SIGN CONVENTION, AND NOTATION

Definitions

Shear strength

The shear strength of a beam is reached when a sudden, inclined tension crack completely traverses the web of the beam.

Ultimate strength

The ultimate strength is reached when the beam continues to deflect with no increase in applied load or when collapse occurs.

Anchorage length

The anchorage length is the length required for a strand to attain its maximum stress.

Anchorage zone

The anchorage zone extends from the end of the prestressed beam to the point where the compressive stress distribution due to the prestress force is essentially the same as the distribution at the center of the beam.

Stress

In this paper, stress will refer exclusively to unit stress.

Sign Convention

Normal stress

Compressive stresses will be positive and tensile stresses will be negative.

Shearing stress

Shearing stresses will be positive when the direction of the shearing force is upward on the left face of a differential element of

the material.

Notation

Cross-sectional constants

A_c	Gross area of concrete section
A'_c	Area of transformed section
A_s	Total steel area
c.g.c.	Center of gravity of the concrete section
c.g.c.′	Center of gravity of the transformed section
c.g.s.	Center of gravity of the steel area
b	Width of flanges
b′	Width of web
d	Effective depth of the section
D	Total depth of the section
y′	Distance from any fiber to c.g.c.′
e′	Eccentricity of c.g.s. with respect to c.g.c.′
I'_c	Moment of inertia of transformed concrete section with respect to c.g.c.′
Q′	First moment of an area of the section with respect to c.g.c.′

Loads

V_c	Applied shear at inclined tension cracking
V_u	Applied shear at ultimate load
M_c	Applied bending moment at inclined tension cracking
P_o	Total applied load at the end of the straight-line portion of load-strain curves for SR-4 gages at the

bottom of the test beams.

F_i Total initial prestress force before release

F Total effective prestress force at time of load test

Stresses

Concrete

f'_c Compressive strength determined from 4-1/2 x 9 inch control cylinders

f'_r Modulus of rupture determined from 6 x 6 x 36-inch flexure specimens

f'_t Tensile strength determined from 4 x 4 x 36-inch tension specimens

f_{PL} Tensile proportional limit of the concrete, measured from flexure specimens

E_c Modulus of elasticity of concrete

f_{F_i} Stress at any fiber due to initial prestressing only

f_F Stress at any fiber due to effective prestressing only

f_{Bi} Stress at bottom fiber at mid-span due to initial prestressing only

f_B Stress at bottom fiber at mid-span due to effective prestressing only

f_L Stress at any fiber due to bending moment caused by applied load

f_{Cx} Normal stress on a vertical plane due to local effect of applied load

f_{Cy}	Normal stress on a horizontal plane due to local effect of applied load
f_{Fy}	Normal stress on a horizontal plane in the anchorage zone due to effect of the prestress force
v_L	Shearing stress due to cross shear caused by the applied load
v_C	Shearing stress due to local effect of the applied load
v_F	Shearing stress due to the effect of the prestress force
S_x	Total normal stress on a vertical plane at a point
S_y	Total normal stress on a horizontal plane at a point
S_s	Total shearing stress on horizontal and vertical planes at a point
S_c	Principal compressive stress
S_t	Principal tensile stress
θ	Angle between horizontal and plane on which one of the principal stresses acts

Steel

f_{si}	Steel stress due to initial prestressing
f_{se}	Effective steel stress after deduction of all losses
E_s	Modulus of elasticity of the steel strand

Other quantities

n	Ratio of E_s to E_c
L	Span of the test specimen

L_s	Length of the shear span
L_o	Length of overhang at the support
L_{az}	Length of the anchorage zone

EXPERIMENTAL INVESTIGATIONS

Test Beams

The test beams for this study had an I-shaped cross-section with proportions which would be typical of beams commonly used in building and bridge structures. Certainly, many other shapes have been used, but it was thought that the I-shaped section would be most representative of the prestressed beams used in Iowa. All of the test specimens had the same cross-section. The section was symmetric with respect to both horizontal and vertical axes. The depth was 18 inches, the flange width 9 inches, and the web thickness 4 inches. The cross-section is shown in Figure 2a. The beams were prestressed with 3/8-inch, seven wire, steel strand. All of the strands were straight for all of the test beams. Possible locations of the strands in the cross-sections are shown in Figure 2b. All of the beams had an overall length of 9 feet 6 inches with the exception of specimens 27-29 which were 6 feet 6 inches in length.

Variables

The variables considered in the study were (1) amount of vertical web reinforcement, (2) prestress stress distribution, (3) length of shear span, (4) length of overhang at the end supports, and (5) concrete strength at time of release of the prestress force.

Web reinforcement The first ten specimens were used to determine the effect of vertical web reinforcement. Specimens 1, 3, 5, 7, and 9 had vertical stirrups uniformly spaced at 12, 6, 18, 9, and 15 inches respectively. Specimens 2, 4, 6, 8, and 10 had no web reinforcement. Specimens 11-33 all had vertical stirrups. Location of stirrups for all

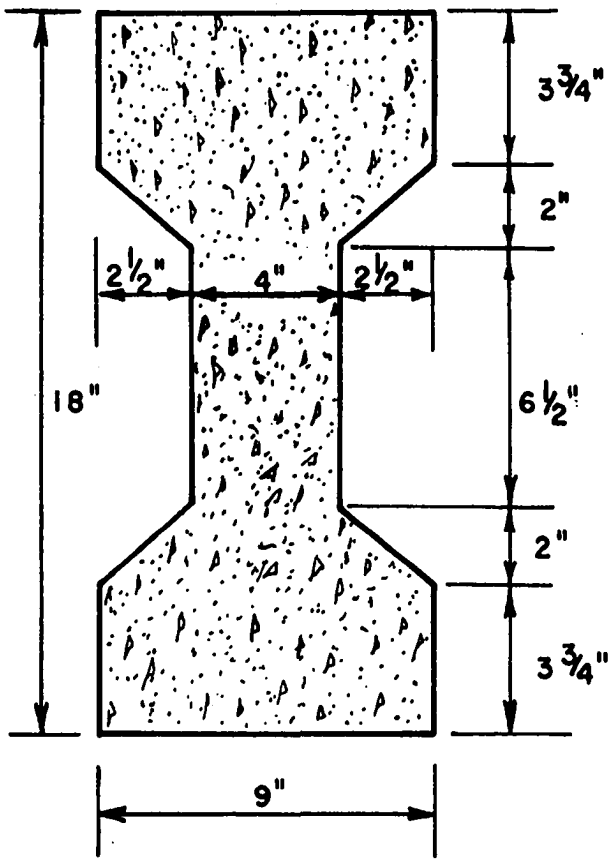

(a) DIMENSIONS

$I_c = 4110 \text{ in.}^4$

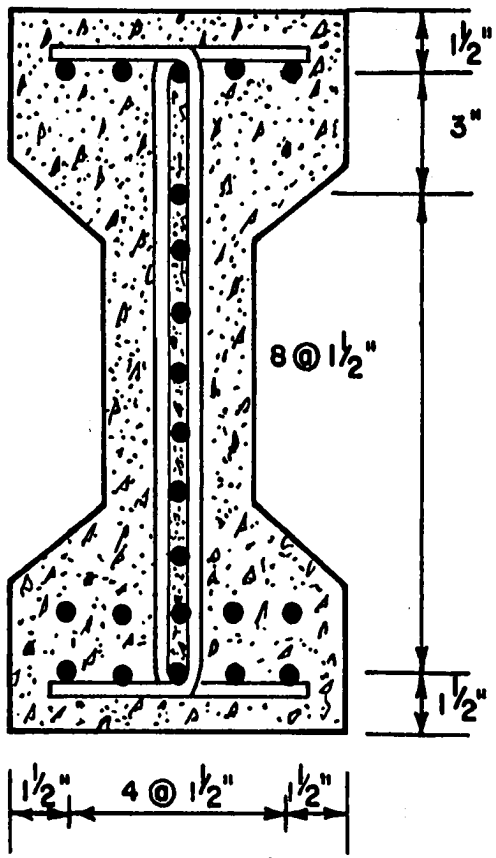

(b) POSSIBLE STRAND LOCATIONS AND SHAPE OF WEB REINFORCEMENT

FIGURE 2. CROSS-SECTION OF TEST BEAMS

test beams is shown in Figure 3.

Prestress stress distribution Specimens 1-10 and 19-33 had a nominal initial prestress stress distribution of 0 at the top and 2400 psi compression at the bottom. Specimens 11 and 12 had a nominal distribution of 0 at the top and 1800 psi compression at the bottom, while 13 and 14 had a distribution of 0 at the top and 1150 psi compression at the bottom. Further, strand patterns were used which produced tensile stresses normally limited to small values by design codes. In specimens 15 and 16, the nominal stresses were 300 psi tension at the top and 2500 psi compression at the bottom, and in 17 and 18 the stresses were 700 psi tension and 2500 psi compression. In all, six different patterns of the steel strand were used to prestress the 33 test beams. The patterns, together with the properties of the transformed sections and nominal initial prestress stress distributions are shown in Figure 4.

Length of shear span The length of shear span was varied from one to three feet as shown in Figure 5.

Length of overhang The length of overhang was varied from 3 to 27 inches. Loading arrangement for all specimens is shown in Figure 5.

Concrete strength The compressive strength of the concrete at the time of release was nominally 5000 psi for specimens 1-29. The prestressing force was released in specimens 30 and 31 when the strength reached 3000 psi, and in specimens 32 and 33 when the strength reached 4000 psi. The concrete mix was the same for all specimens.

Construction of the test beams

The test beams were fabricated in a prestressing bed located at

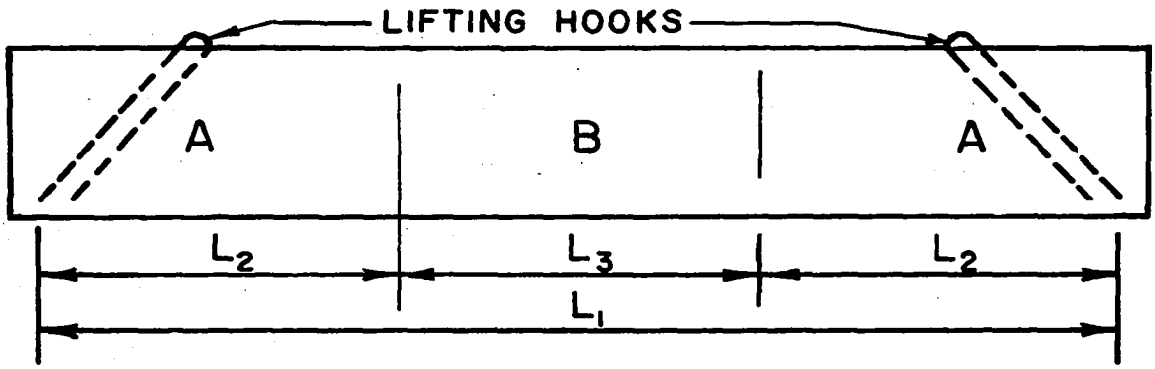

SPECIMEN	STIRRUPS	L_1, FT.	L_2, FT.	L_3, FT.	STIRRUP SPACING, IN. ENTIRE BEAM	ZONE A	ZONE B
1	YES	9	—	—	12	—	—
2	NO	9	—	—	—	—	—
3	YES	9	—	—	6	—	—
4	NO	9	—	—	—	—	—
5	YES	9	—	—	18	—	—
6	NO	9	—	—	—	—	—
7	YES	9	—	—	9	—	—
8	NO	9	—	—	—	—	—
9	YES	9	—	—	15	—	—
10	NO	9	—	—	—	—	—
11	YES	9	3	3	—	6	12
12	YES	9	—	—	12	—	—
13	YES	9	3	3	—	6	12
14	YES	9	—	—	12	—	—
15	YES	9	3	3	—	6	12
16	YES	9	—	—	12	—	—
17	YES	9	3	3	—	6	12
18	YES	9	—	—	12	—	—
19	YES	9	3	3	—	6	12
20	YES	9	—	—	12	—	—
21	YES	9	3	3	—	6	12
22	YES	9	—	—	12	—	—
23	YES	9	3	3	—	6	12
24	YES	9	—	—	12	—	—
25	YES	9	3	3	—	6	12
26	YES	9	—	—	12	—	—
27	YES	6	—	—	6	—	—
28	YES	6	—	—	12	—	—
29	YES	6	—	—	9	—	—
30	YES	9	3	3	—	6	12
31	YES	9	—	—	12	—	—
32	YES	9	3	3	—	6	12
33	YES	9	—	—	12	—	—

FIGURE 3. SPACING OF WEB REINFORCEMENT

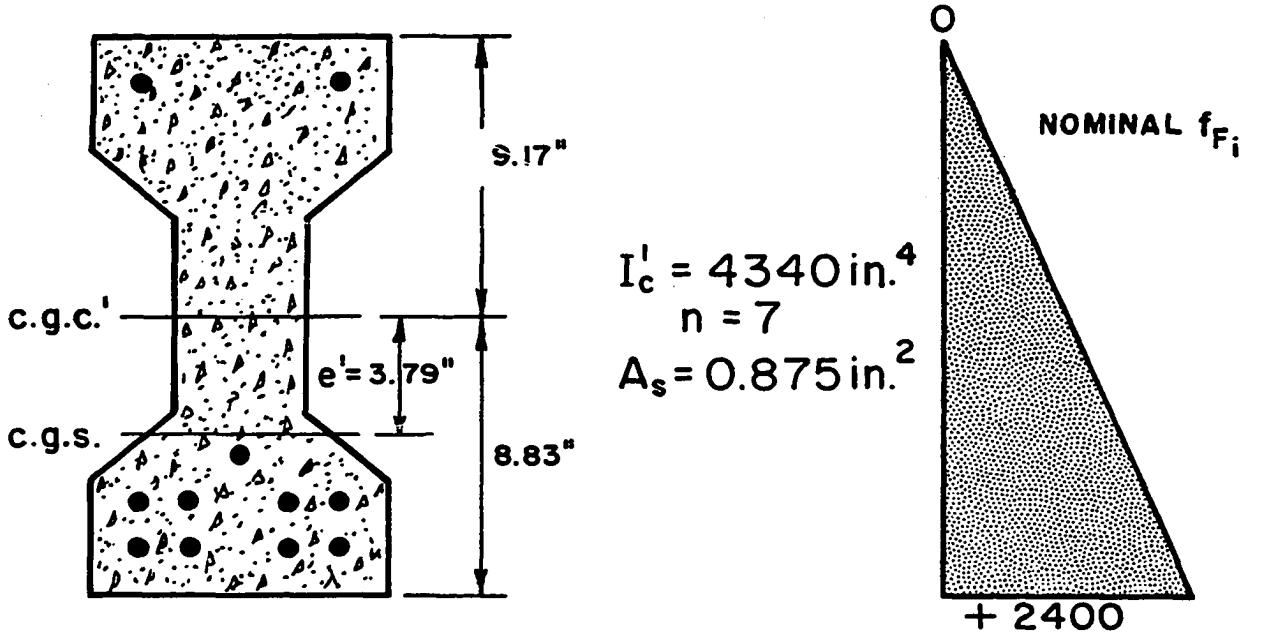

STRAND PATTERN I

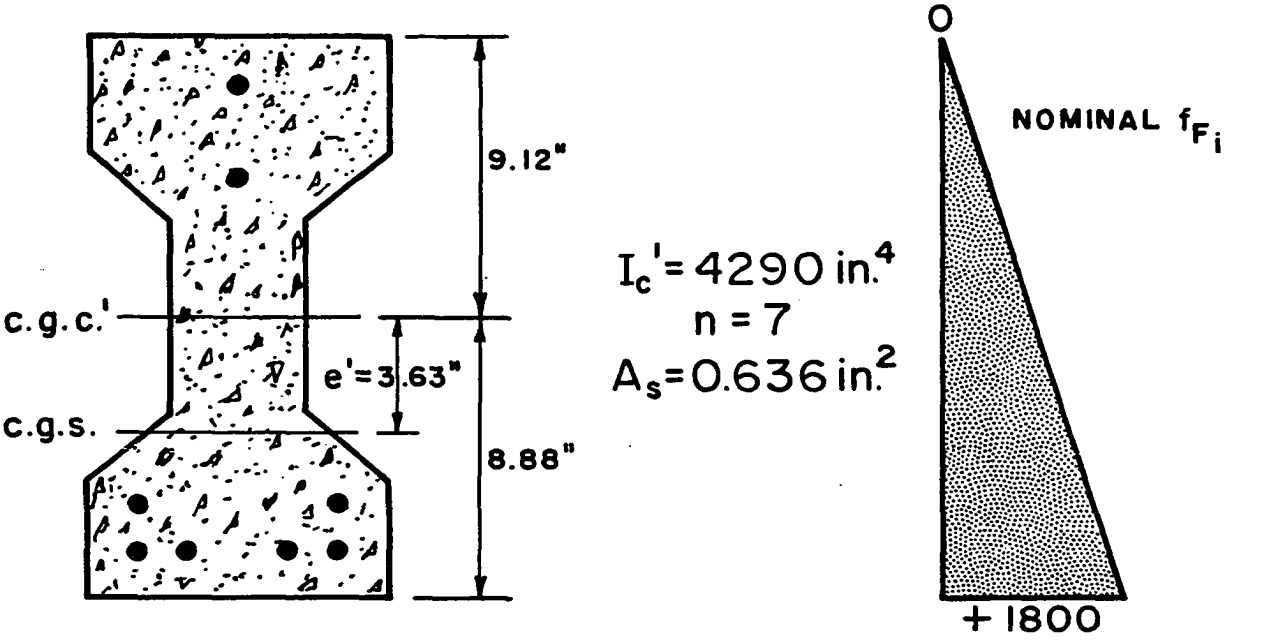

STRAND PATTERN II

FIGURE 4. STRAND PATTERNS AND PROPERTIES OF TRANSFORMED SECTIONS

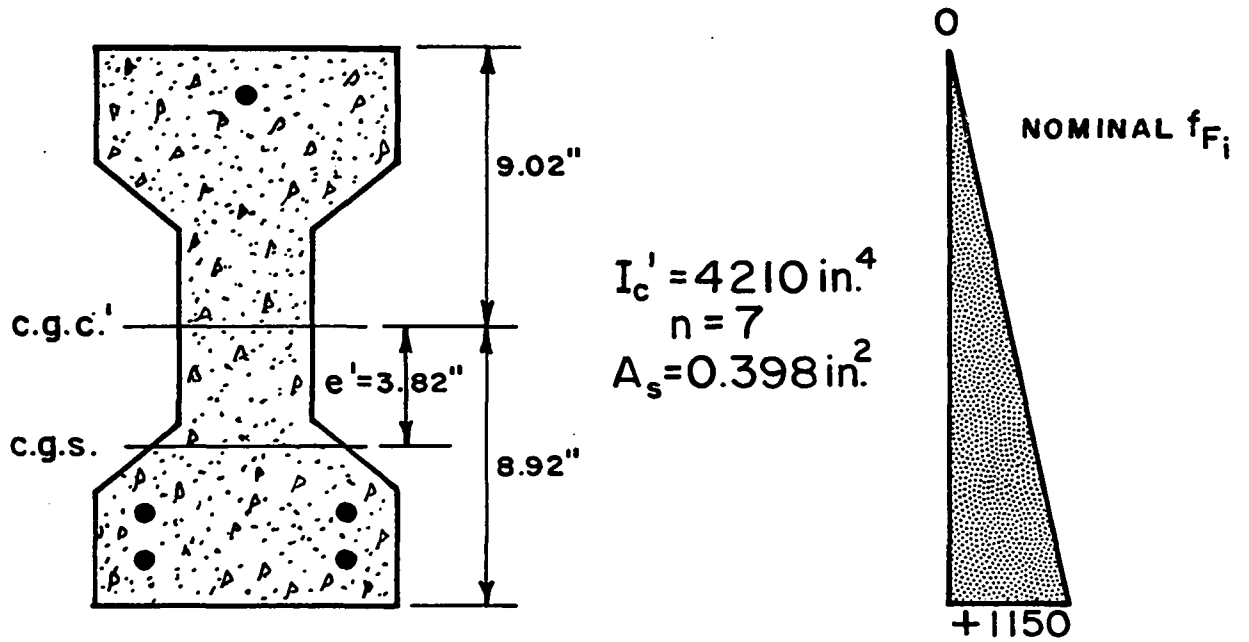

STRAND PATTERN III

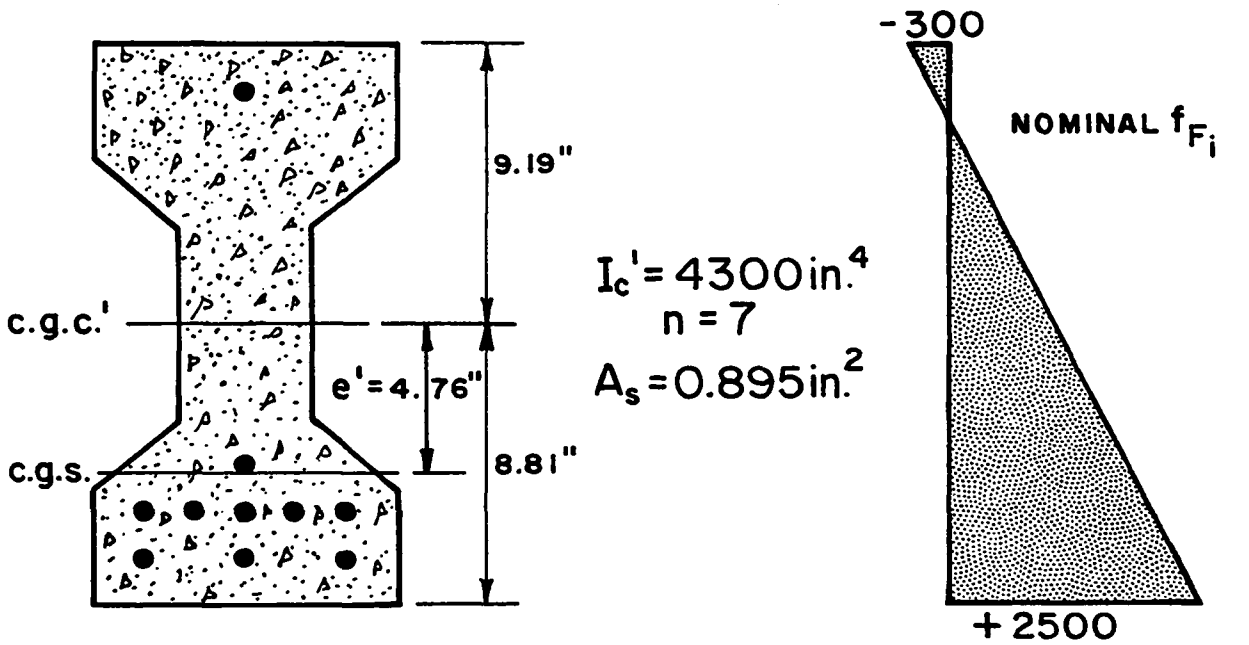

STRAND PATTERN IV

FIGURE 4.(continued) STRAND PATTERNS AND PROPERTIES OF TRANSFORMED SECTIONS

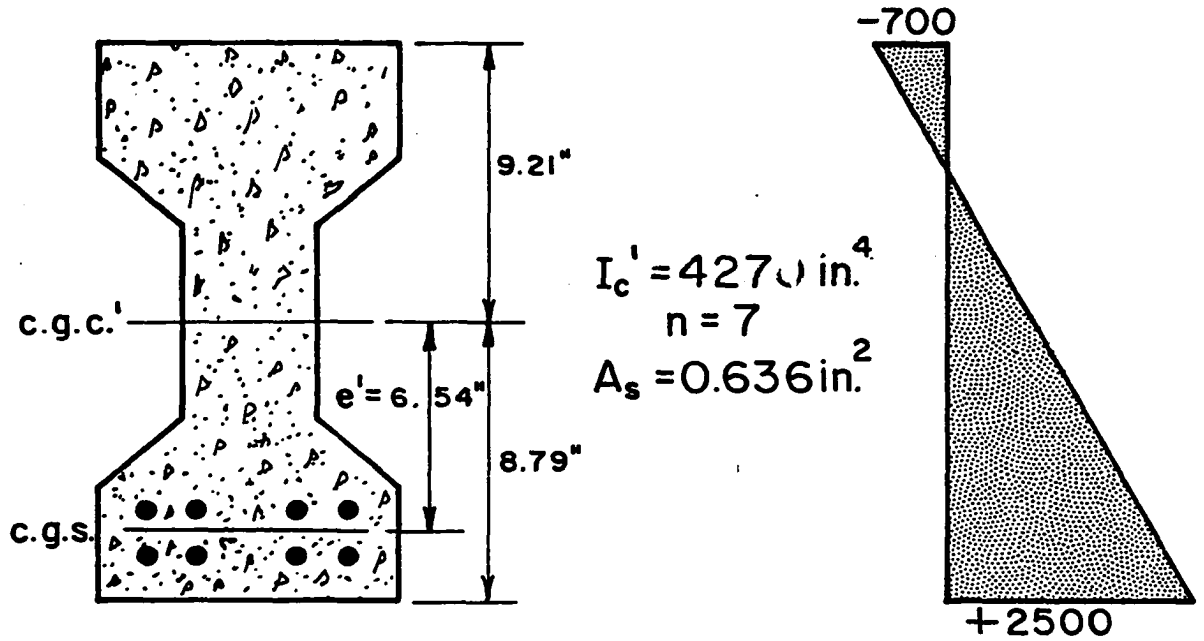

STRAND PATTERN V

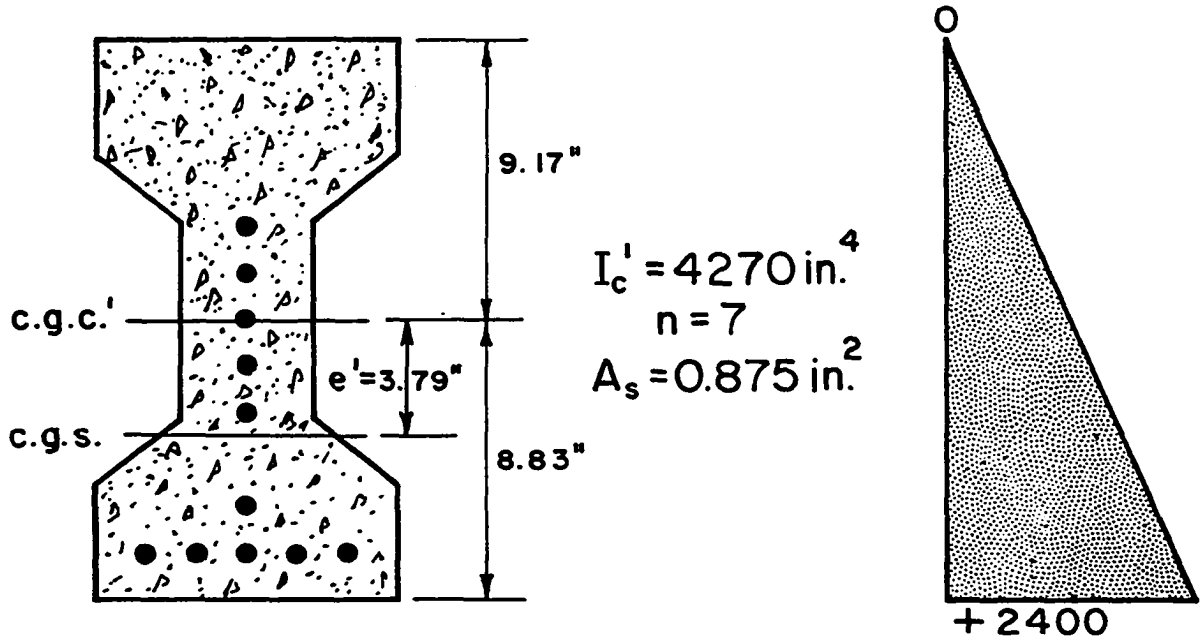

STRAND PATTERN VI

FIGURE 4. (continued) STRAND PATTERNS AND PROPERTIES OF TRANSFORMED SECTIONS

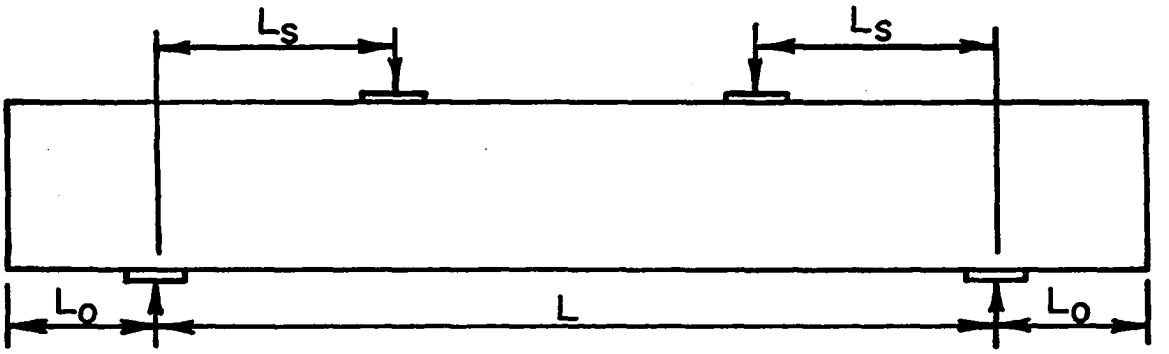

BEAM	L_S, INCHES	L_O, INCHES	L, INCHES
1	36	3	108
2	36	3	108
3	36	3	108
4	36	3	108
5	36	3	108
6	36	3	108
7	36	3	108
8	36	3	108
9	36	3	108
10	36	3	108
11	36	3	108
12	36	3	108
13	36	3	108
14	36	3	108
15	36	3	108
16	36	3	108
17	36	3	108
18	36	3	108
19	24	3	108
20	24	3	108
21	24	15	84
22	36	15	84
23	12	27	60
24	36	21	72
25	36	3	108
26	36	15	84
27	36	3	72
28	12	3	72
29	18	3	72
30	36	3	108
31	36	15	84
32	36	15	84
33	36	3	108

FIGURE 5. SPAN DIMENSIONS FOR TEST BEAMS

the Iowa Engineering Experiment Station Laboratory. The initial step in the fabrication process consisted of threading the steel strand first through the steel templates which formed the ends of the beams and then through the anchorage plates at the ends of the bed. The anchorage plate at one end was stationary, while the plate at the other end was movable. Next, Steelcase Strandvise grips were slipped over the ends of the strands to provide anchorage for fabrication. Load cells were inserted between the grip and the movable anchorage plate on four of the strands to provide a means for measuring the initial prestress force in the strands. A description of the prestressing bed and the load cells was given by Monson (14).

Each strand was tensioned individually to a force of 500 pounds to set the grips and to insure that all strands would have essentially the same force. A hydraulic jack was then used to pull the movable head to the position required to tension the strands to the desired initial force. When the strands had reached the proper tension, movable nuts were tightened to secure the movable head, thus allowing removal of the jack. After the strands had been tensioned, the vertical web reinforcement and lifting hooks were wired into place. The greased side forms were then bolted into place and spacers were installed at the top of the forms. The test beams were cast in pairs, except specimens 27-29 which, because of their shorter length, were cast at the same time.

The concrete was placed in the forms and consolidated with an internal vibrator. At intervals during the placing procedure, samples

of the concrete were used to cast a total of fifteen 4-1/2 x 9-inch compression cylinders, five 6 x 6 x 36-inch flexure specimens, and four 4 x 4 x 36-inch tension specimens. To cure the concrete, wet burlap was kept in contact with all exposed surfaces until the time of release of the prestressing strands.

After the concrete had attained the required strength, the side forms for the test beams were removed and the prestressing strands were released slowly with the hydraulic jack. At the time of release, initial and final readings were taken on the load cell strain gages to measure the actual initial prestressing force. Also, at the time of release, the cylinders, flexure specimens, and tension specimens of the concrete were removed from the forms. The test beams and concrete specimens were then set aside until the load tests were performed.

Materials

Concrete The concrete mix for all of the test beams was a typical mix used in the production of prestressed bridge beams in Iowa. Quantities of materials required for one cubic yard of concrete are:

35 gallons of water

8-3/4 sacks of cement

1175 pounds of fine aggregate

1763 pounds of coarse aggregate

The maximum size of aggregate was 3/4 inch. The nominal slump for each batch was two inches. All concrete was provided by Ames Concrete, Inc. Sixteen one-yard batches were required to produce the 35 test beams and the concrete specimens.

Prestressing steel strand All of the steel used for prestressing was 3/8-inch, stress relieved, seven wire strand. The strand was the same type used in commercial beams, and had a specified minimum ultimate strength of 250,000 psi.

Web reinforcement and lifting hooks The vertical web reinforcement was fabricated from ordinary No. 3 structural steel deformed bars. The shape and general dimensions of the stirrups are shown in Figure 2b. The lifting hooks were formed from short lengths of strand and are shown in place in Figure 3.

Testing Procedure

Test beams

All of the beams were loaded to ultimate failure in one load cycle in an hydraulic testing machine. The load was applied in 5-kip increments, either as two symmetrically placed vertical concentrated loads or as a single concentrated load at the center of the span. The beams were simply supported on 1 x 6-inch steel plates which extended across the entire width and served to distribute the reaction. A condition of no-lateral-restraint was provided by supporting each plate on a 2-inch diameter steel bar. Each load was transmitted by a 1-inch diameter steel bar acting on a 1 x 6-inch steel plate which served to distribute the load. A thin layer of plaster of Paris was placed between each of the 1 x 6-inch plates and the surface of the beam. The manner of supporting and loading the beams is shown in Figure 6.

The primary quantities measured during the load test were (1) the load at which shear strength was reached and (2) the location of the

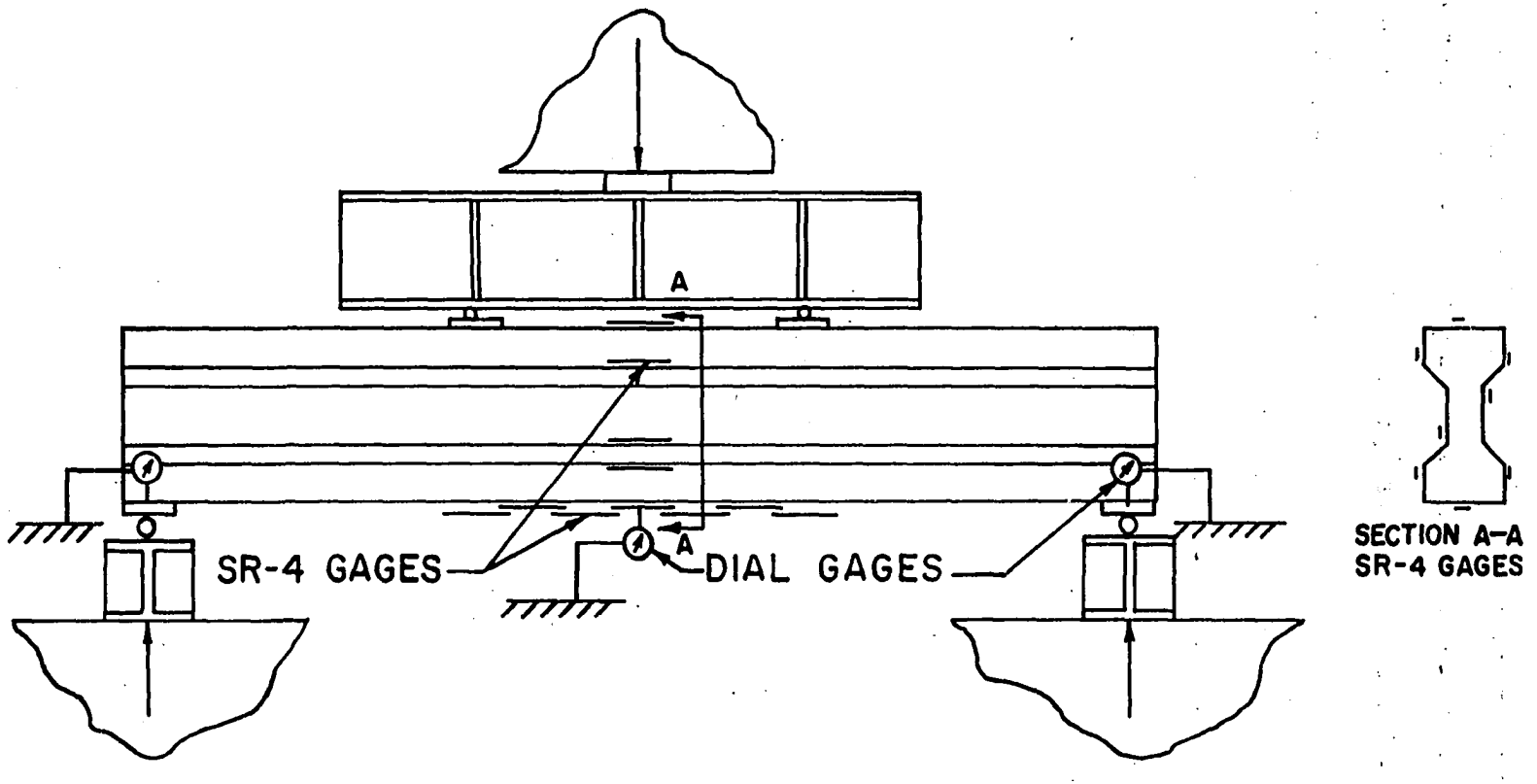

FIGURE 6. LOADING ARRANGEMENT FOR TEST BEAMS

inclined tension crack which indicated the attainment of the shear strength. Other measurements taken during the load test were (3) the load at which the first flexural cracks occurred at the bottom of the beam, (4) ultimate load, (5) the deflection of the beam at mid-span, and (6) flexural strain distribution around the cross-section at mid-span. Measuring the load at which the shear strength was reached consisted of recording the load on the testing machine at which the inclined tension crack appeared. The location of the inclined tension cracks were measured immediately after the cracks appeared.

Measurement of the load at which the first flexural cracks occurred at the bottom of the beam was a problem of a different type. A line of SR-4 strain gages, A-9 type, was placed along the bottom of the test beams covering the region exposed to the maximum moment. The gages were overlapped slightly to give a continuous line. As the load was applied in the lower load range, the strain readings on each gage exhibited a uniform change in strain for each load increment. As the load reached higher values, the concrete at the bottom of the beam was subjected to high tensile stresses resulting in the formation of tiny cracks. When the cracks formed, some of the strain gages exhibited either a larger or a smaller change in strain than the change shown for loads in the lower range. At the first sign of non-uniformity shown by the bottom gages, the cracks were too small to be detected by the unaided eye. But, as the loads were increased, the cracks first appeared under the gages which had first shown the non-uniform gain in strain.

Measurement of the ultimate load consisted of recording the maximum

load that the beam would accept. Mid-span deflections were measured with dial gages located on each side of the beam at the end reactions, and on each side at mid-span. Also during the load test, strain measurements were recorded from SR-4 gages, A-9 type, placed around the cross-section at mid-span. Location of the dial gages and all of the SR-4 gages is shown in Figure 6.

Concrete specimens

Cylinders The 4-1/2 x 9-inch cylinder specimens were loaded to failure by direct compression. During the load test of each cylinder, a compressometer was attached for measurement of longitudinal strain. The compressometer had a gage length of five inches and a multiplication ratio of two. A dial gage with a least count of 0.0001 inch was used to measure the total strain. As the load was applied in 5-kip increments, strain readings were taken up to the ultimate load. The rate of loading was approximately one kip per second. At least three cylinders were tested (1) at the time of release of the prestress force and (2) at the time the test beam was loaded to failure.

Flexure specimens The 6 x 6 x 36-inch flexure specimens were used to determine (1) the modulus of rupture of the concrete and (2) the stress-strain characteristics of the concrete subjected to bending. The beams were tested with third point loading over a 30-inch span. Two SR-4 strain gages, A-9 type, were cemented to the bottom side of each of the specimens between the load points. The load was applied in 500-pound increments until the specimen was fractured. Readings of the SR-4 gages were taken at each load increment. The rate of loading was approxi-

mately 200 pounds per minute.

Tension specimens The tension specimens (10) were 4 x 4-inches in cross-section and had a length of 36 inches. The cross-section was constant over a 16-inch portion of the specimen and was enlarged into bulb-shaped ends for gripping. The specimens were loaded to fracture at a rate of approximately 100 pounds per second. The ultimate load was determined, but no strain measurements were taken.

THEORETICAL ANALYSIS

The problem of predicting the susceptibility of a prestressed beam to a shear-type failure can be approached through two methods. In the first method, experimentally determined empirical equations can be used, provided that the properties of the given beam fall within the restrictions imposed in the derivation of the equations. In light of the research work completed and the equations now available, it appears that the use of this method is very limited. The second method involves the determination of principal stresses produced in the beam plus a comparison of these stresses with limiting stresses dictated by a theory of failure for the concrete. In this study, the theoretical analysis will be focused on the determination of the principal stresses produced in the test beams.

The test beams were loaded to determine the load at which the sudden inclined tension crack completely traversed the web. For each of the test beams, principal stresses were computed at a number of points in the web section, considering the applied load as the load which produced this sudden crack. To identify the points at which principal stresses were determined, a grid system was used as shown in Figure 7.

The principal stresses at a point in a condition of plane stress are given by:

$$S_c = \frac{S_x + S_y}{2} + \sqrt{\left[\frac{S_x - S_y}{2}\right]^2 + S_s^2} \qquad (1)$$

$$S_t = \frac{S_x + S_y}{2} - \sqrt{\left[\frac{S_x - S_y}{2}\right]^2 + S_s^2} \qquad (2)$$

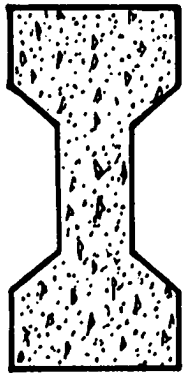

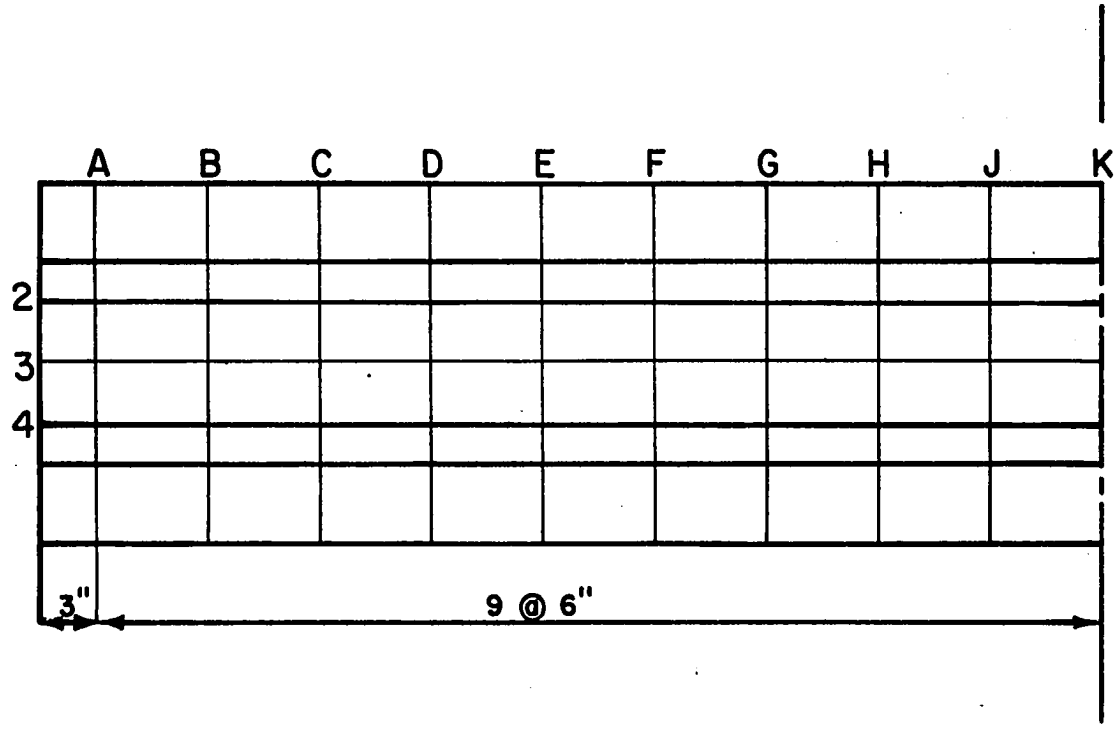

FIGURE 7. GRID SYSTEM

The angle between a horizontal plane and the plane on which one of the principal stresses acts is represented by θ. The angle θ can be found from the expression:

$$\tan 2\theta = \frac{-2S_s}{S_x - S_y} \tag{3}$$

The stresses S_x and S_y represent the total normal stresses and S_s represents the total shearing stress on vertical and horizontal planes at a point in the beam.

Stress Analysis

The several factors which produce the stresses are (1) the cross shear and bending moment caused by the dead load and the applied load, (2) the direct compressive force produced by the prestressing steel, (3) the stress conditions in the anchorage zone caused by build-up of the prestressing force through bond, and (4) the local effects of the end reactions and applied concentrated loads.

Stresses due to cross shear and bending moment

Since the effect of the dead load is very small as compared to the effect of the applied load, dead load stresses will be ignored. Thus, the shearing stresses which result from the effect of cross shear are given by:

$$v_L = \frac{V_c Q'}{I'_c b'} \tag{4}$$

The normal stresses caused by the bending moment are found from:

$$f_L = \frac{M_c y'}{I'_c} \tag{5}$$

Direct prestress stresses

For cross-sections of the beam which are in the center portion between the ends of the anchorage zones, the initial direct prestress stresses are given by:

$$f_{F_i} = \frac{F_i}{A'_c} \mp \frac{F_i e' y'}{I'_c} \tag{6}$$

The effective direct prestress stresses are given by:

$$f_F = \frac{F}{A'_c} \mp \frac{F e' y'}{I'_c} \tag{7}$$

For cross-sections of the beam which are in the anchorage zone, the manner in which the direct prestress stresses develop from the end of the beam to the end of the anchorage zone must be known. In Monson's study (14), the manner in which the prestress stresses develop was determined for a beam having the same cross-section used in this study and having strand pattern I. The results of Monson's study are shown in modified form in Figure 8a. The stresses are presented as fractions of the stress at the bottom fiber at mid-span, f_B, due to effective prestressing only. The procedure used to determine the value of f_B for each beam is explained in the Results section.

From the results presented in Figure 8a, the graph in Figure 9a was developed. The graph represents the build-up of the effective prestress stress along horizontal grid lines 2, 3, and 4 from the end of the beam to mid-span. The abscissa represents the distance from the end of the beam, while the ordinate represents the effective prestress

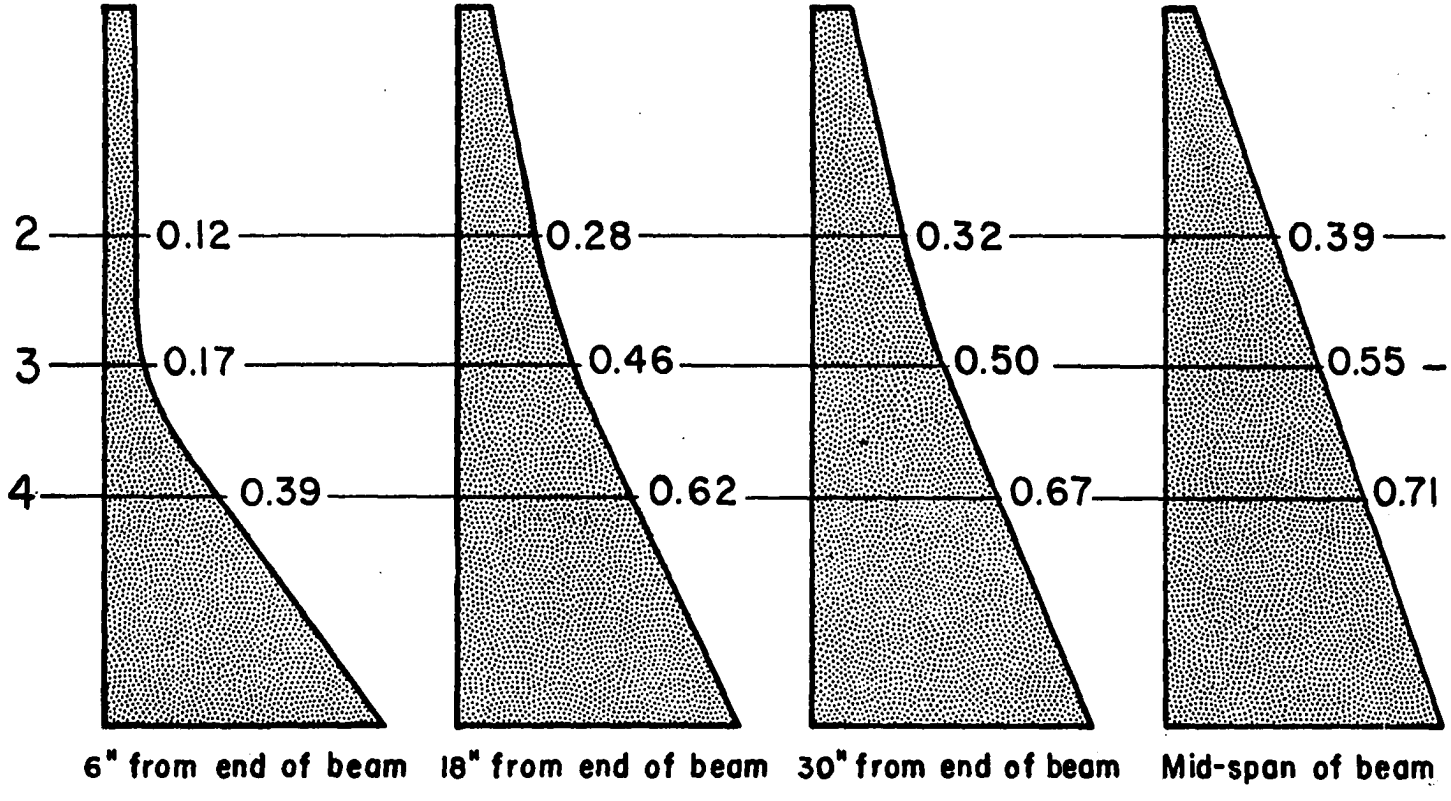

FIGURE 8a. PRESTRESS STRESS (f_F) DISTRIBUTION FOR STRAND PATTERNS I, II, AND III

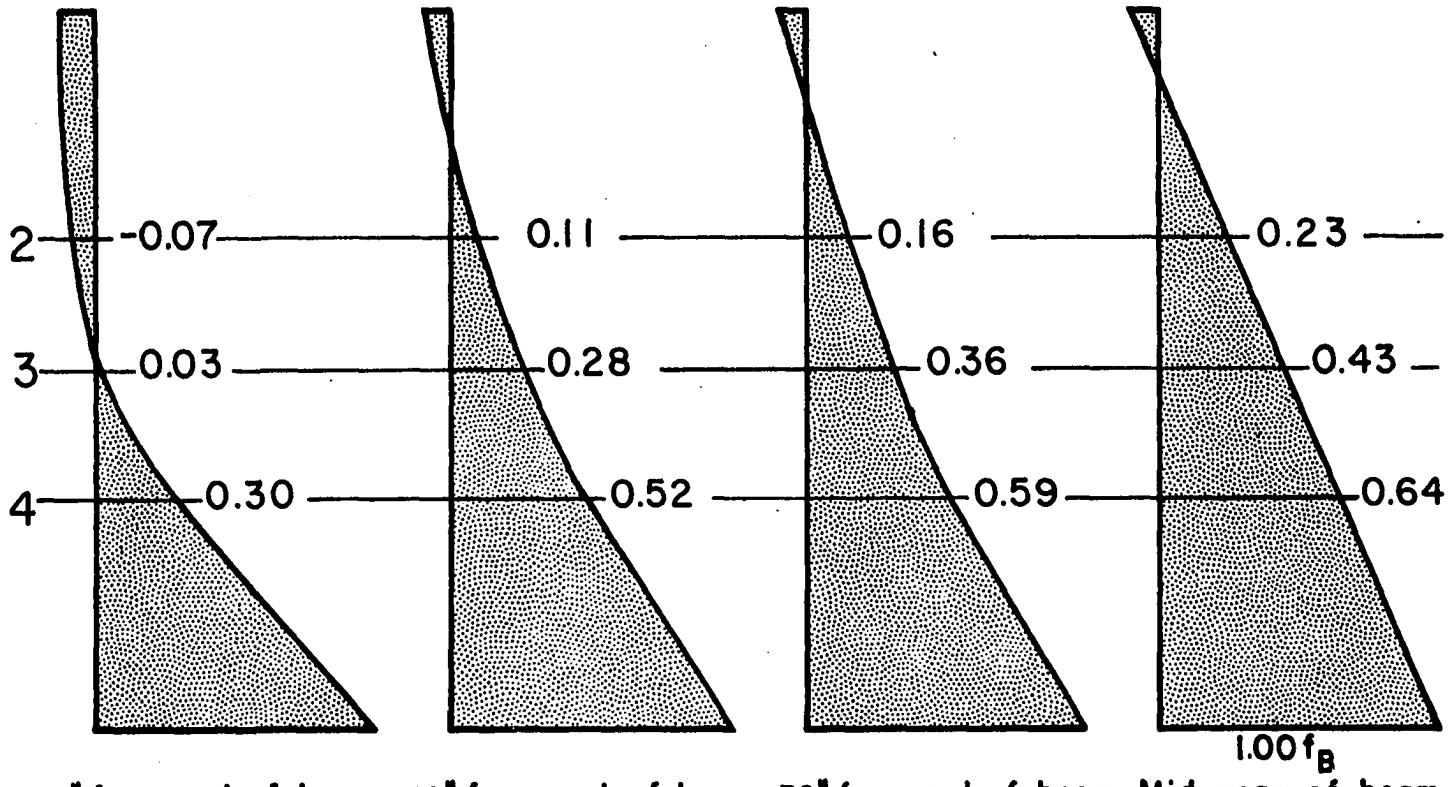

FIGURE 8b. PRESTRESS STRESS (f_B) DISTRIBUTION FOR STRAND PATTERN IV

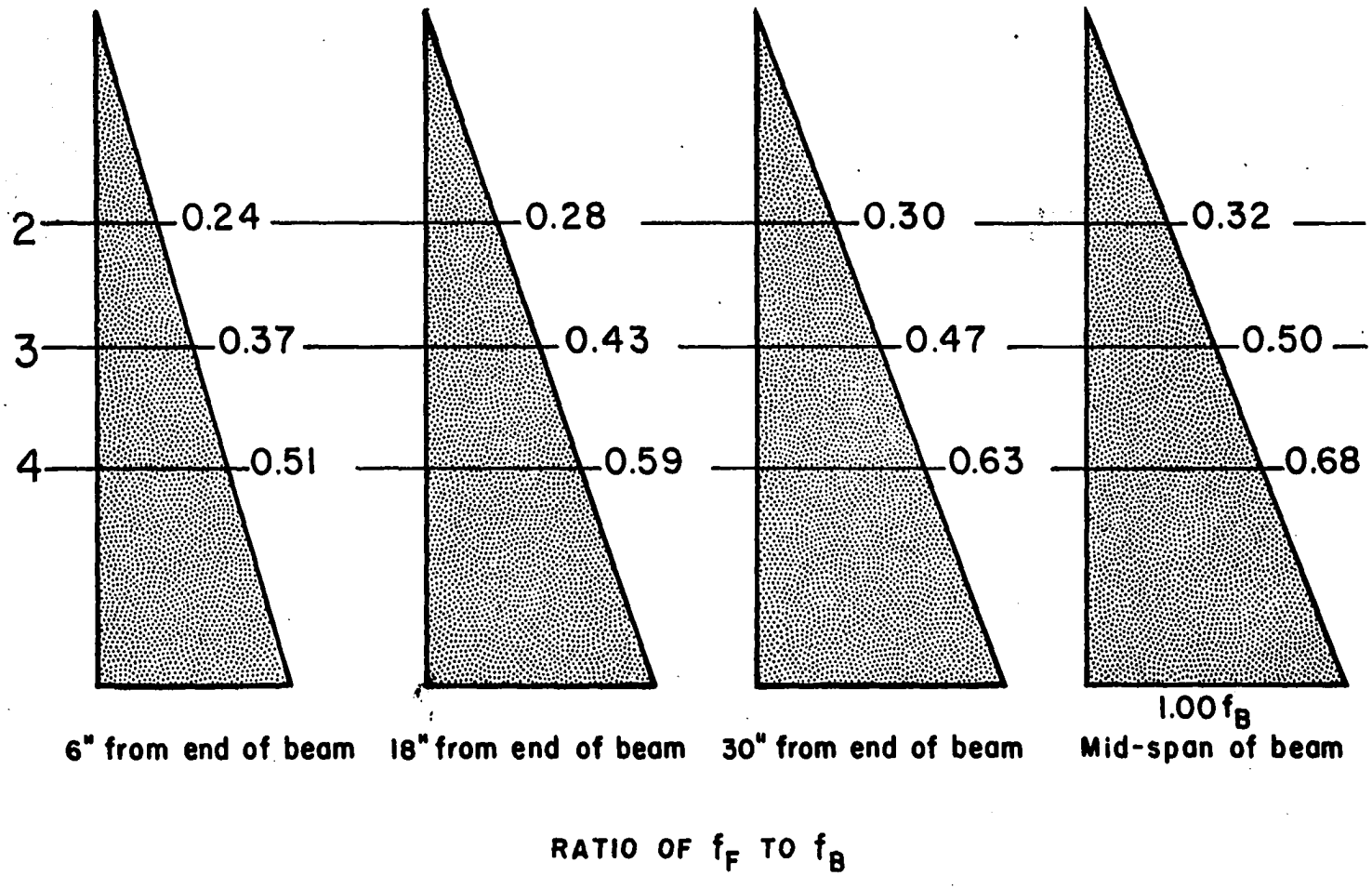

FIGURE 8c. PRESTRESS STRESS (f_F) DISTRIBUTION FOR STRAND PATTERN VI

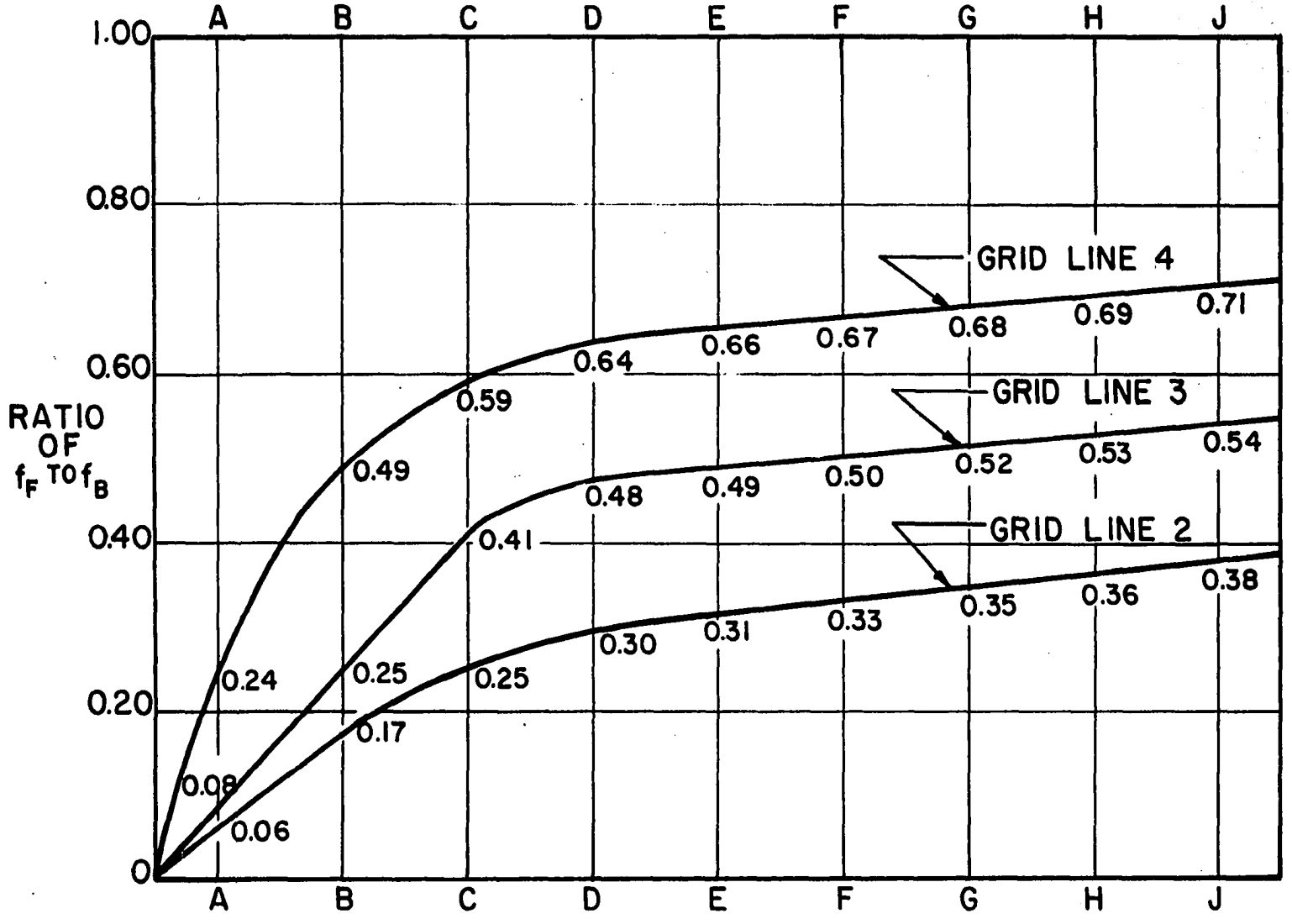

FIGURE 9a. PRESTRESS STRESS (f_F) VARIATION ALONG HORIZONTAL GRID LINES FOR STRAND PATTERNS I, II, AND III

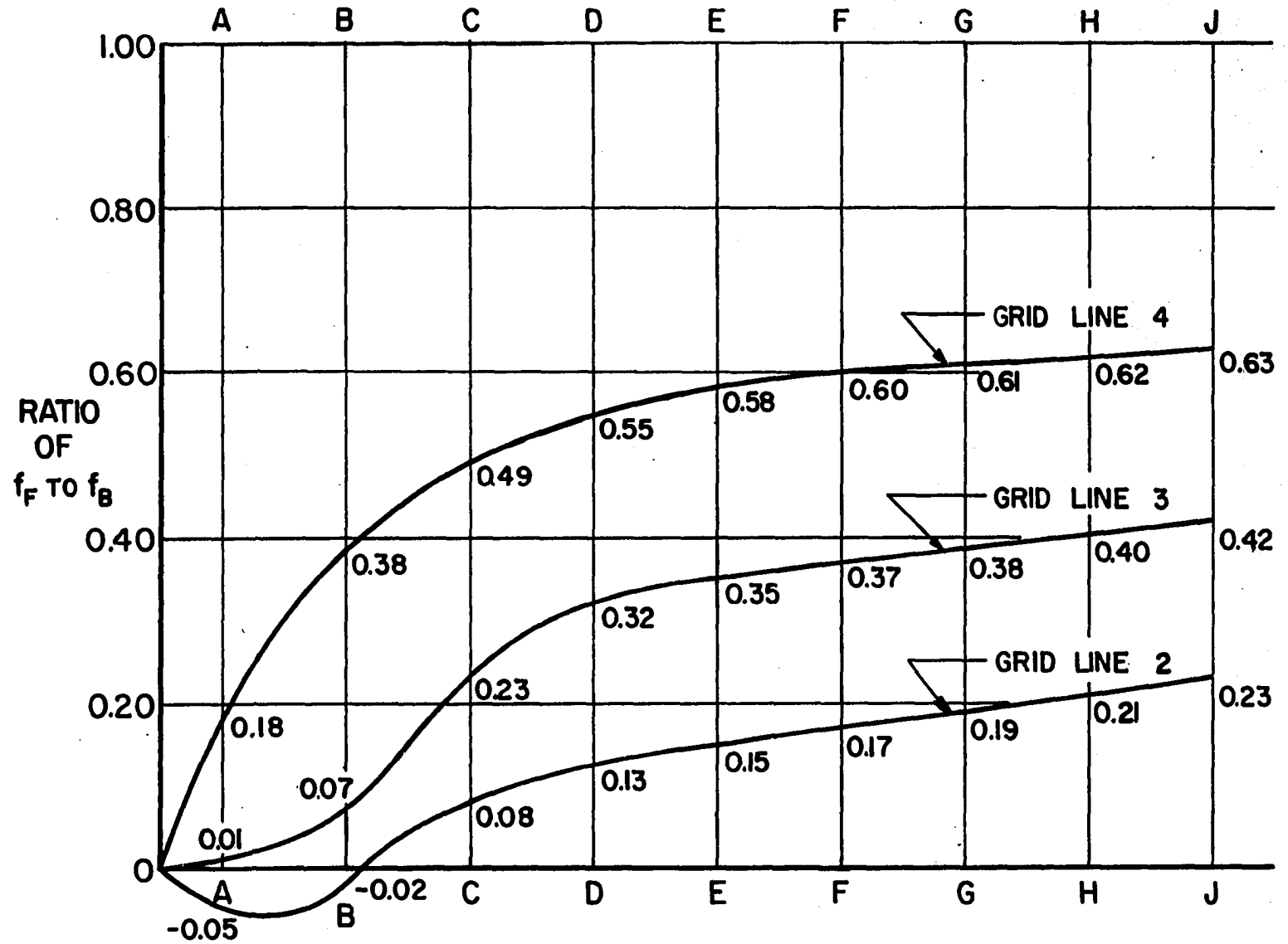

FIGURE 9b. PRESTRESS STRESS (f_F) VARIATION ALONG HORIZONTAL GRID LINES FOR STRAND PATTERN IV

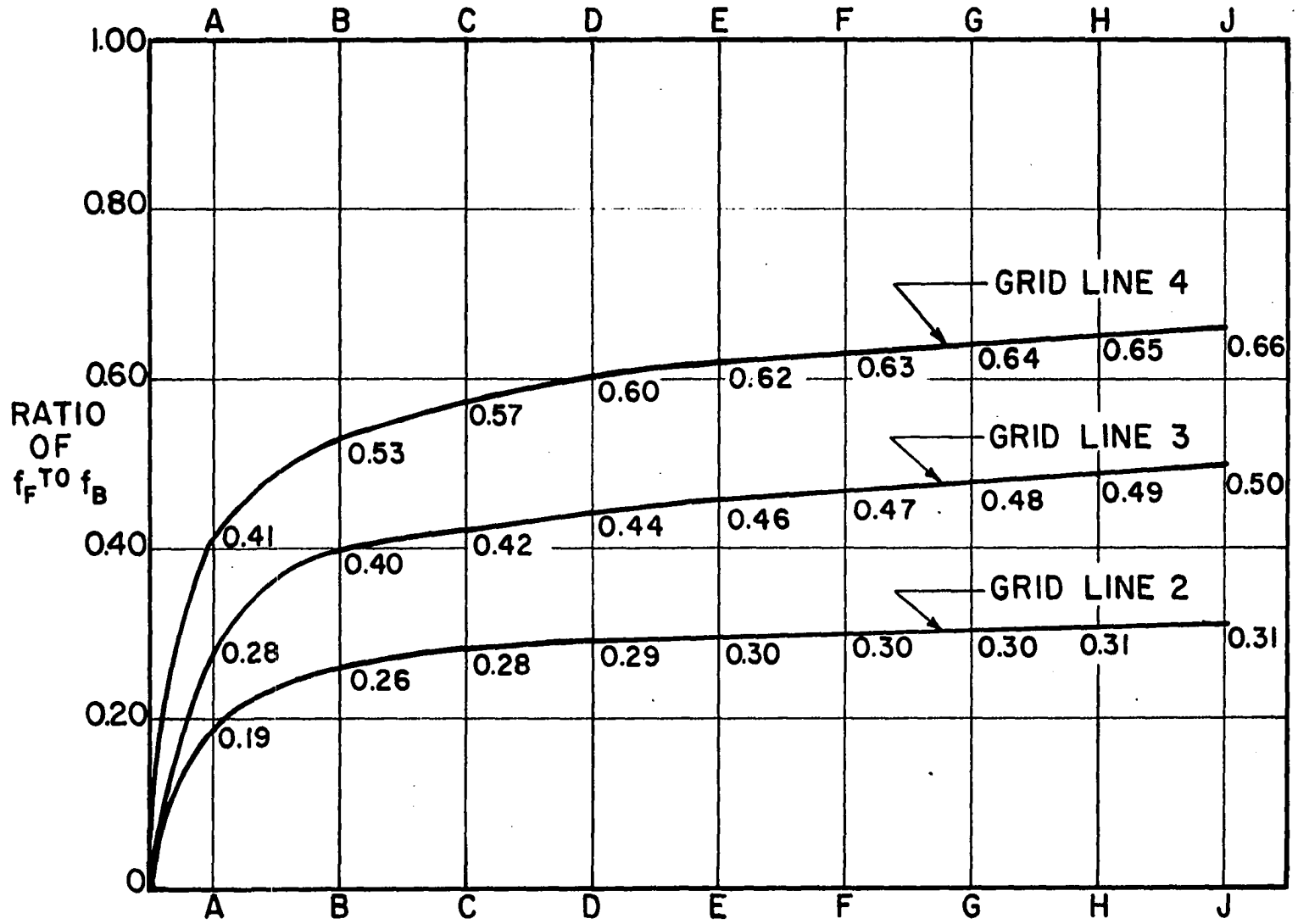

FIGURE 9c. PRESTRESS STRESS (f_F) VARIATION ALONG HORIZONTAL GRID LINES FOR STRAND PATTERN VI

stress as a fraction of f_B. Values of stress at grid lines 2, 3, and 4 were plotted for the four sections shown in Figure 8a, and smooth curves were drawn through the plotted points. Figure 9a was used to develop Figure 10a which shows the stress distributions for cross-sections A, B, C, D, and E. Thus, the stresses f_F at the grid points can be determined by multiplying the coefficients in Figure 10a by the stress f_B. However, the results of Monson's study refer only to beams prestressed with strand pattern I, which would include beams 1-10, 19-24, and 27-33. The following assumptions were used to determine effective prestress stress distributions for the remaining beams. Since the general shape of the prestress stress distribution was essentially the same for strand patterns I, II, and III, the results of Monson's study were assumed to apply to beams 11-14. But, because tensile stresses were produced by patterns IV and V, and because pattern VI differed from pattern I, assumptions were made to cover beams 15-18 and 25-26. The assumptions, which were made by modifying the results given in Figure 8a, are presented in Figures 8b and 8c and represent patterns IV and VI. In assuming the distributions given in Figure 8b, the same general shapes of the distributions in Figure 8a were retained, since the majority of the cables were located in the bottom flange in patterns I, II, and III. But, due to the distribution of strands through the web in pattern VI, it was thought that straight line distributions given in Figure 8c would be appropriate. An assumption was not made for pattern V because tensile cracks which formed at the time of release of the prestressing force made it impossible to complete a theoretical analysis for beams 17 and 18. The development of

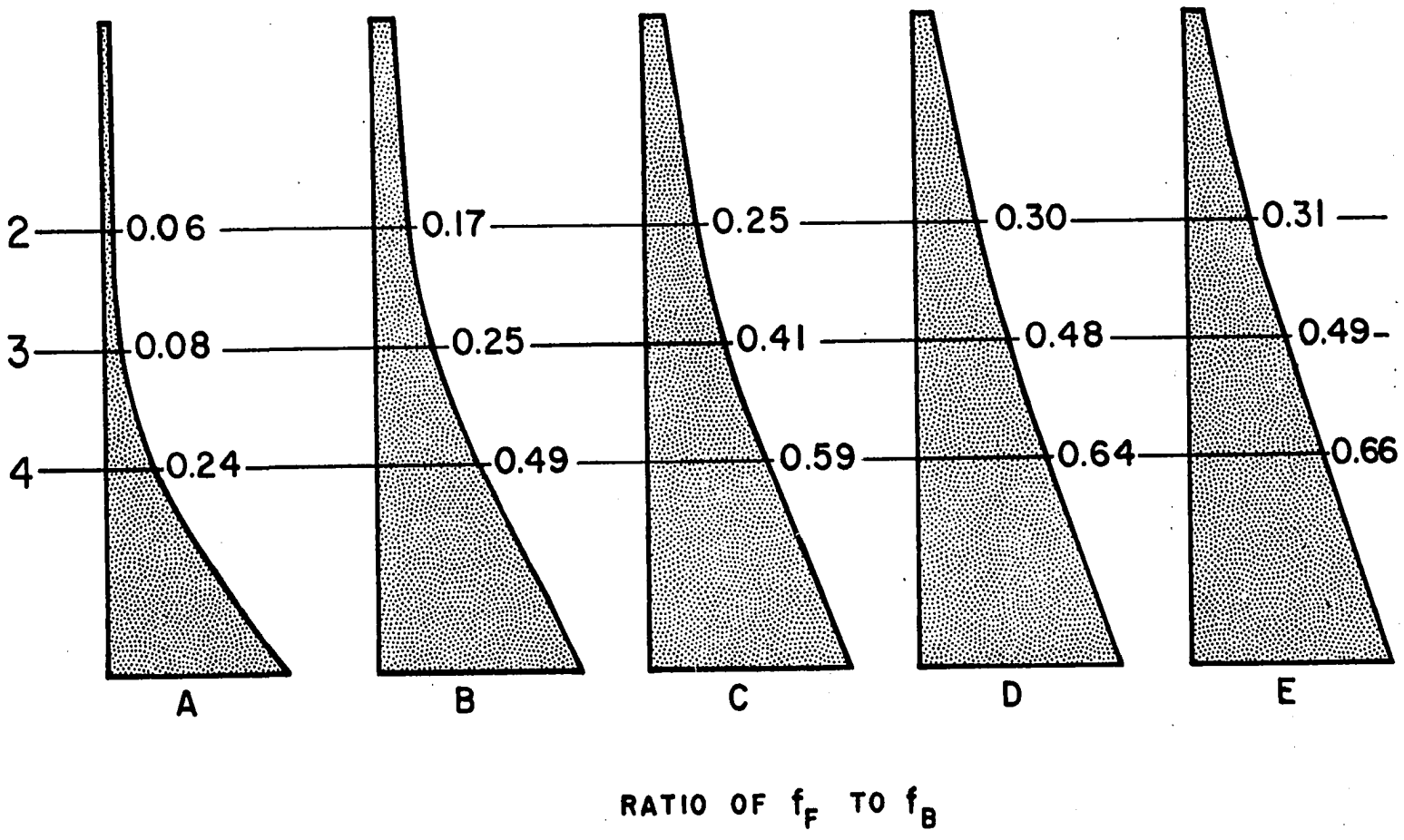

FIGURE 10a. PRESTRESS STRESS (f_F) DISTRIBUTION ALONG VERTICAL GRID LINES FOR STRAND PATTERNS I, II, AND III

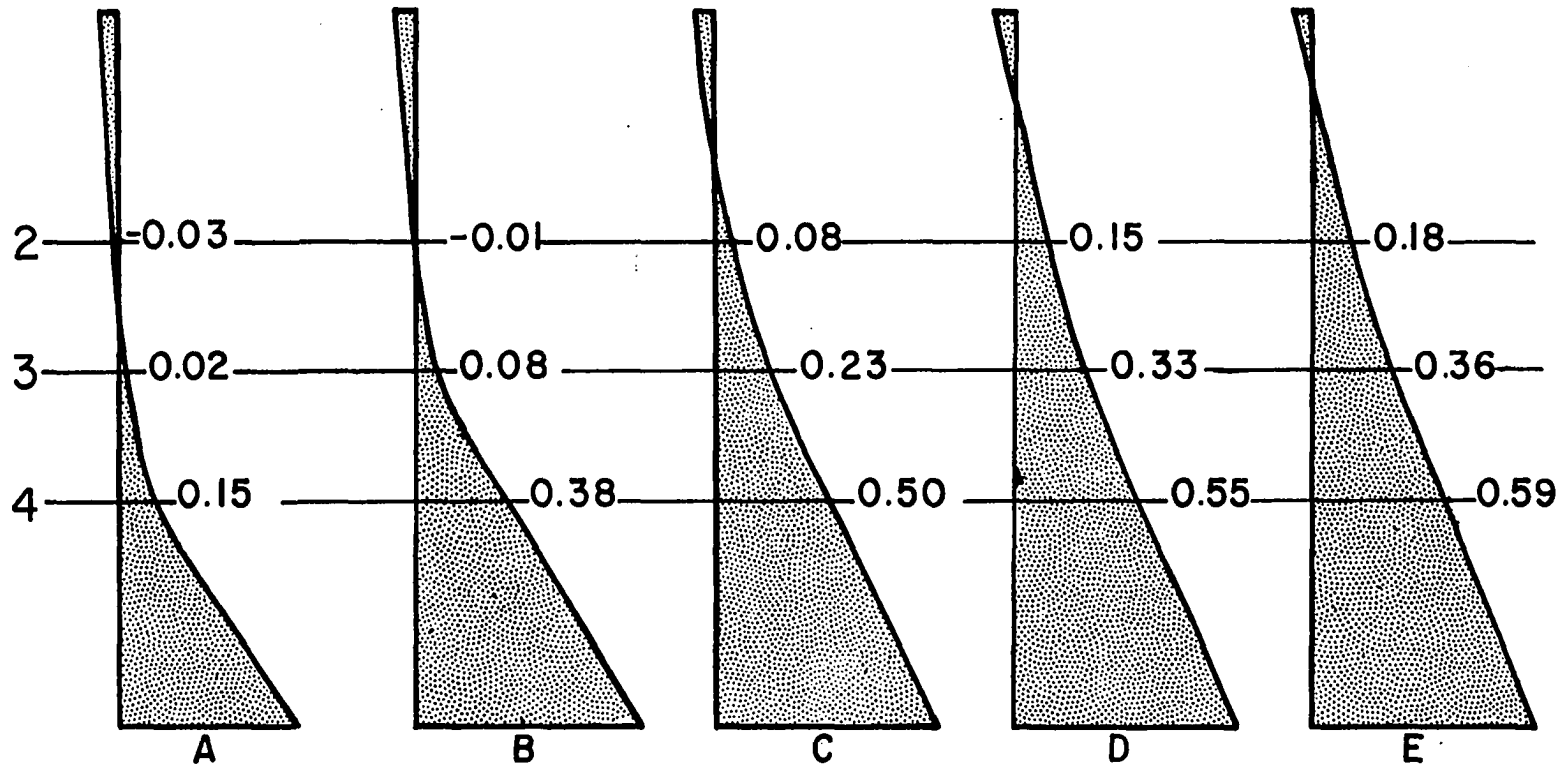

FIGURE 10b. PRESTRESS STRESS (f_F) DISTRIBUTION ALONG VERTICAL GRID LINES FOR STRAND PATTERN IV

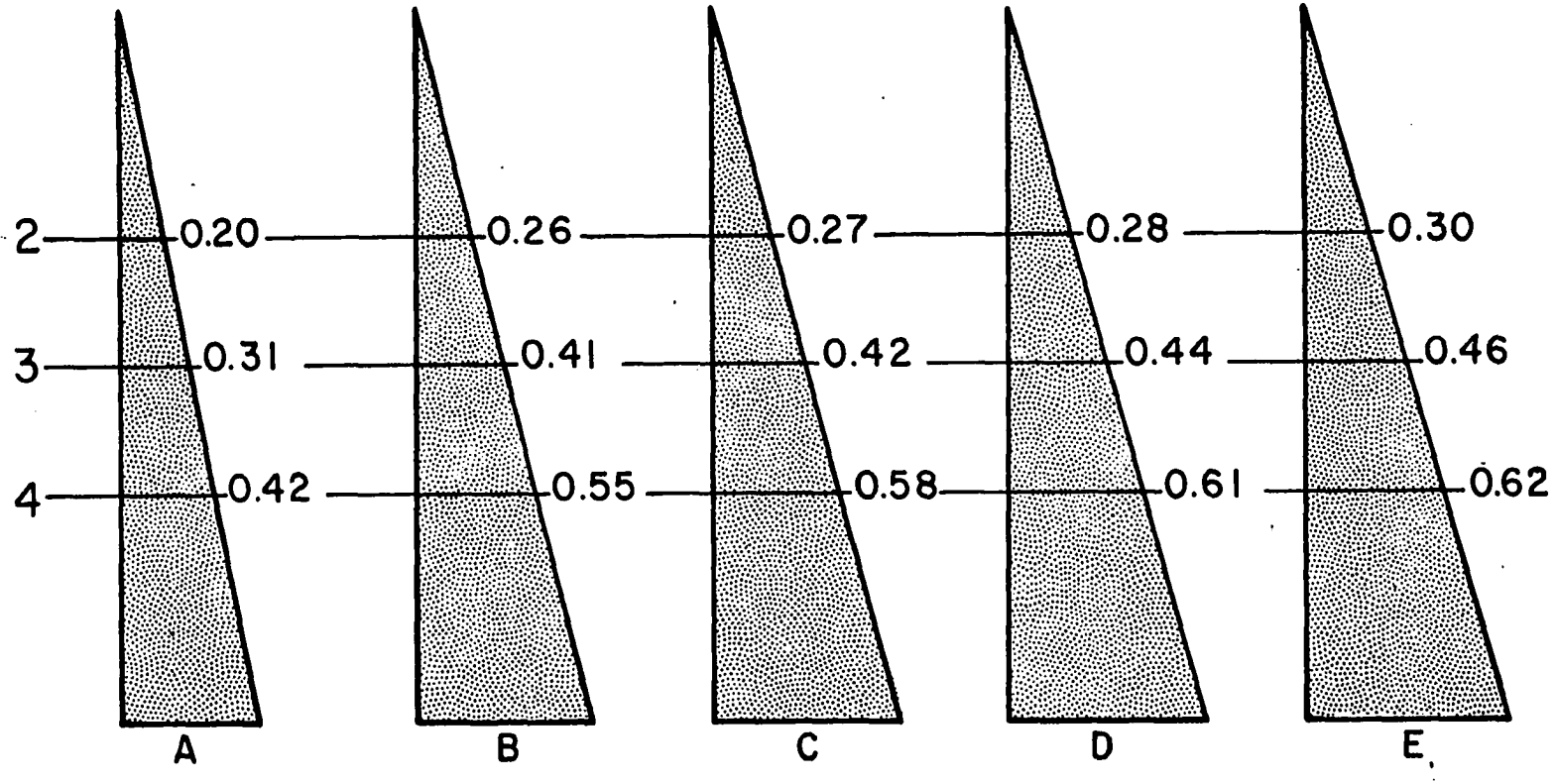

FIGURE 10c. PRESTRESS STRESS (f_F) DISTRIBUTION ALONG VERTICAL GRID LINES FOR STRAND PATTERN VI

Figures 9b, 9c, 10b, and 10c paralleled the previous development of Figures 9a and 10a.

Stresses caused by build-up of the prestressing force

In consideration of the information presented in Figures 9a-10c, the length of the anchorage zone, L_{az}, was taken as 30 inches for all test beams. In Figure 11b, consider the free body diagram of the section of the beam indicated by the dotted line in Figure 11a. On the right face of the free body, a pressure, f_F, is exerted by the effective prestress stress and a tensile force, F, is produced by the prestressing steel. To maintain equilibrium, a shear, V, and a moment, M, must exist on the bottom face.

In the determination of the manner in which the shearing stress caused by V is developed, consider the free body diagram in Figure 11d. The pressure distributions, $(f_F)_B$ and $(f_F)_C$, can be evaluated from Figure 10 for any of the test beams. With reference to Irelan's study (9), assumptions are made regarding the anchorage length for the strands which appear in the free body diagrams. The strands which are located in the top flange are assumed to attain their effective stress uniformly in a 30-inch length. Likewise, for all strands located in the web, the length is assumed to be 21 inches. The force, v, which is required to preserve equilibrium, is a part of the total force, V. The shearing stress, v_F, is assumed to be uniformly distributed over the bottom surface of the free body diagram shown. The shearing stress was determined similarly for the other free body diagrams bounded by the vertical grid lines and grid line 2.

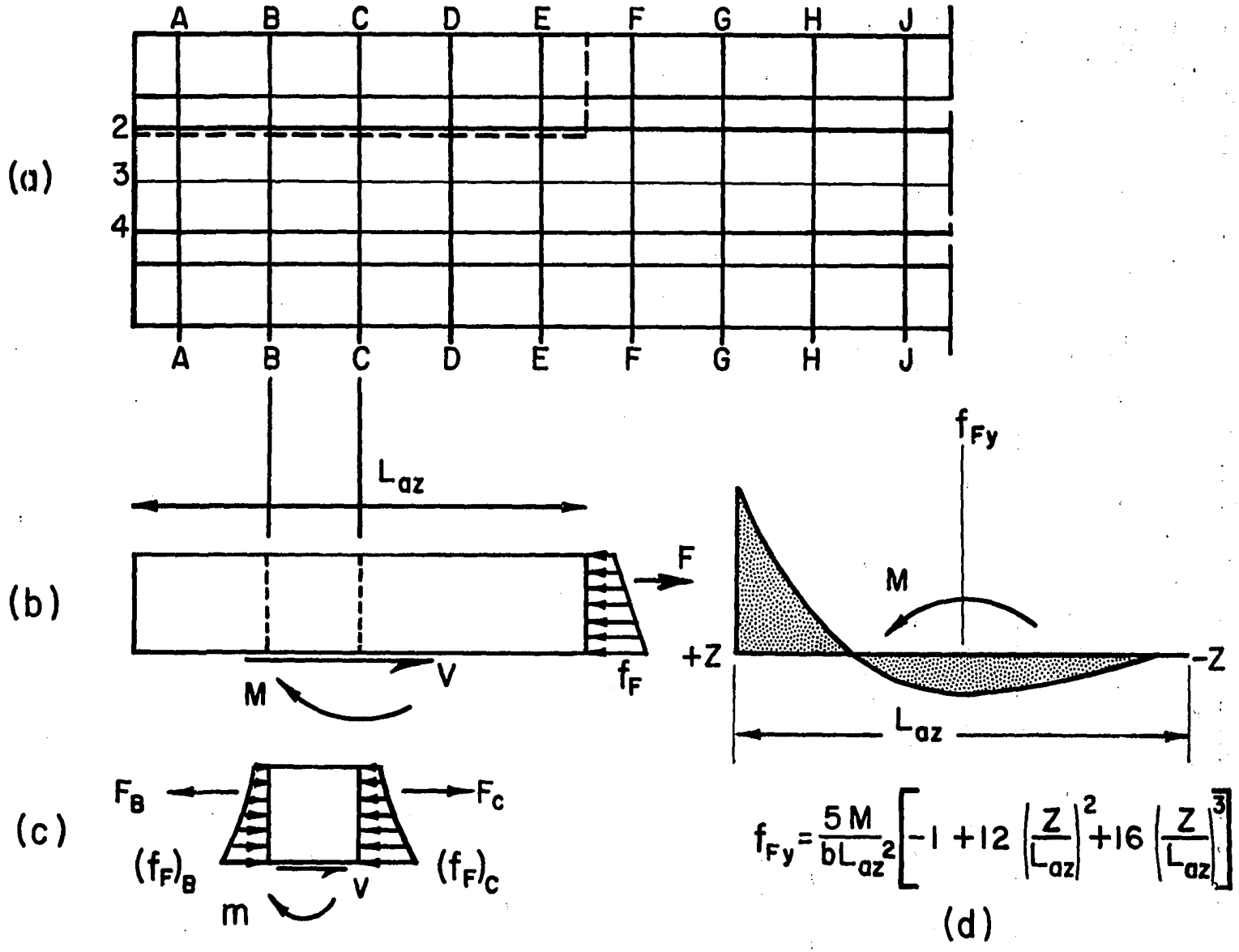

FIGURE 11. SKETCHES USED FOR COMPUTATION OF BUILD-UP STRESSES

The shearing stress distribution from the end of the beam to the end of the anchorage zone was then obtained by plotting the stress values at their respective locations. The distribution of shearing stress along grid lines 3 and 4 was determined in the same manner. The results of the determinations for beams having strand patterns I and II are shown in Figure 12a. Similar stress variations for patterns III, IV, and VI are given in Figures 12b, 12c, and 12d. Thus, from Figure 12, the shearing stress at each of the grid points can be expressed as:

$$v_F = C_1 f_B \tag{8}$$

Values for the constant C_1 are given in Table 1. It is emphasized that the shearing stresses discussed here are due solely to the build-up of the prestress force in the anchorage zone.

Magnel (13) presents an assumption regarding the distribution of fiber stresses produced by the moment, M, in Figure 11b. The assumption is shown in Figure 11c. Values of M, expressed in terms of f_B, were computed for each of the strand patterns, and the stress distribution given by Magnel was used. Thus, the normal stresses produced at the grid points by the moment, M, can be expressed as:

$$f_{F_y} = C_2 f_B \tag{9}$$

Values of the constant C_2 are given in Table 2.

Stresses caused by local effects of concentrated loads

A local effect is produced in a beam at the point of application of a concentrated load. To evaluate the effect, consider the theory

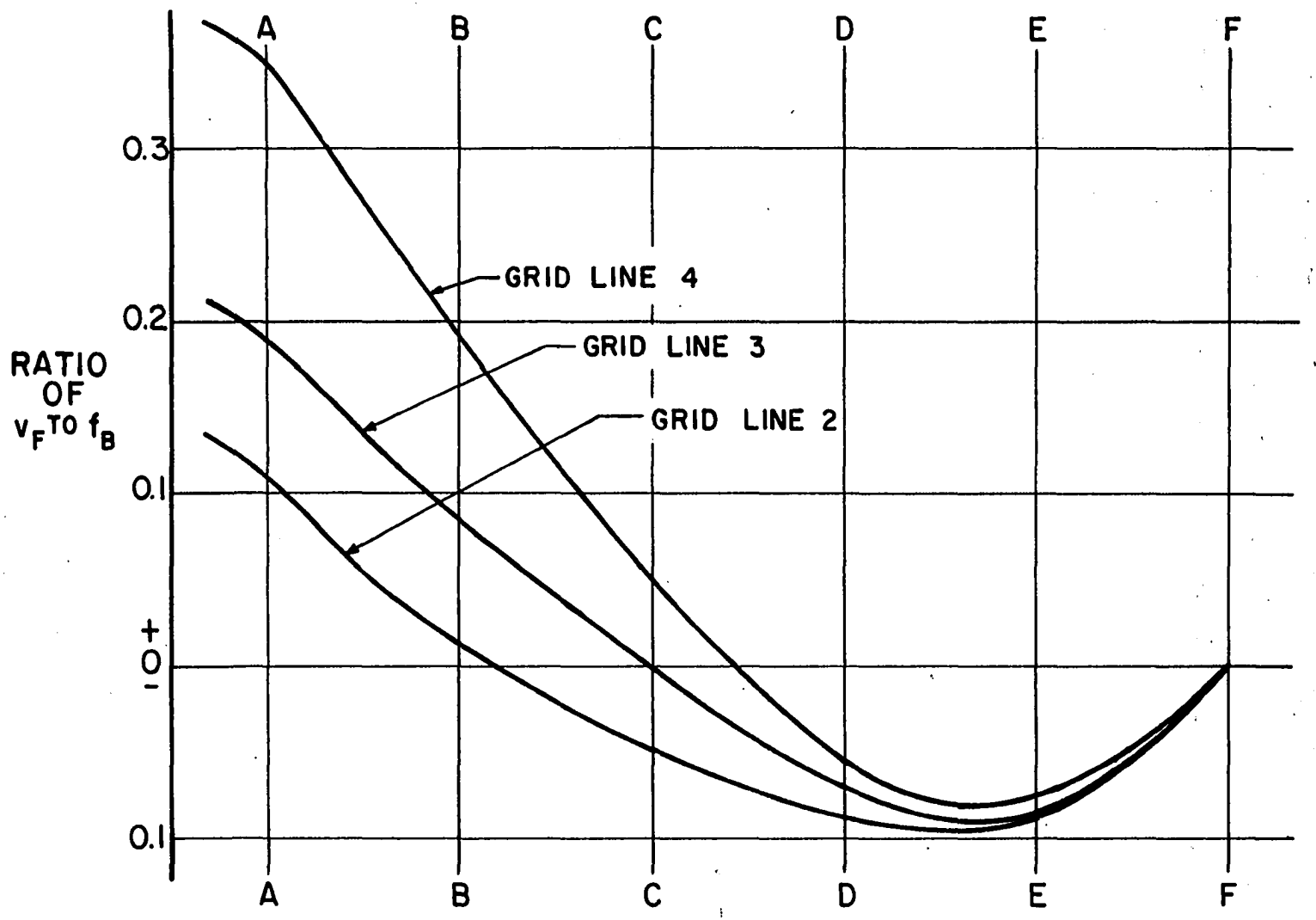

FIGURE 12 a. SHEARING STRESS (v_F) VARIATION ALONG HORIZONTAL GRID LINES FOR STRAND PATTERNS I AND II

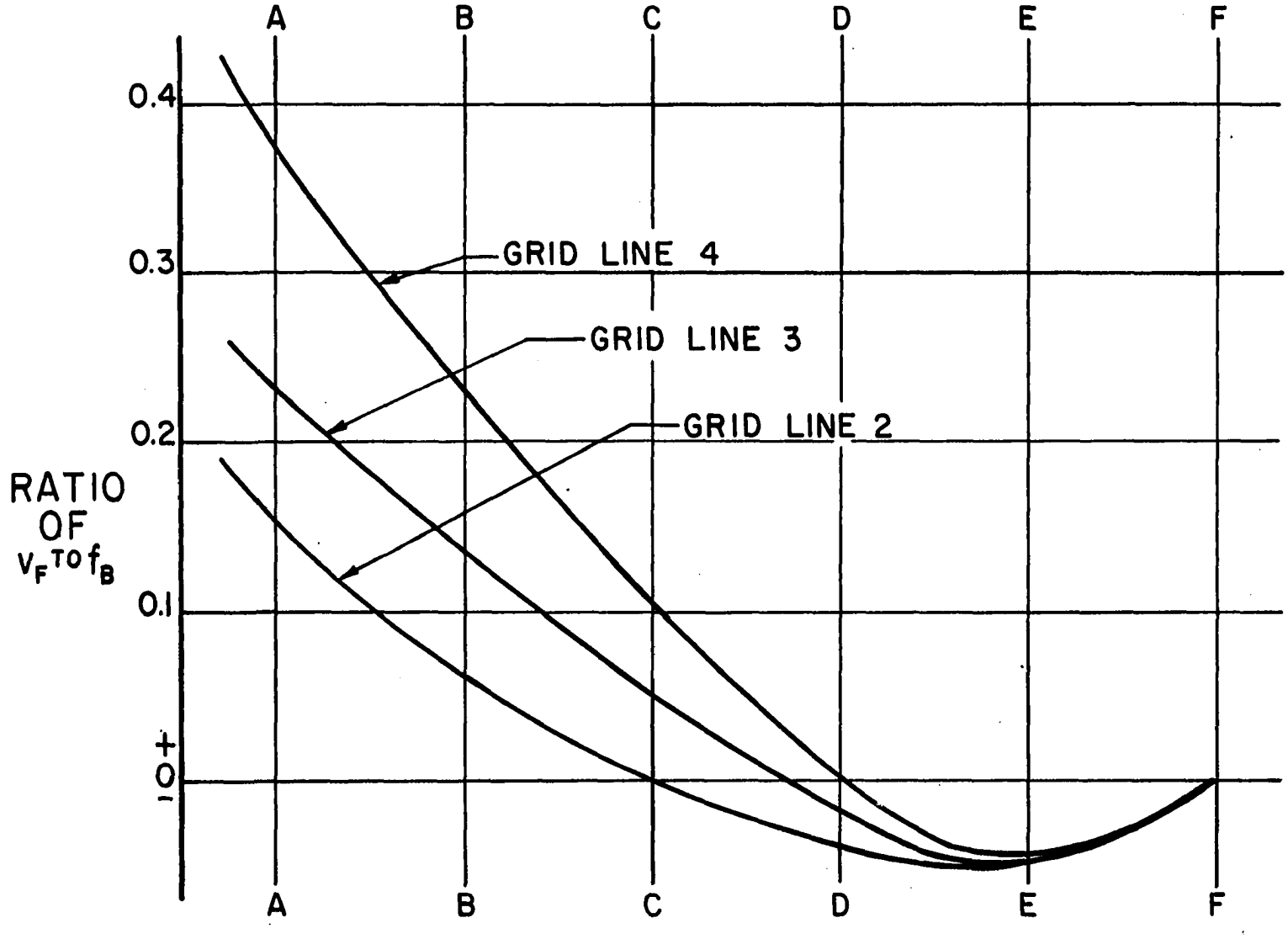

FIGURE 12b. SHEARING STRESS (V_F) VARIATION ALONG HORIZONTAL GRID LINES FOR STRAND PATTERN III

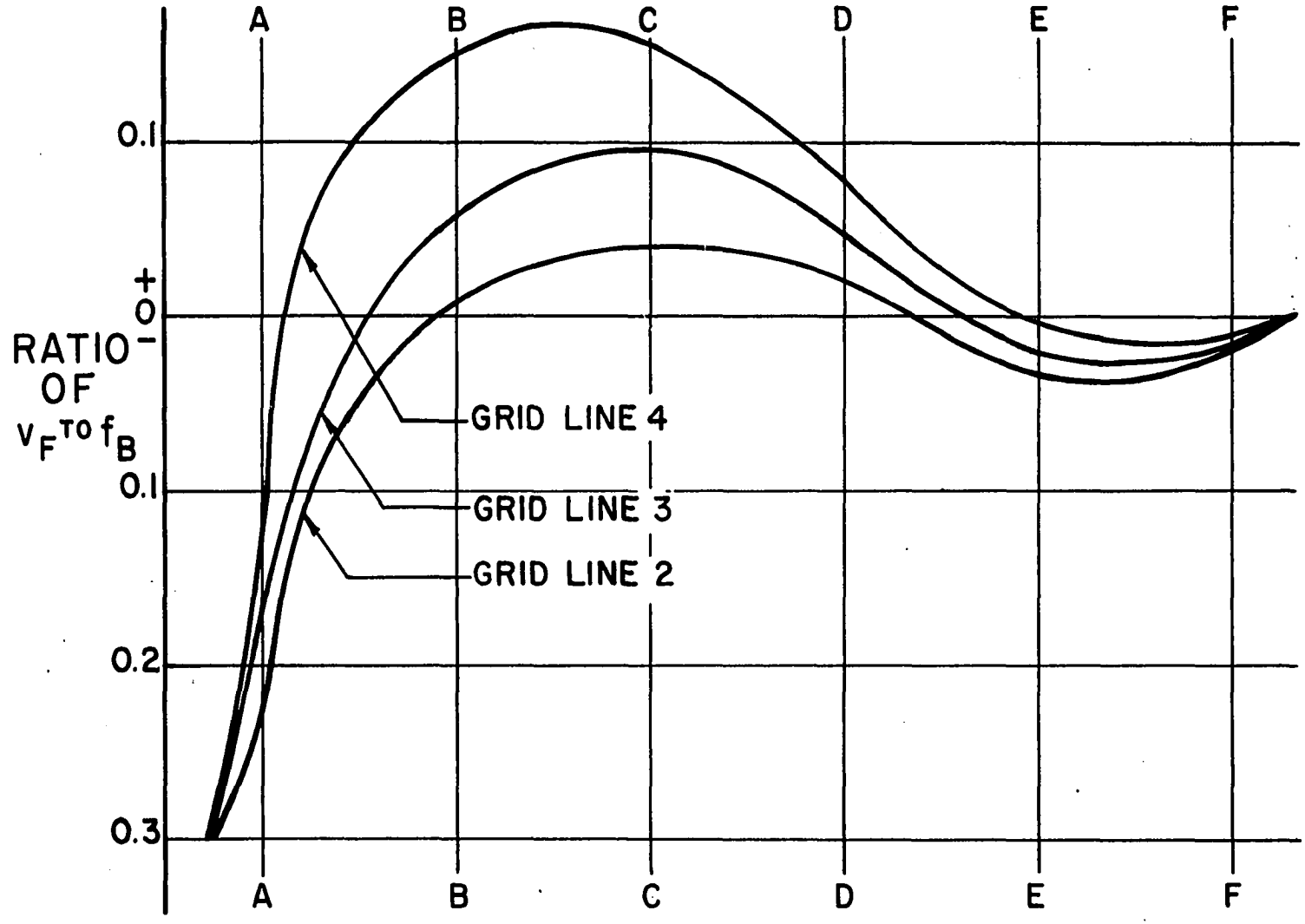

FIGURE 12c. SHEARING STRESS (V_F) VARIATION ALONG HORIZONTAL GRID LINES FOR STRAND PATTERN IV

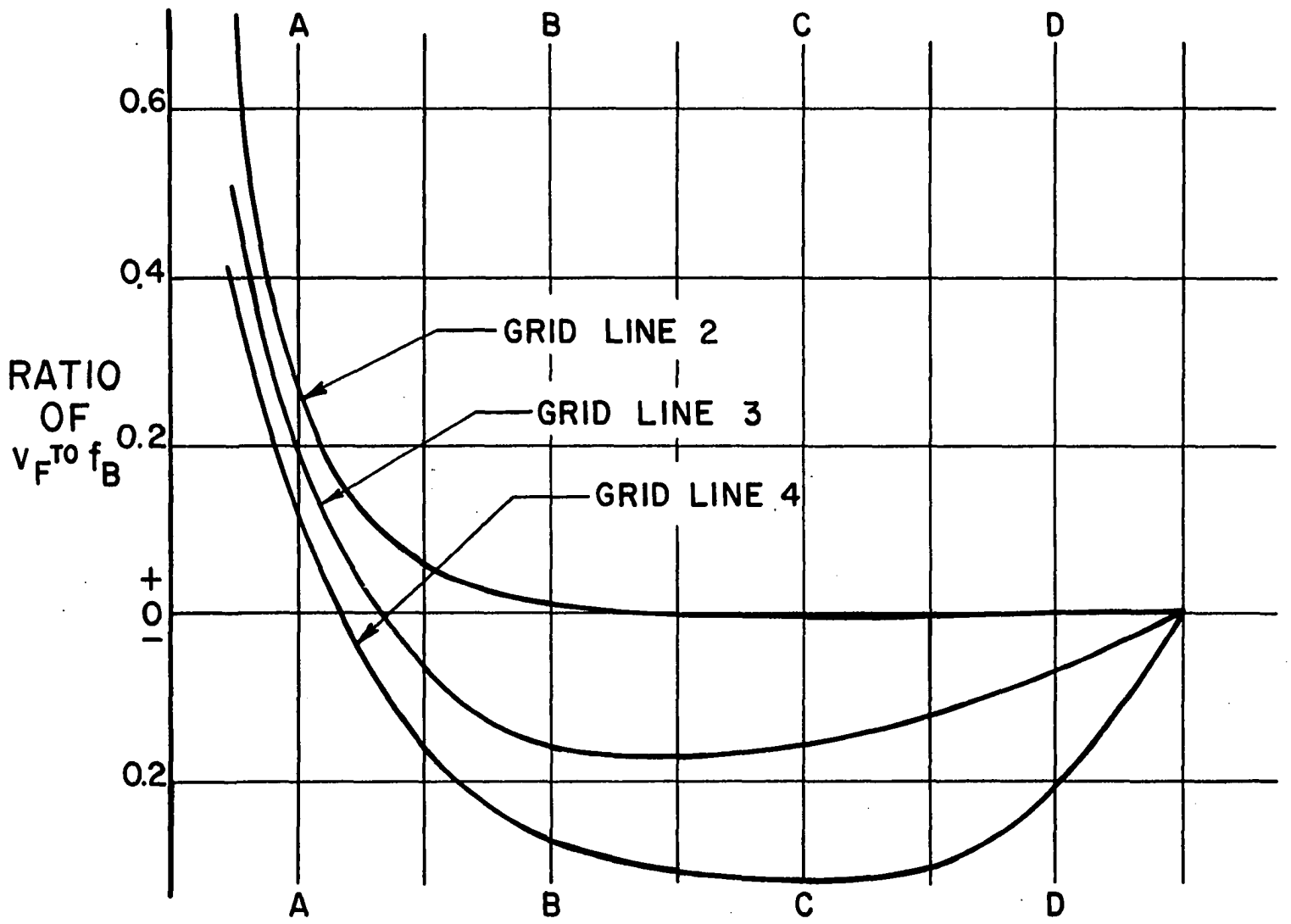

FIGURE 12 d. SHEARING STRESS (V_F) VARIATION ALONG HORIZONTAL GRID LINES FOR STRAND PATTERN VI

Table 1. Values of C_1

$v_F = C_1 f_B$

Grid point	Patterns I and II	Pattern III	Pattern IV	Pattern VI
A-2	+0.112	+0.155	-0.175	+0.200
3	+0.192	+0.230	-0.225	+0.200
4	+0.350	+0.375	-0.125	+0.225
B-2	+0.010	+0.062	+0.008	+0.018
3	+0.085	+0.135	+0.055	-0.130
4	+0.177	+0.225	+0.150	-0.268
C-2	-0.050	0.000	+0.040	+0.005
3	0.000	+0.050	+0.098	-0.170
4	+0.055	+0.102	+0.155	-0.320
D-2	-0.090	-0.038	+0.020	0.000
3	-0.073	-0.018	+0.048	-0.090
4	-0.060	0.000	+0.078	-0.200
E-2	-0.085	-0.048	-0.035	0.000
3	-0.085	-0.045	-0.022	0.000
4	-0.075	-0.040	-0.005	0.000

Table 2. Values of C_2

$f_{F_y} = C_2 f_B$

Grid point	Pattern I	Pattern II	Pattern III	Pattern IV	Pattern VI
A-2	-0.0670	-0.0192	+0.0027	-0.0700	+0.0214
3	-0.0660	-0.0167	+0.0573	-0.0811	+0.0368
4	-0.0094	+0.0400	+0.1682	-0.0386	+0.0030
B-2	+0.0135	+0.0039	-0.0005	+0.0141	-0.0043
3	+0.0133	+0.0034	-0.0115	+0.0163	-0.0074
4	+0.0019	-0.0081	-0.0337	+0.0078	-0.0006
C-2	+0.0344	+0.0099	-0.0014	+0.0360	-0.0110
3	+0.0339	+0.0086	-0.0294	+0.0416	-0.0189
4	+0.0049	-0.0205	-0.0859	+0.0199	-0.0015
D-2	+0.0223	+0.0064	-0.0009	+0.0233	-0.0071
3	+0.0220	+0.0056	-0.0191	+0.0270	-0.0122
4	+0.0032	-0.0133	-0.0557	+0.0129	-0.0010
E-2	+0.0036	+0.0010	-0.0001	+0.0037	-0.0011
3	+0.0035	+0.0009	-0.0030	+0.0043	-0.0020
4	+0.0005	-0.0021	-0.0089	+0.0021	-0.0002

presented by Timoshenko (21) concerning the effects of a concentrated force at a point of a straight boundary. With reference to Figure 13, the load, P, is distributed uniformly along the thickness of the plate. Since the thickness of the plate is taken as unity, P is the load per unit thickness. The stress function which represents the stress distribution is of the form:

$$\phi_1 = \frac{P}{\pi} r\beta\sin\beta \tag{10}$$

Therefore, the only stress which is produced at a point in the material is a radial stress given by:

$$\sigma_r = \frac{2P}{\pi} \frac{\cos\beta}{r} \tag{11}$$

The circumferencial stress, σ_θ, and the shearing stress, $\gamma_{r\theta}$, are 0. The stresses produced on horizontal and vertical planes are given by:

$$\sigma_y = \frac{2P}{\pi a} \cos^4\beta \tag{12}$$

$$\sigma_x = \frac{2P}{\pi a} \sin^2\beta\cos^2\beta \tag{13}$$

$$\gamma_{xy} = \frac{2P}{\pi a} \sin\beta\cos^3\beta \tag{14}$$

The limitations imposed by the derivation of the equations should be recognized before modifications are made to permit application to the test beams. The derivations are made on the basis that the plate is infinitely large and has a constant thickness. Consider first the constant thickness. In an I-beam, the web normally carries the major

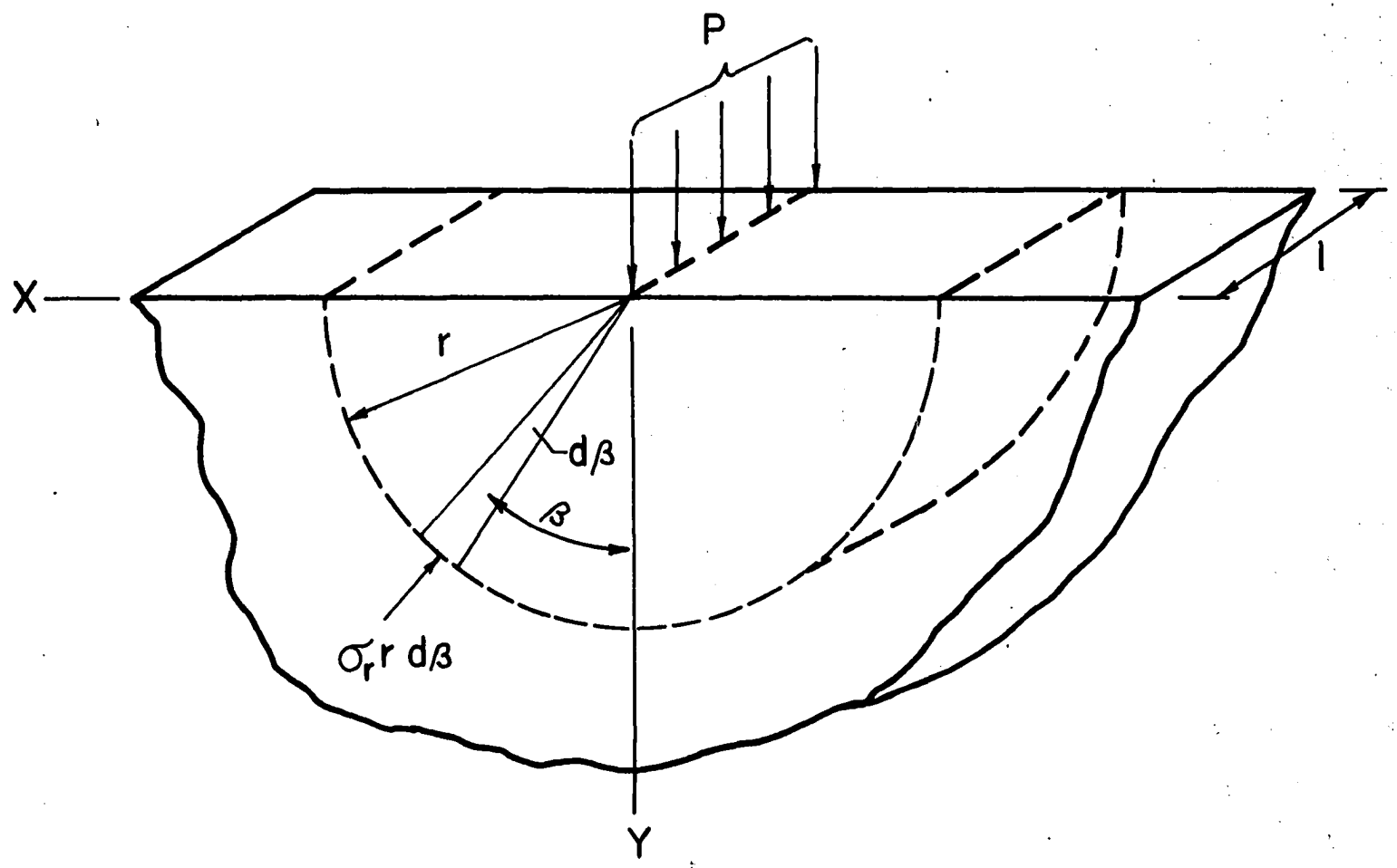

FIGURE 13. LOCAL EFFECT DEFINED BY STRESS FUNCTION ϕ_1

part of a shearing force. If the shearing stress distribution due to cross shear is considered, a rectangular part of the cross-section, bounded by the top and bottom surfaces of the beam and the edges of the web portion, carries 77.5% of the shear. Therefore, it was assumed that 77.5% of a concentrated load applied to the test beam would be effective in producing local stresses in the web in the vicinity of the load. Next, consider the infinite size stipulation. The bottom surface of the beam creates a finite boundary to the material, but since the stresses produced by the force diminish rapidly as the distance from the point of application increases, it was considered that the expressions apply to the rectangular section described. Thus, P is taken as:

$$P = \frac{(V_c)(0.775)}{b'} = (0.193)(V_c) \tag{15}$$

The modified equations are of the form:

$$f_{C_y} = \frac{(0.386)(V_c)}{\pi a} \cos^4\beta \tag{16}$$

$$f_{C_x} = \frac{(0.386)(V_c)}{\pi a} \sin^2\beta\cos^2\beta \tag{17}$$

$$v_C = \frac{(0.386)(V_c)}{\pi a} \sin\beta\cos^3\beta \tag{18}$$

Since the local effect diminishes rapidly, the effect was considered for a distance of 18 inches on either side of a concentrated load. Thus, the equations 16, 17, and 18 can be applied at all load points and at all end reactions which act at or between cross-section C and mid-span of a

test beam. Coefficients useful in solution of equations 16, 17, and 18 can be found in Figure 14.

For end reactions at cross-section A, another solution was required. Consider Figure 15. The stress function which represents the stress distribution for this case is:

$$\phi_2 = \frac{(0.707)Pa}{A_o \cos\beta} \left[\beta\frac{\pi}{2}\sin\beta + 2\left(\frac{\pi}{4}\right)^2\cos\beta + \beta\cos\beta + \frac{\pi}{4}\sin\beta \right] \tag{19}$$

The term A_o is given by:

$$A_o = 2\left[\left(\frac{\pi}{4}\right)^2 - \left(\frac{1}{2}\right)^2\right] \tag{20}$$

The normal and shearing stresses produced on horizontal and vertical planes are given by:

$$f_{C_y} = \frac{(0.386)(V_c)}{A_o a} \left[\frac{\pi}{2}\cos^4\beta - \sin\beta\cos^3\beta\right] \tag{21}$$

$$f_{C_x} = \frac{(0.386)(V_c)}{A_o a} \left[\frac{\pi}{2}\cos^2\beta\sin^2\beta - \sin^3\beta\cos\beta\right] \tag{22}$$

$$v_C = \frac{(0.386)(V_c)}{A_o a} \left[\frac{\pi}{2}\cos^3\beta\sin\beta - \sin^2\beta\cos^2\beta\right] \tag{23}$$

Equations 21, 22, and 23 were used to determine the local effects produced by an end reaction at cross-section A. It was assumed that the 3-inch overhang did not measurably influence the derived effect of the end reaction. Coefficients useful in solution of equations 21, 22, and 23 can be found in Figure 16.

After evaluating the various effects responsible for producing

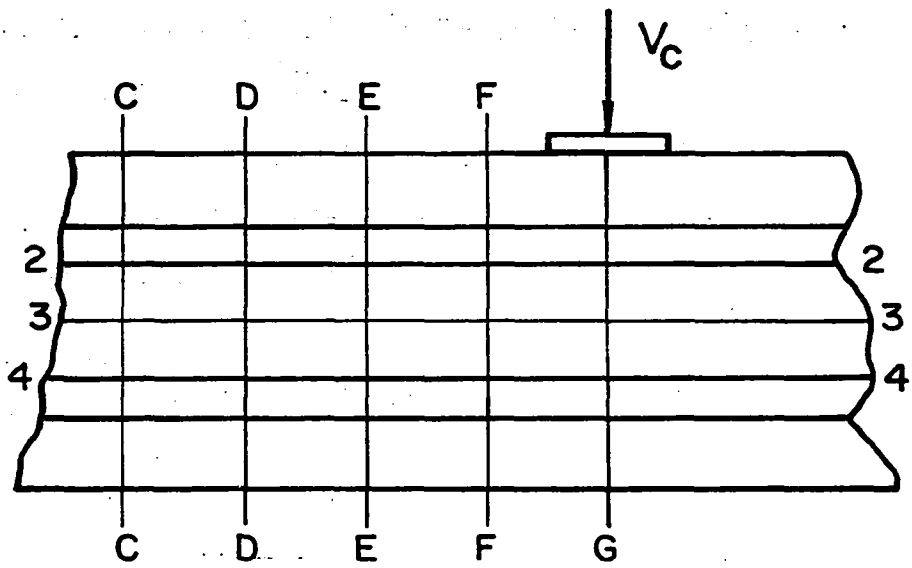

$$f_{Cy} = K_0 (0.193 V_C)$$

$$f_{Cx} = K_1 (0.193 V_C)$$

$$V_C = K_2 (0.193 V_C)$$

	K_0	K_1	K_2
G – 4	+0.0519	0	0
3	+0.0707	0	0
2	+0.1105	0	0
F – 4	+0.0337	+0.0081	+0.0165
3	+0.0339	+0.0150	+0.0226
2	+0.0253	+0.0276	+0.0265
E – 4	+0.0135	+0.0130	+0.0132
3	+0.0092	+0.0163	+0.0122
2	+0.0039	+0.0168	+0.0081
D – 4	+0.0052	+0.0112	+0.0008
3	+0.0028	+0.0113	+0.0057
2	+0.0007	+0.0079	+0.0023

FIGURE 14. COEFFICIENTS USED TO DETERMINE LOCAL EFFECT DEFINED BY ϕ_1

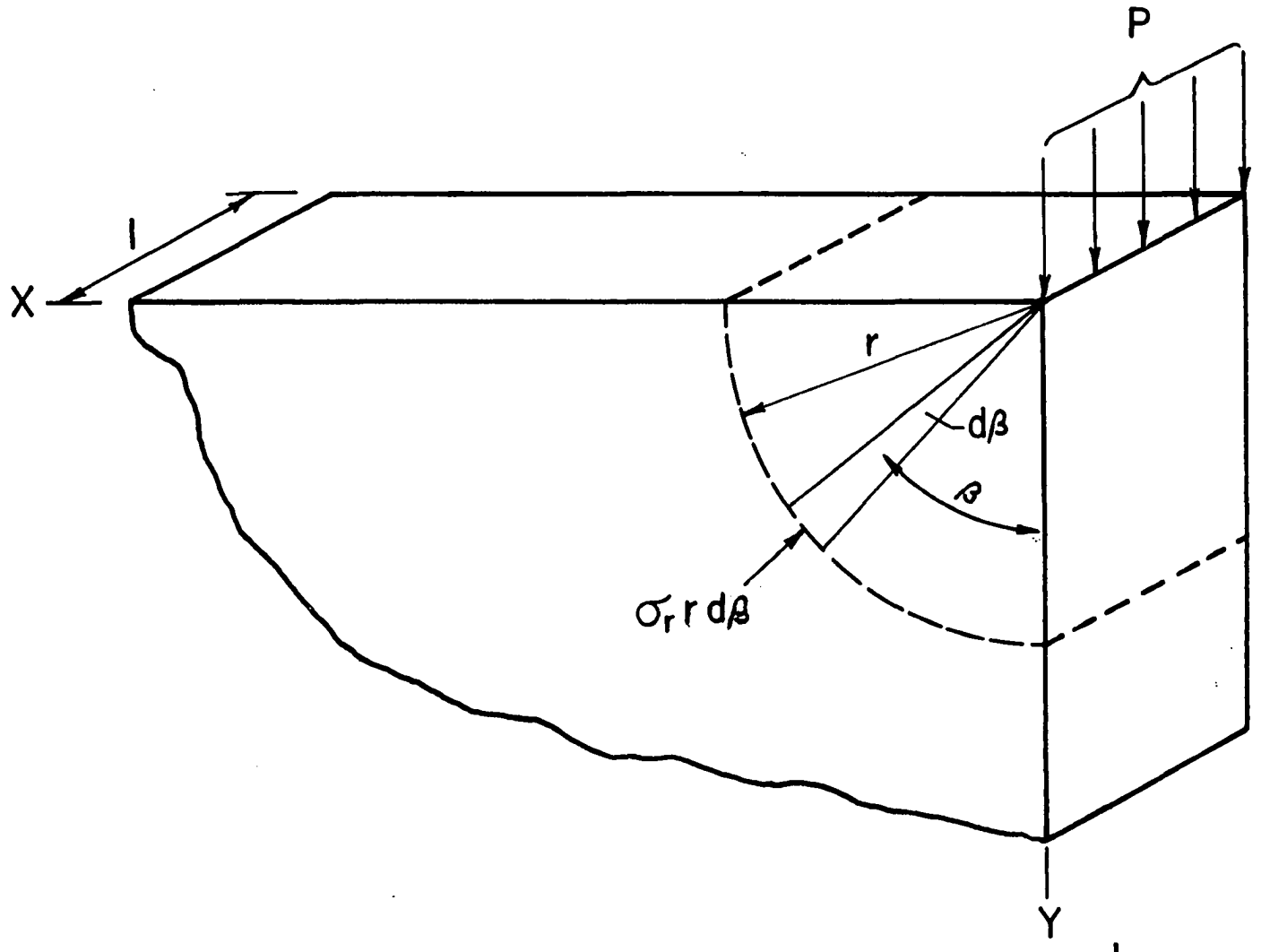

FIGURE 15. LOCAL EFFECT DEFINED BY STRESS FUNCTION ϕ_2

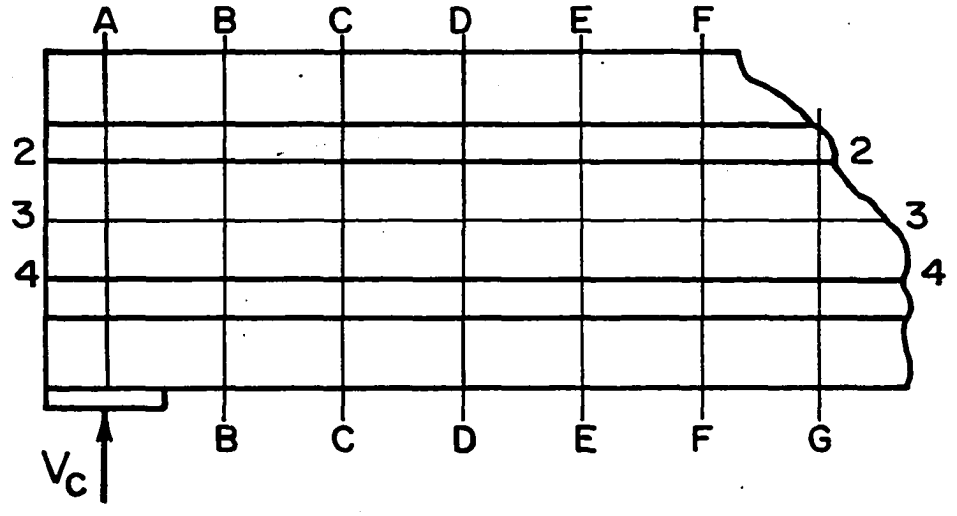

$$f_{cy} = K_3 \ (0.193 V_C)$$

$$f_{cx} = K_4 \ (0.193 V_C)$$

$$V_C = K_5 \ (0.193 V_C)$$

	K_3	K_4	K_5
A – 2	+0.174	0	0
3	+0.238	0	0
4	+0.372	0	0
B – 2	+0.078	+0.019	+0.038
3	+0.066	+0.029	+0.044
4	+0.028	+0.031	+0.030
C – 2	+0.017	+0.016	+0.017
3	+0.005	+0.008	+0.006
4	−0.004	−0.018	−0.009
D – 2	+0.016	+0.002	−0.021
3	−0.003	−0.011	−0.005
4	−0.003	−0.032	−0.009

FIGURE 16. COEFFICIENTS USED TO DETERMINE LOCAL EFFECT DEFINED BY ϕ_2

stresses in the beams, the stresses S_x, S_y, and S_s were determined at each grid point by adding, algebraically, the normal and shearing stresses produced by each of the effects. The principal stresses, S_c and S_t, and the angle θ were then computed from equations 1, 2, and 3.

RESULTS AND DISCUSSION

Results

Test beams

The stress f_B and the prestress loss for each of the test beams were computed in the following manner.

1. The value of the tensile proportional limit of the concrete, f_{PL}, was obtained from load-strain curves for SR-4 gages on the tension side of the flexure specimens.
2. P_o was taken as the load at the end of the straight line portion of the load-strain curves for SR-4 gages at the bottom of the test beams. The stress, f_L^b, due to P_o was computed.
3. The value of f_B was computed from

$$f_B = f_L^b - f_{PL}$$

   The determination of f_B is based on the assumption that the actual resultant tensile stress at the bottom of the beam loaded with P_o is equal to the tensile proportional limit obtained from the flexure specimens of the concrete.
4. The initial prestress force was measured for a number of strands in each of the beams. The average of these values was then multiplied by the number of strands to obtain the total prestress force, F_i. Measured values used to obtain the initial prestress force are shown in Table 3.
5. The prestress stress f_{Bi} was computed, using the actual

Table 3. Determination of values of F_i

Beams	Force in load cell	Avg. force k	F_i k	Beams	Force in load cell	Avg. force k	F_i k
1-2	14.9			17-18	14.2		
	14.9				14.4		
	14.8				14.4		
	15.3	15.0	165.0		-	14.3	114.4
3-4	14.3			19-20	13.9		
	14.1				14.2		
	14.3				14.3		
	14.6	14.3	157.3		-	14.1	155.1
5-6	14.3			21-22	13.4		
	14.0				13.6		
	14.4				13.5		
	14.4	14.3	157.3		-	13.5	148.5
7-8	14.5			23-24	13.7		
	13.9				13.7		
	14.2				13.6		
	14.7	14.3	157.3		13.7	13.7	150.7
9-10	14.5			25-26	14.2		
	14.2				14.2		
	14.5				13.8		
	14.5	14.4	158.4		14.1	14.1	155.0
11-12	13.7			27-28-29	13.8		
	13.1				14.0		
	13.7				13.8		
	13.4	13.5	108.0		14.5	14.0	154.0
13-14	12.4			30-31	13.9		
	13.2				13.7		
	13.3				13.9		
	-	13.0	65.0		14.4	14.0	154.0
15-16	14.3			32-33	14.0		
	14.0				13.6		
	14.1				14.0		
	14.0	14.1	141.0		13.6	13.8	151.8

value of the prestress force from step 4.

6. The stress loss at the bottom of the beam was computed as

$$\text{Loss} = f_{Bi} - f_B$$

The loss was expressed as a percentage of f_{Bi}.

As an example, consider the computations for test beam 1. Four of the seven load-strain curves for gages at the bottom of the beam are shown in Figure 17. The applied load which produced f_{PL} at the bottom of the beam was taken from the load-strain curves as 70 kips. In the load-strain curves shown in Figure 17, two of the gages show a deviation at 70 kips while the others continue linearly to a higher load. For all of the test beams, it was common for several of the gages to indicate the same load at the end of the straight line portion. This load was normally the lowest load at which the straight line portion ended, and was taken as the applied load in computing f_L^b. In beam 1, the stress f_L^b produced by the 70-kip load was computed to be -2560 psi. The stress-strain curves for the flexure specimens for beam 1 are shown in Figure 18. The average of the three values of f_{PL} was -370 psi. Therefore, f_B = +2190 psi and the stress loss is 410 psi or 15.8%. Values of the prestressing force, in addition to values of f_{Bi}, f_B, and the prestress loss are given in Table 4 for each of the test beams.

Theoretical analyses were completed for test beams 1, 3-16, and 19-33. Beam 2 was fractured before the load test and will be discussed in a later section. Theoretical analyses were not made for beams 17 and 18 because of cracks which were caused by high initial tensile stresses

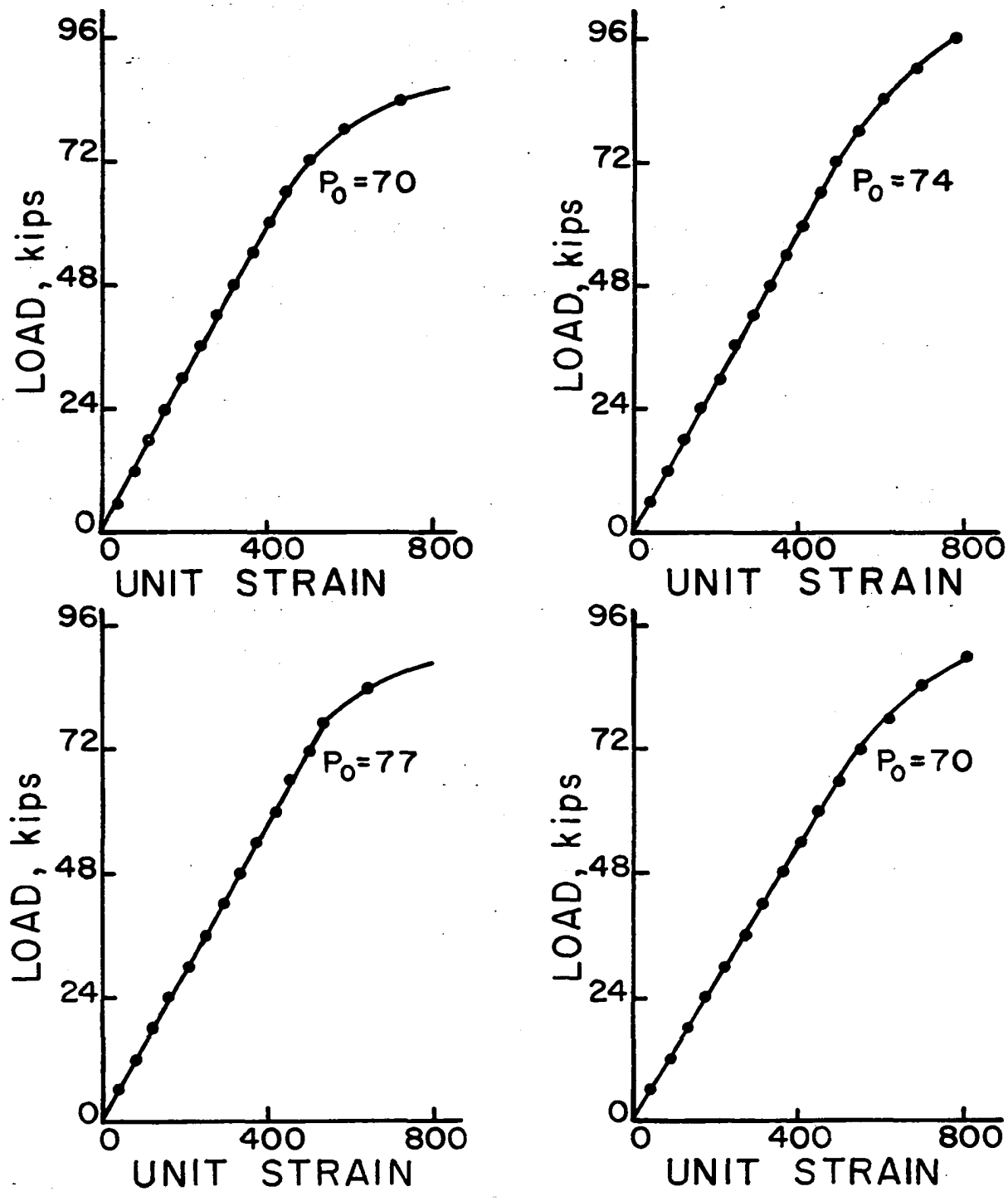

FIGURE 17. TYPICAL LOAD-STRAIN CURVES FOR BOTTOM SR-4 GAGES – BEAM I

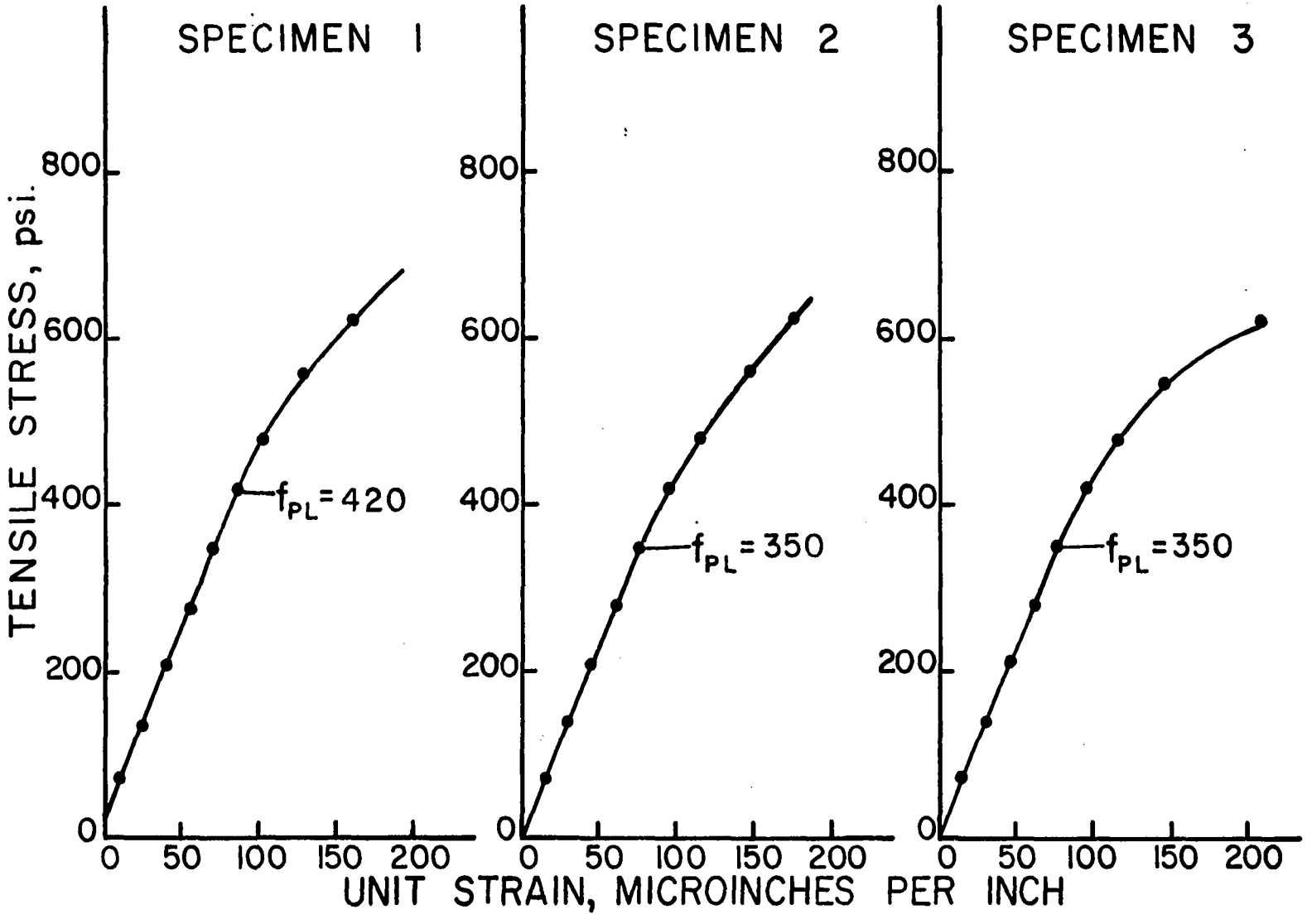

FIGURE 18. STRESS-STRAIN CURVES — FLEXURE SPECIMENS — BEAM I

Table 4. Initial prestress force and selected test results

Beam	F_{se} k	f_{Bi} psi	f_B psi	% Loss	V_c k	V_u k	f'_t psi	π_1	π_2	L_s in.
1	165.0	2600	2190	15.8	37.5	51.0	470	2.00	2.94	36
2	165.0	2600	-	-	-	-	470	-	2.94	36
3	157.3	2480	1890	23.8	37.5	53.0	490	1.92	2.68	36
4	157.3	2480	1860	25.0	43.0	43.0	490	2.19	2.68	36
5	157.3	2480	1830	26.2	32.5	42.5	510	1.59	2.58	36
6	157.3	2480	1760	29.0	38.0	38.0	510	1.86	2.58	36
7	157.3	2480	1800	27.4	39.0	45.0	520	1.86	2.53	36
8	157.3	2480	1800	27.4	37.5	37.5	520	1.80	2.53	36
9	158.4	2490	1680	32.6	31.0	45.0	545	1.43	2.44	36
10	158.4	2490	1760	29.4	35.0	35.0	545	1.61	2.44	36
11	108.0	1685	1240	26.4	39.5	47.0	545	1.69	1.66	36
12	108.0	1685	1240	26.4	40.0	43.5	545	1.72	1.66	36
13	65.0	1060	720	32.0	31.0	55.5	560	1.33	0.97	36
14	65.0	1060	810	23.4	32.5	32.5	560	1.41	0.97	36
15	141.0	2510	1860	25.9	40.0	55.5	570	1.80	2.07	36
16	141.0	2510	1800	28.3	40.0	51.0	570	1.80	2.07	36
17	114.4	2480	1885	24.0	40.0	40.0	590	1.63	1.62	36
18	114.4	2480	1925	22.4	30.0	36.0	590	1.23	1.62	36
19	155.1	2440	1835	24.8	40.0	51.5	495	1.35	2.62	24
20	155.1	2440	1695	30.5	37.5	55.0	495	1.25	2.62	24
21	148.5	2340	1800	23.0	55.0	99.0	505	1.81	2.46	24
22	148.5	2340	1800	23.0	41.5[a]	70.0	505	2.05	2.46	36
23	150.7	2370	1850	22.0	-	90.0+	550	-	2.29	12
24	150.7	2370	1800	24.0	45.0	71.5	550	2.04	2.29	36
25	155.0	2460	1835	25.4	37.5	56.0	535	1.70	2.42	36
26	155.0	2460	1895	23.0	47.5	72.5	535	2.14	2.42	36
27	154.0	2420	1845	23.7	42.0	50.0	510	2.05	2.52	36
28	154.0	2420	1845	23.7	70.0	85.0	510	1.13	2.52	12
29	154.0	2420	1845	23.7	52.5	81.5	510	1.28	2.52	18
30	154.0	2420	1870	22.7	37.5	46.5	525	1.78	2.45	36
31	154.0	2420	1770	26.9	43.5	69.0	525	2.06	2.45	36
32	151.8	2390	1875	21.5	45.0	76.0	520	2.16	2.44	36
33	151.8	2390	1865	22.0	37.0	45.0	520	1.78	2.44	36

[a]At 90.0 k, inclined tension crack had not formed

$$\pi_1 = \frac{V_c L_s}{f_t b d^2 \sqrt{\frac{b'}{b}}} \qquad \pi_2 = \frac{F_{se}}{A_c f'_t}$$

$b = 9$
$b' = 4$
$D = 18$
$A_c = 119.5$

produced by the prestressing at time of release. Stress trajectories which resulted from the theoretical analyses are shown in Figure 19-48. The inclined tension cracks, which formed when the shear strength was reached, are shown, in addition to the principal tensile stresses computed at each of the grid points.

In addition, the results of the load tests are presented in another form. Using the variables considered in Sozen's paper (20), and taking

$$\pi_1 = \frac{V_c L_s}{f_t b d^2 \sqrt{\frac{b'}{b}}} \tag{24}$$

$$\pi_2 = \frac{F_{se}}{A_c f'_t} \tag{25}$$

π_1 is plotted against π_2 as shown in Figure 49. Values of π_1 and π_2 are given in Table 4.

It was found that the information obtained from the deflection data and the SR-4 gages located around the cross-section at mid-span was not necessary in evaluating shear strength of the test beams. Therefore, this information is not presented.

Concrete specimens

Compression cylinders Results of the tests used to evaluate f'_c are given in Table 5.

Flexure specimens The results of the tests performed on the flexure specimens are given in Table 6. An example of the stress-strain curves for the SR-4 gages is shown in Figure 18.

Tension specimens The values of f'_t are given in Table 7.

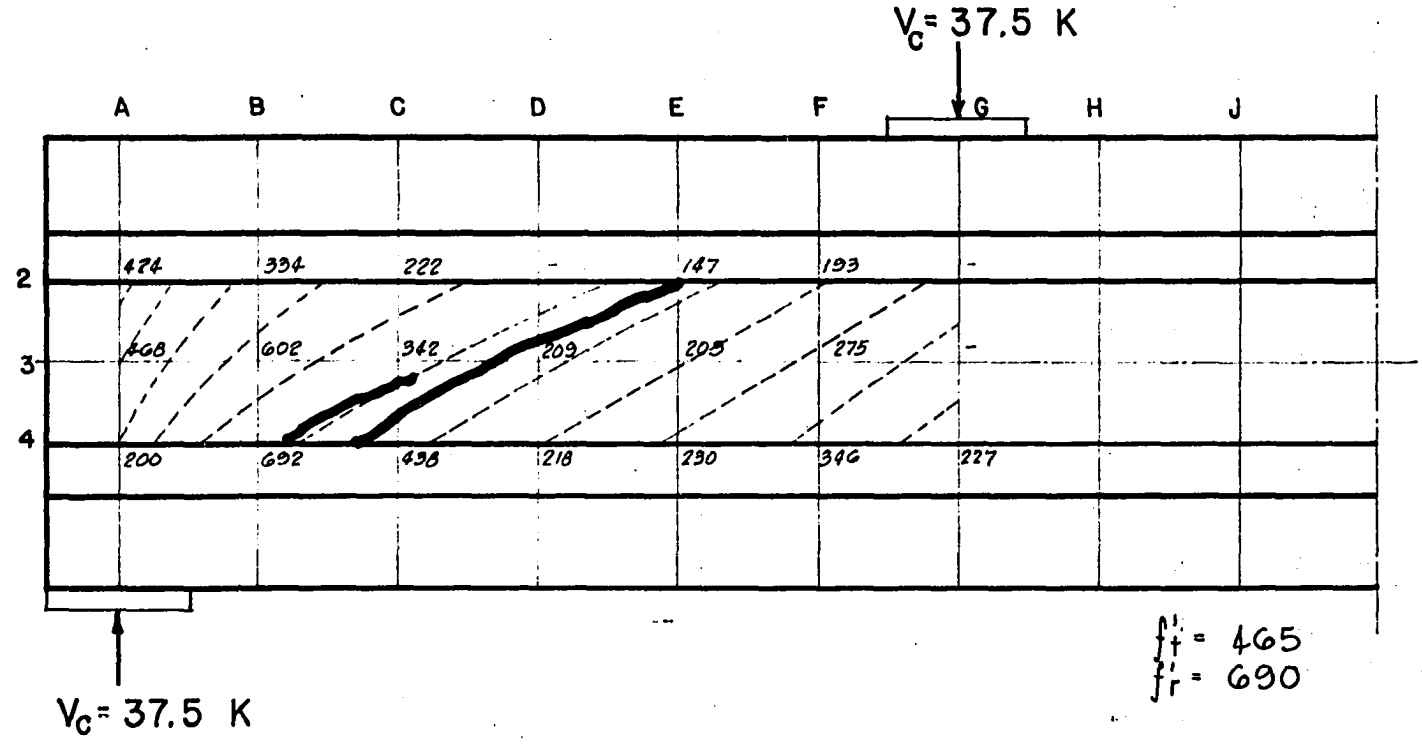

FIGURE 19. STRESS TRAJECTORIES, CRACK PATTERN, AND PRINCIPAL TENSILE STRESSES. BEAM 1

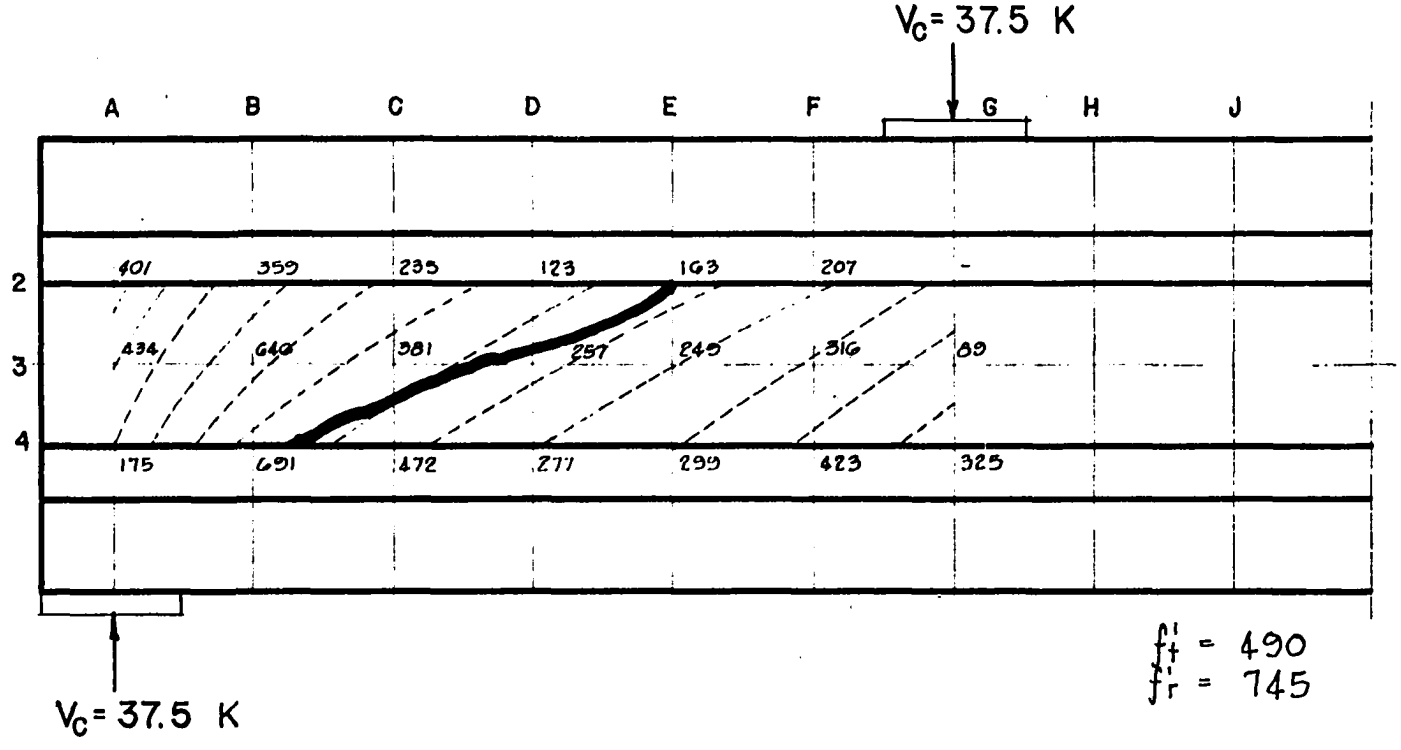

FIGURE 20. STRESS TRAJECTORIES, CRACK PATTERN, AND PRINCIPAL TENSILE STRESSES. BEAM 3

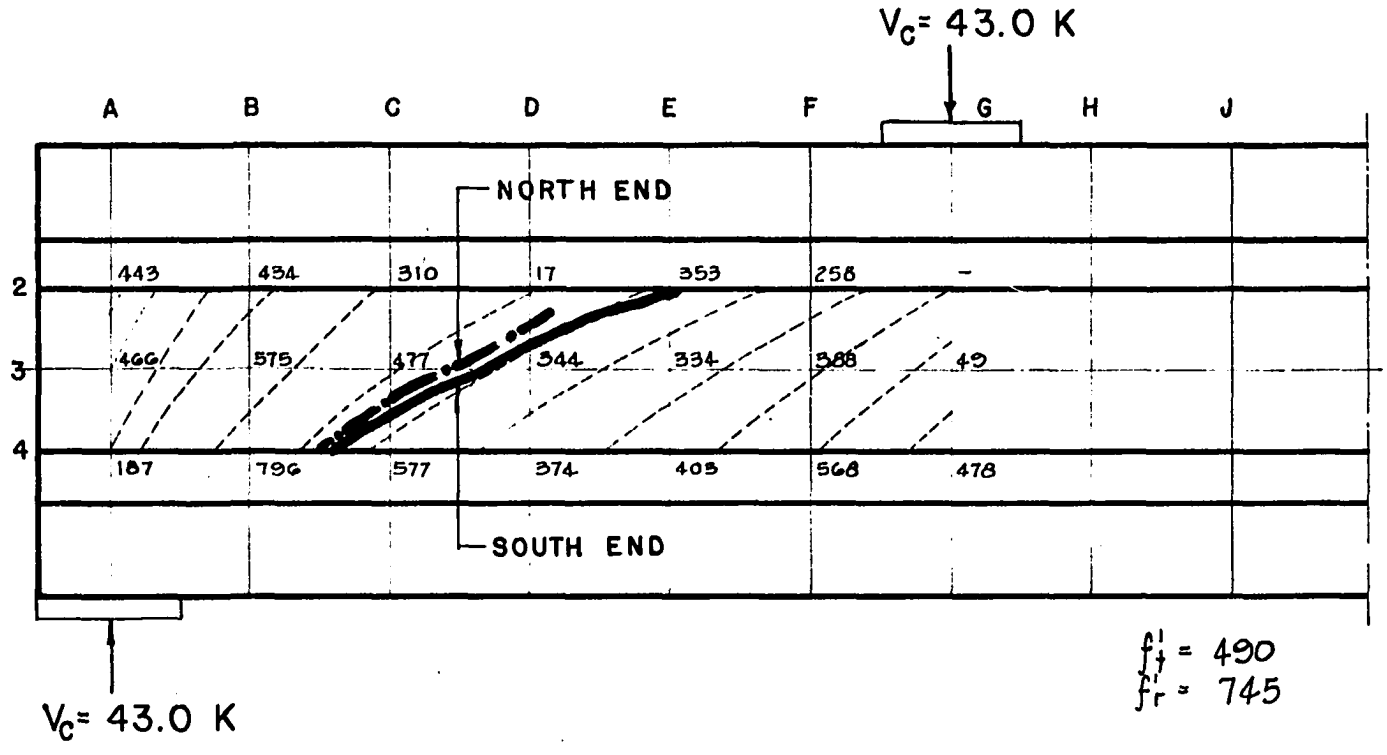

FIGURE 21. STRESS TRAJECTORIES, CRACK PATTERN, AND PRINCIPAL TENSILE STRESSES. BEAM 4

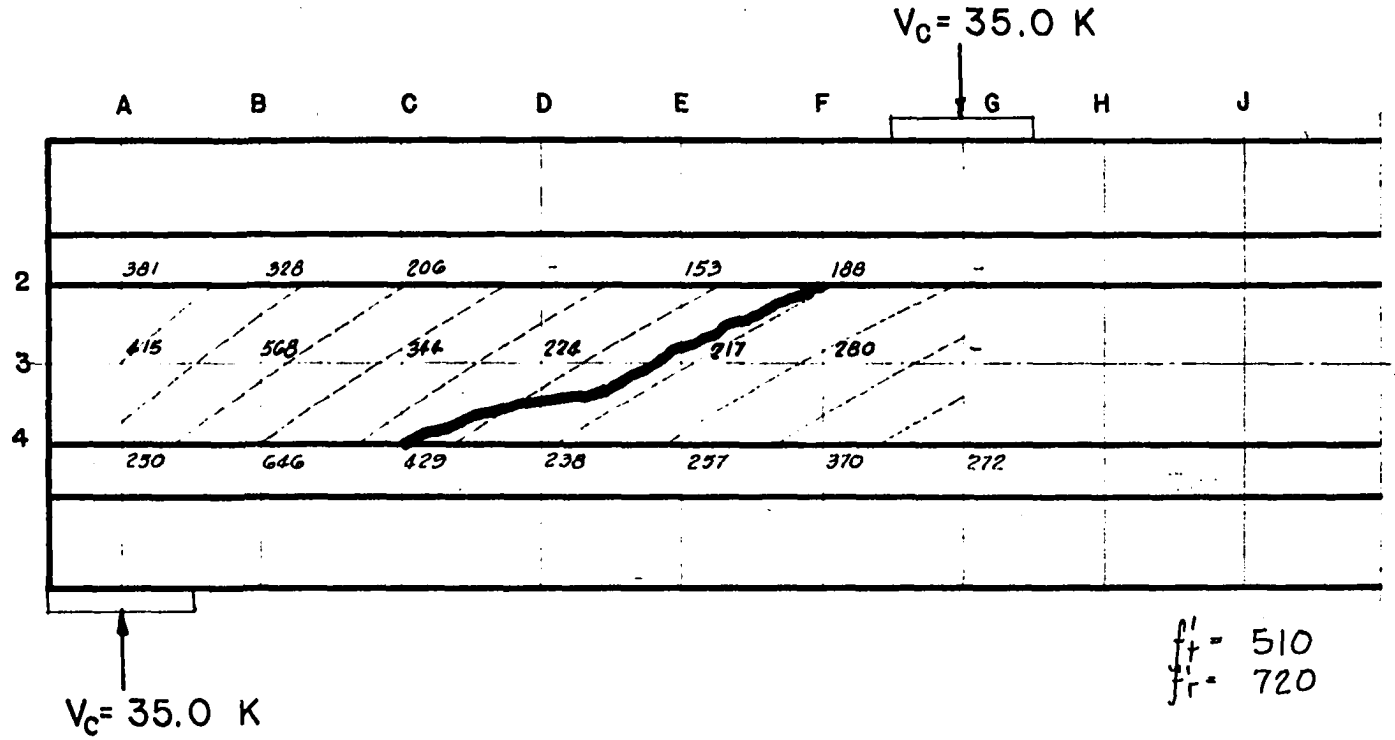

FIGURE 22. STRESS TRAJECTORIES, CRACK PATTERN, AND PRINCIPAL TENSILE STRESSES. BEAM 5

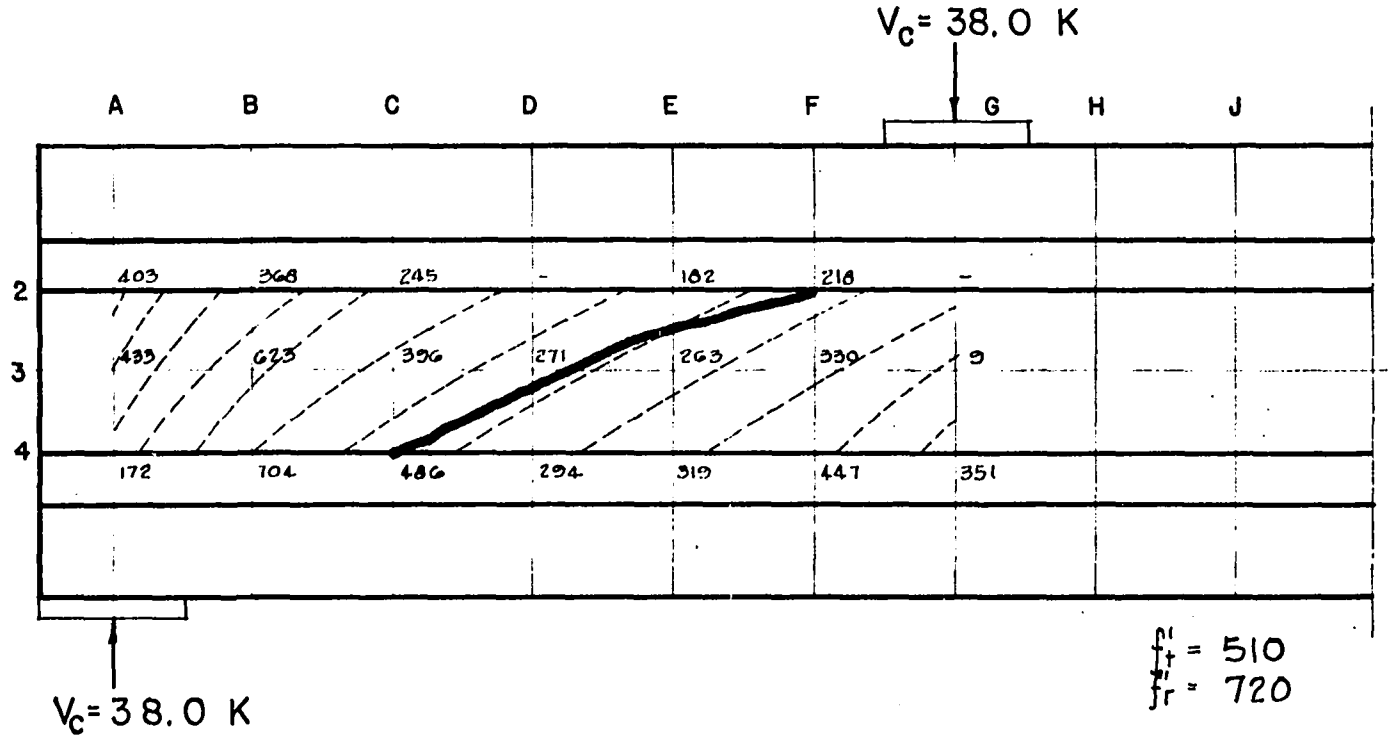

FIGURE 23. STRESS TRAJECTORIES, CRACK PATTERN, AND PRINCIPAL TENSILE STRESSES. BEAM 6

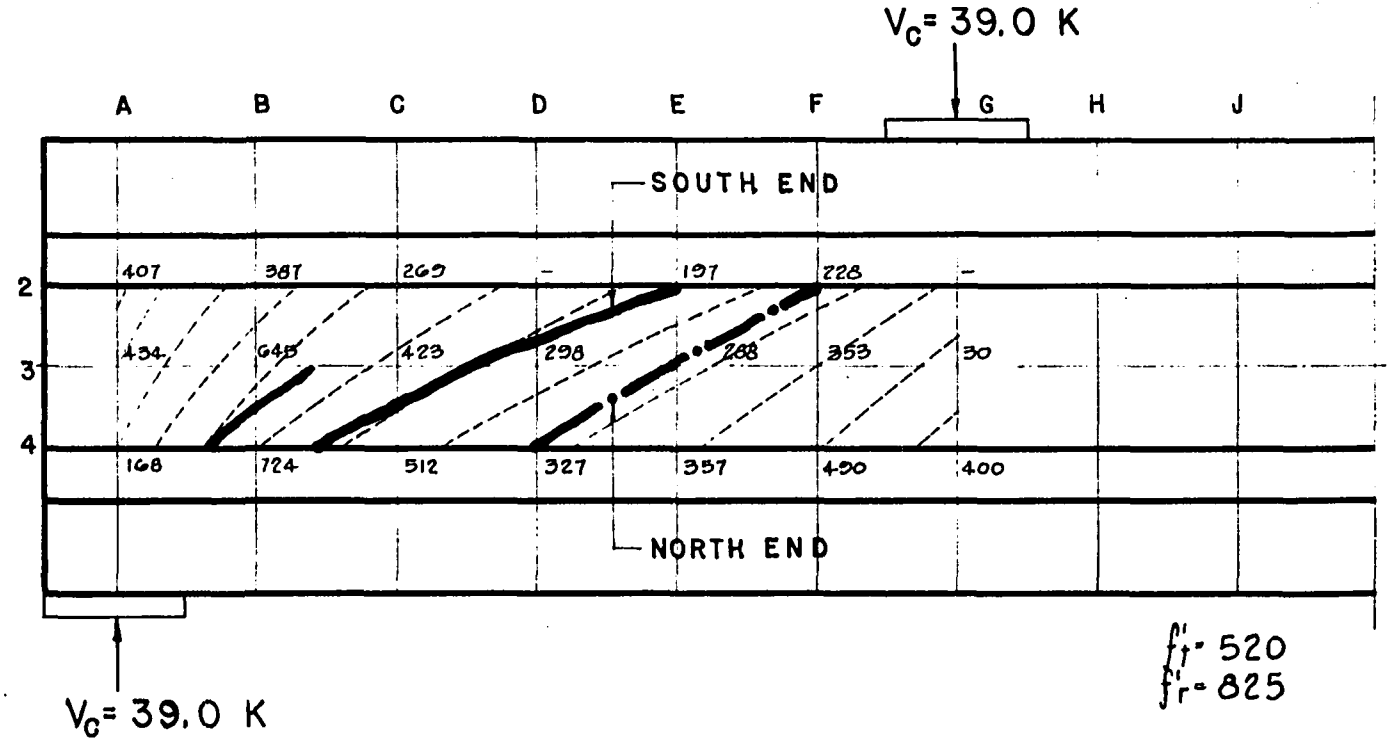

FIGURE 24. STRESS TRAJECTORIES, CRACK PATTERN, AND PRINCIPAL TENSILE STRESSES. BEAM 7

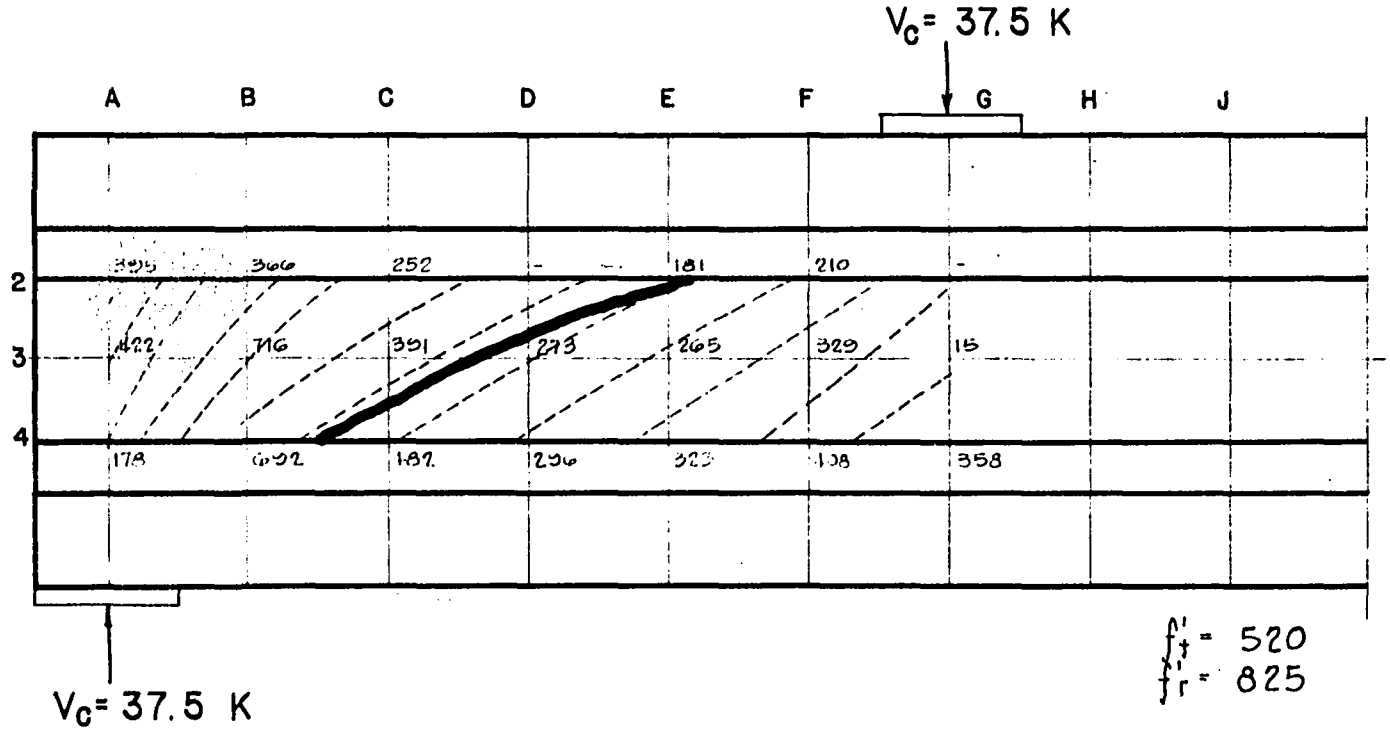

FIGURE 25. STRESS TRAJECTORIES, CRACK PATTERN, AND PRINCIPAL TENSILE STRESSES. BEAM 8

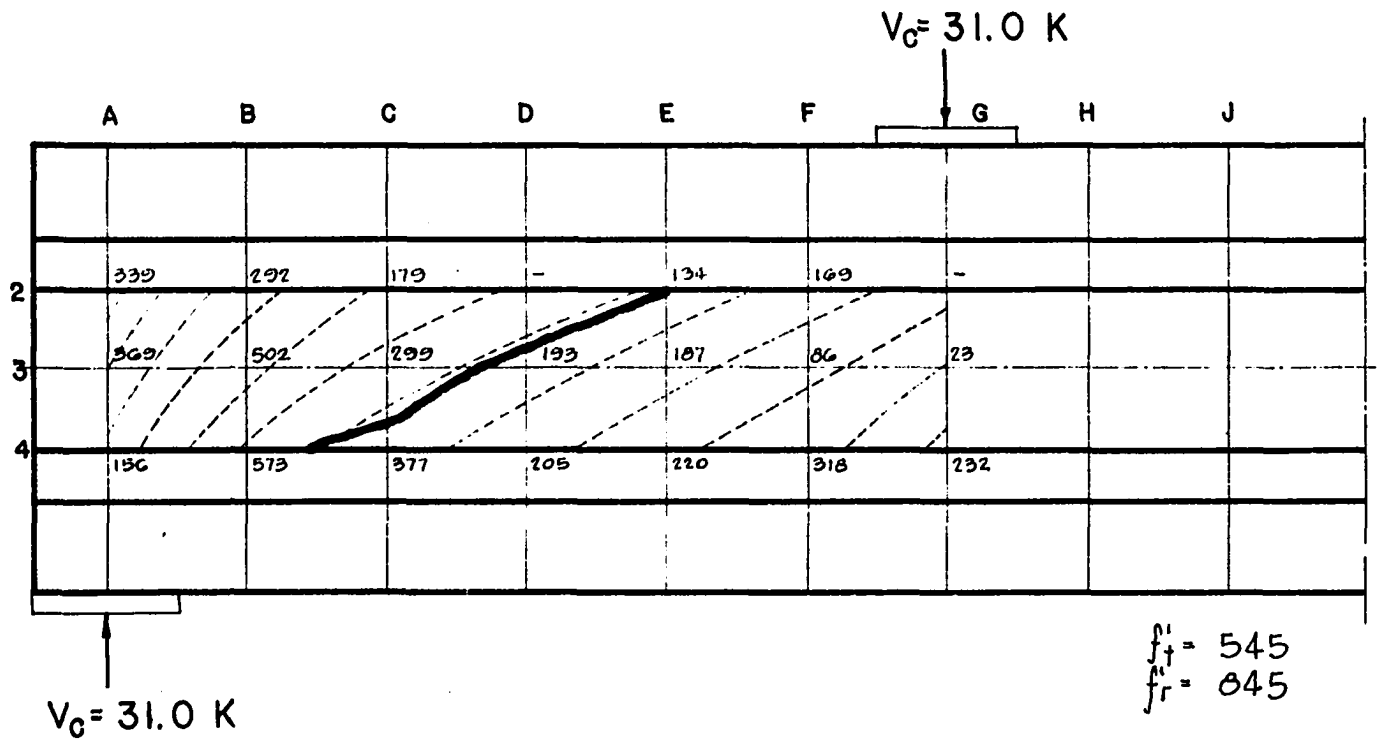

FIGURE 26. STRESS TRAJECTORIES, CRACK PATTERN, AND PRINCIPAL TENSILE STRESSES. BEAM 9

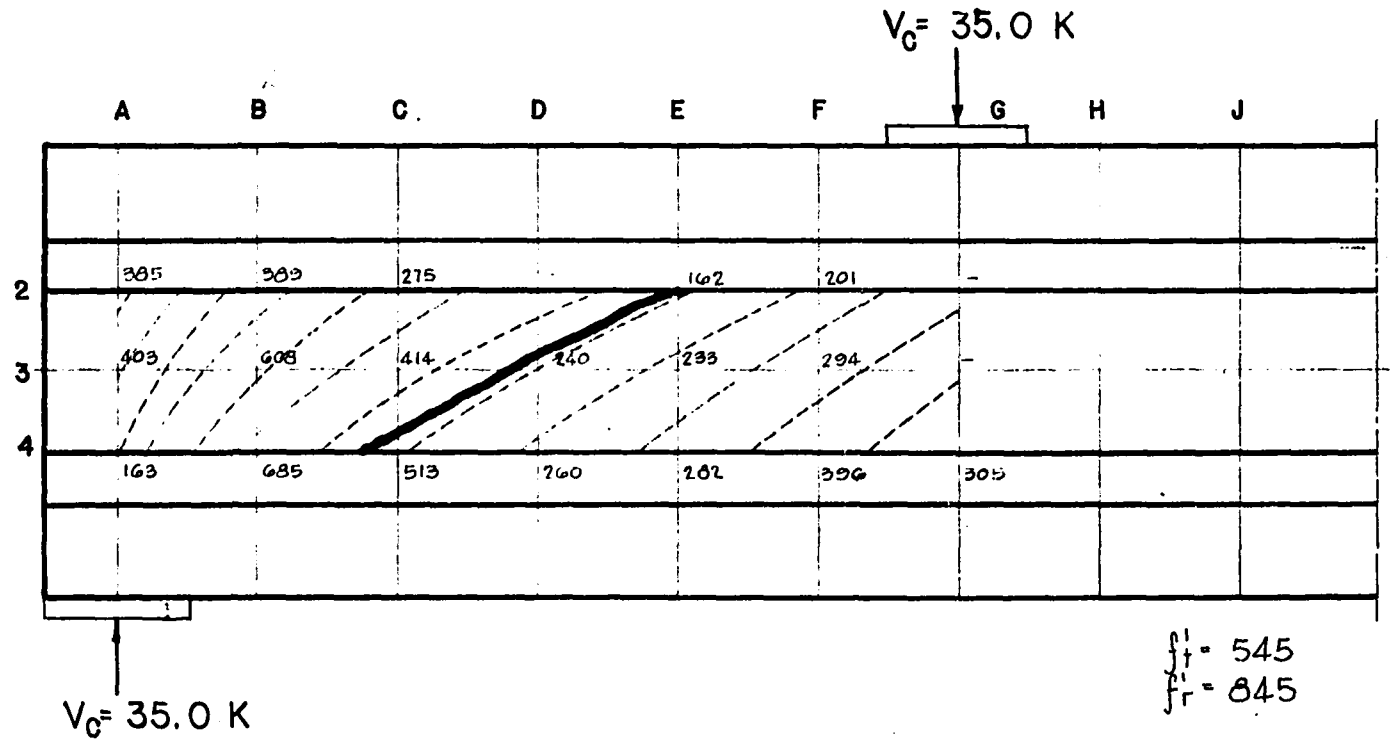

FIGURE 27. STRESS TRAJECTORIES, CRACK PATTERN, AND PRINCIPAL TENSILE STRESSES. BEAM 10

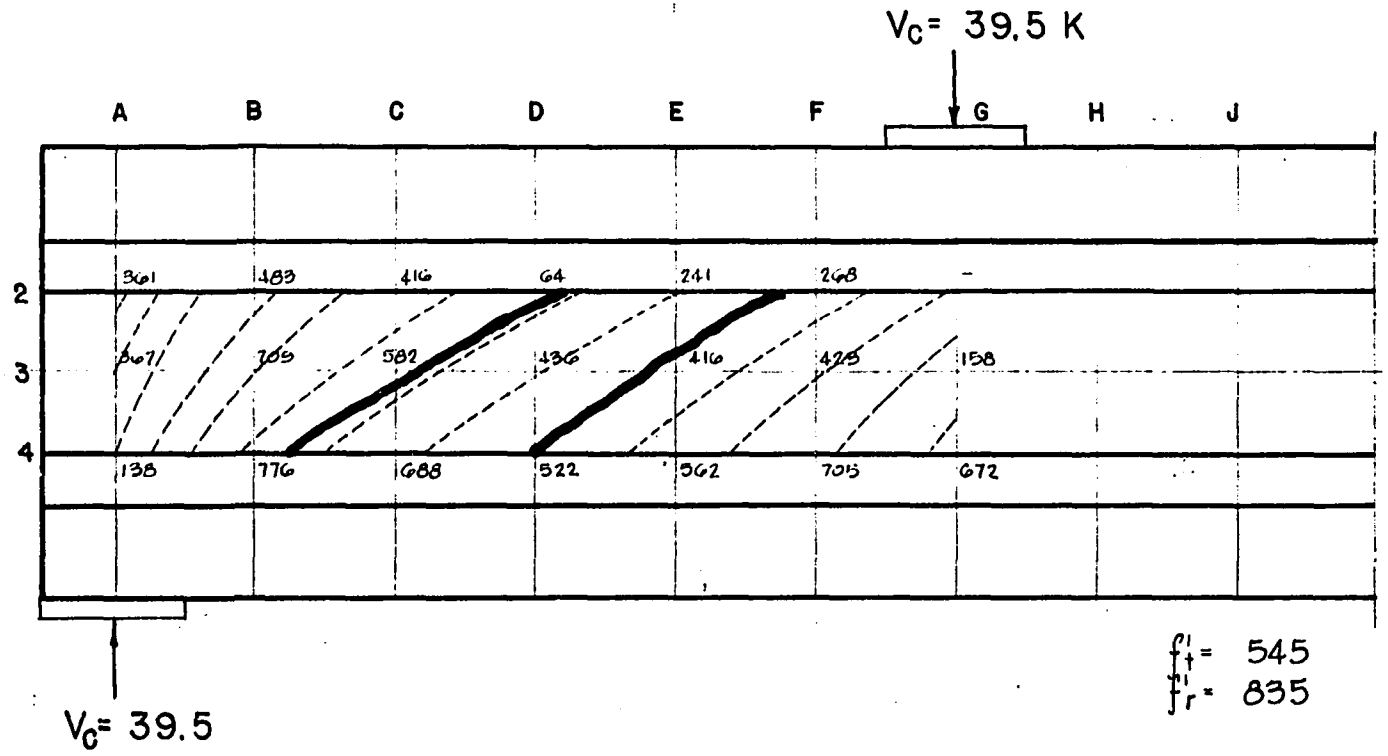

FIGURE 28. STRESS TRAJECTORIES, CRACK PATTERN, AND PRINCIPAL TENSILE STRESSES. BEAM 11

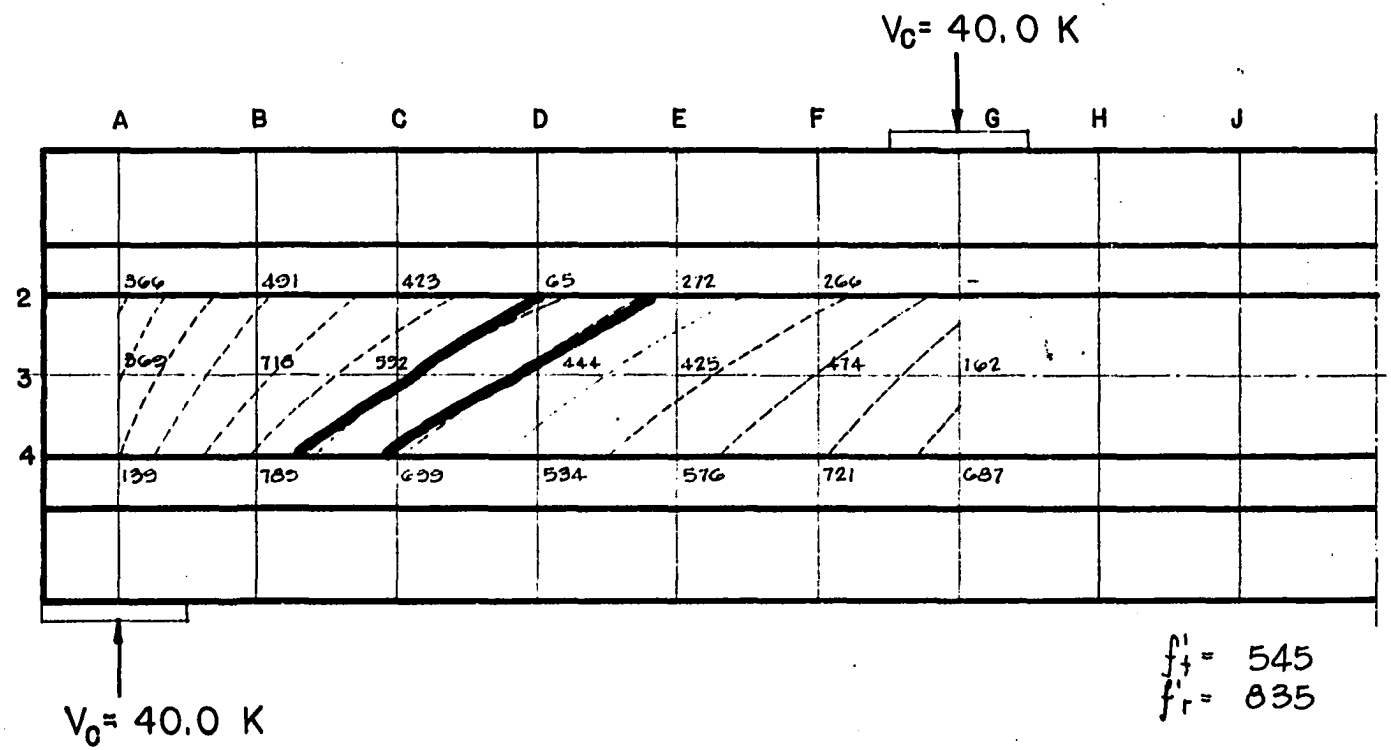

FIGURE 29. STRESS TRAJECTORIES, CRACK PATTERN, AND PRINCIPAL TENSILE STRESSES. BEAM 12

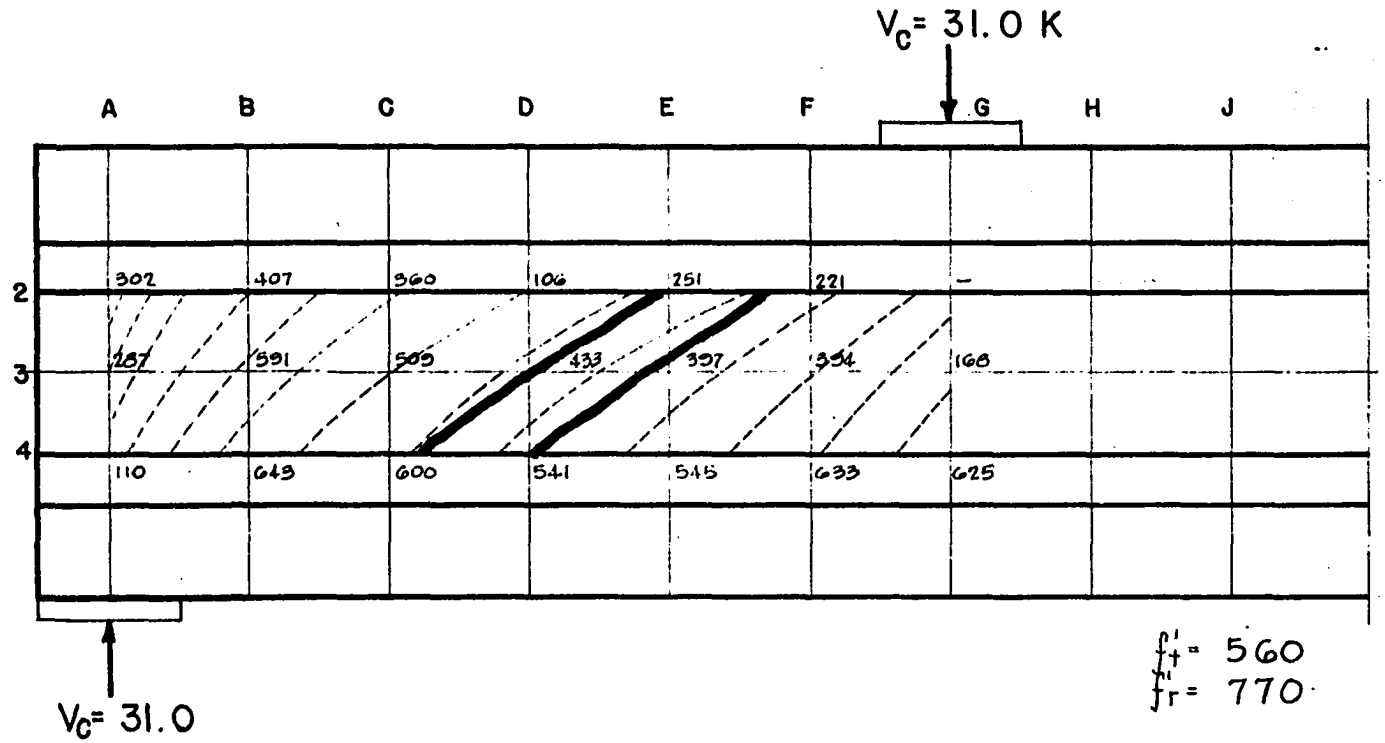

FIGURE 30. STRESS TRAJECTORIES, CRACK PATTERN, AND PRINCIPAL TENSILE STRESSES. BEAM 13

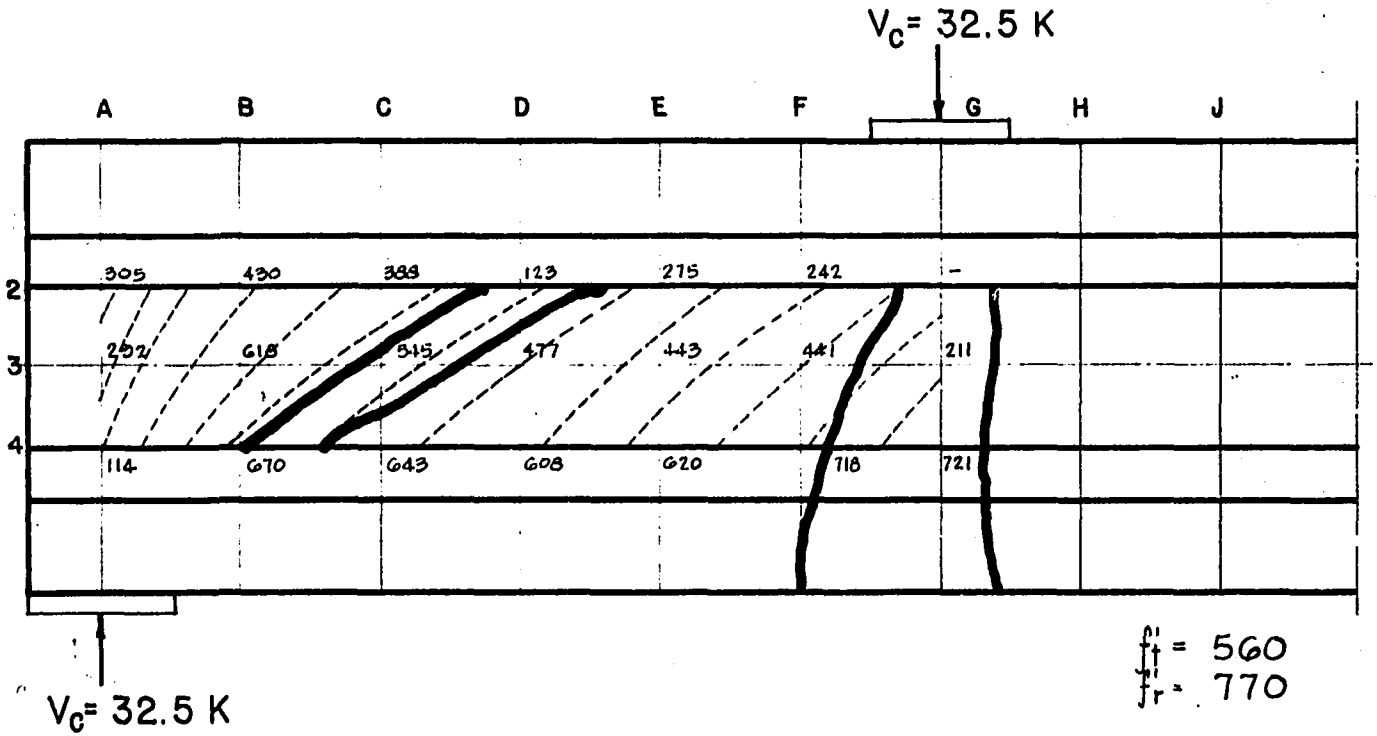

FIGURE 31. STRESS TRAJECTORIES, CRACK PATTERN, AND PRINCIPAL TENSILE STRESSES. BEAM 14

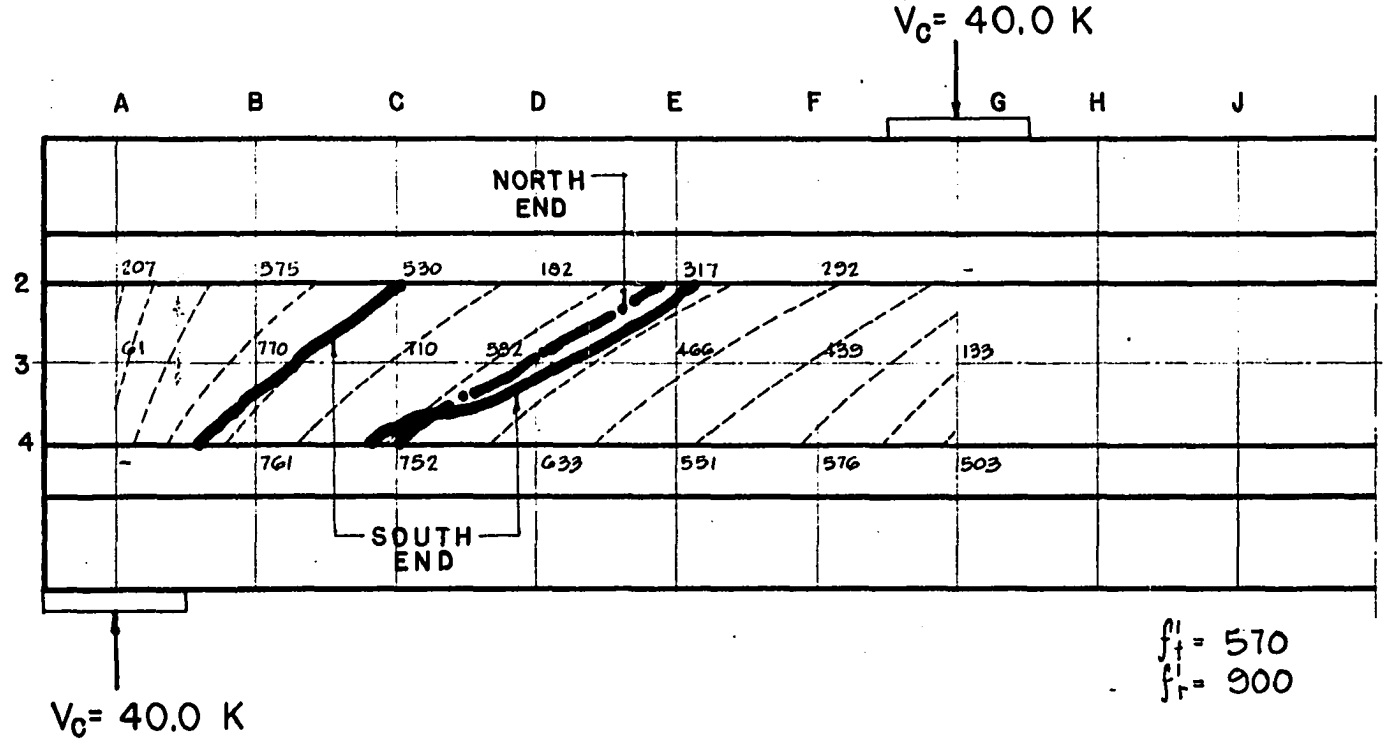

FIGURE 32. STRESS TRAJECTORIES, CRACK PATTERN, AND PRINCIPAL TENSILE STRESSES. BEAM 15

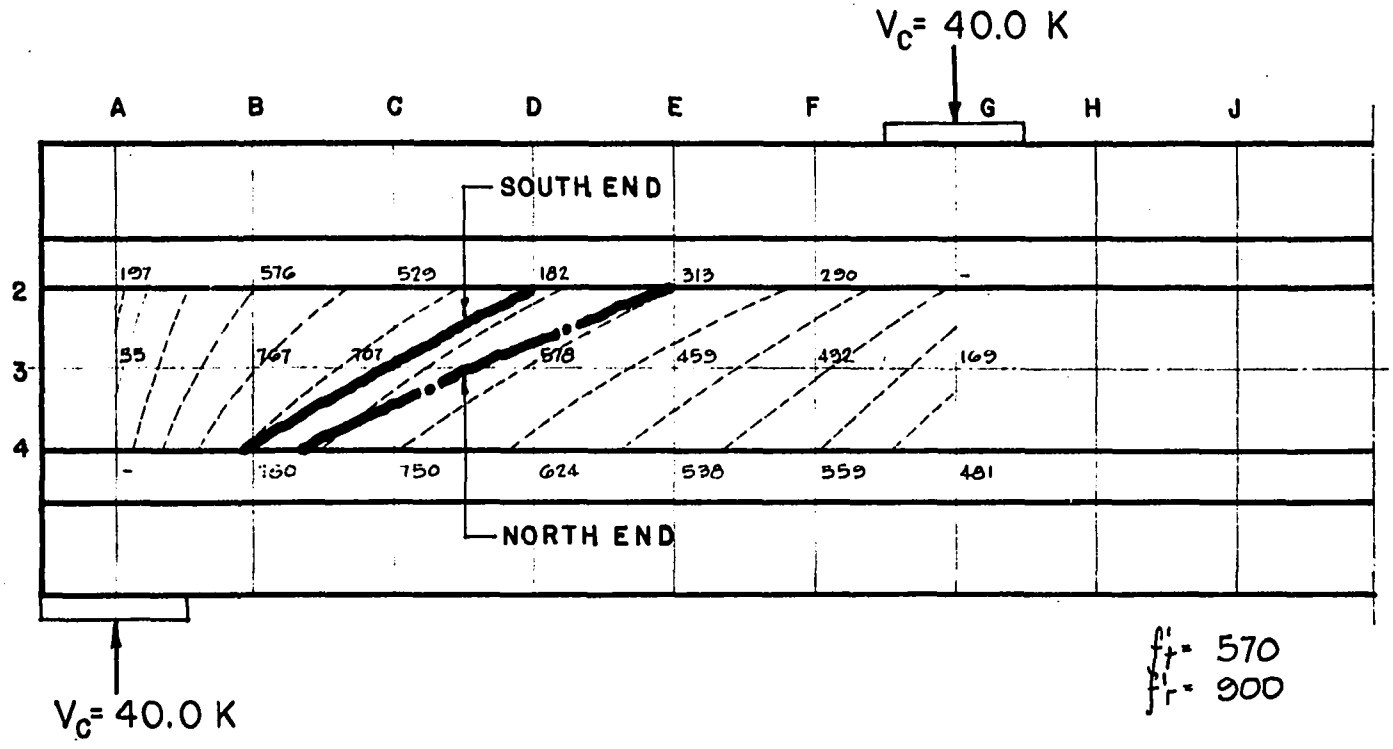

FIGURE 33. STRESS TRAJECTORIES, CRACK PATTERN, AND PRINCIPAL TENSILE STRESSES. BEAM 16

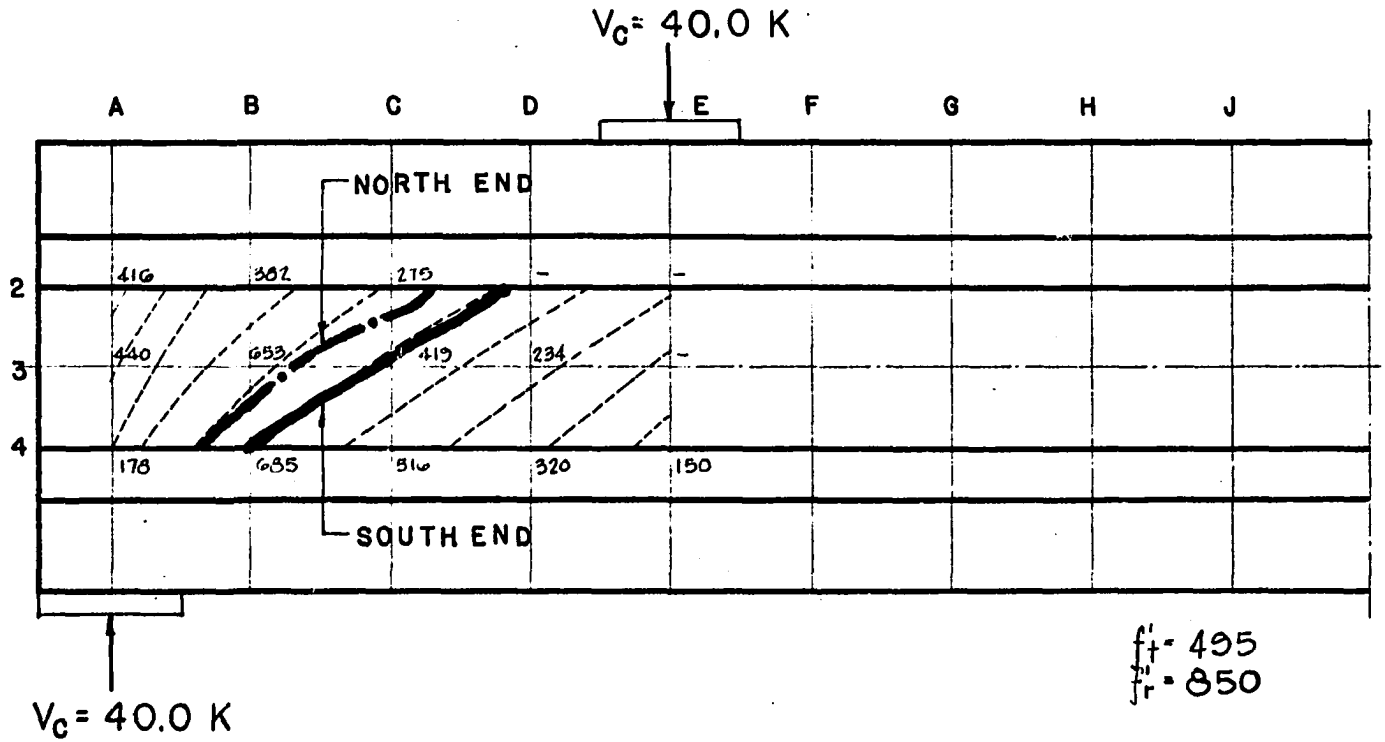

FIGURE 34. STRESS TRAJECTORIES, CRACK PATTERN, AND PRINCIPAL TENSILE STRESSES. BEAM 19

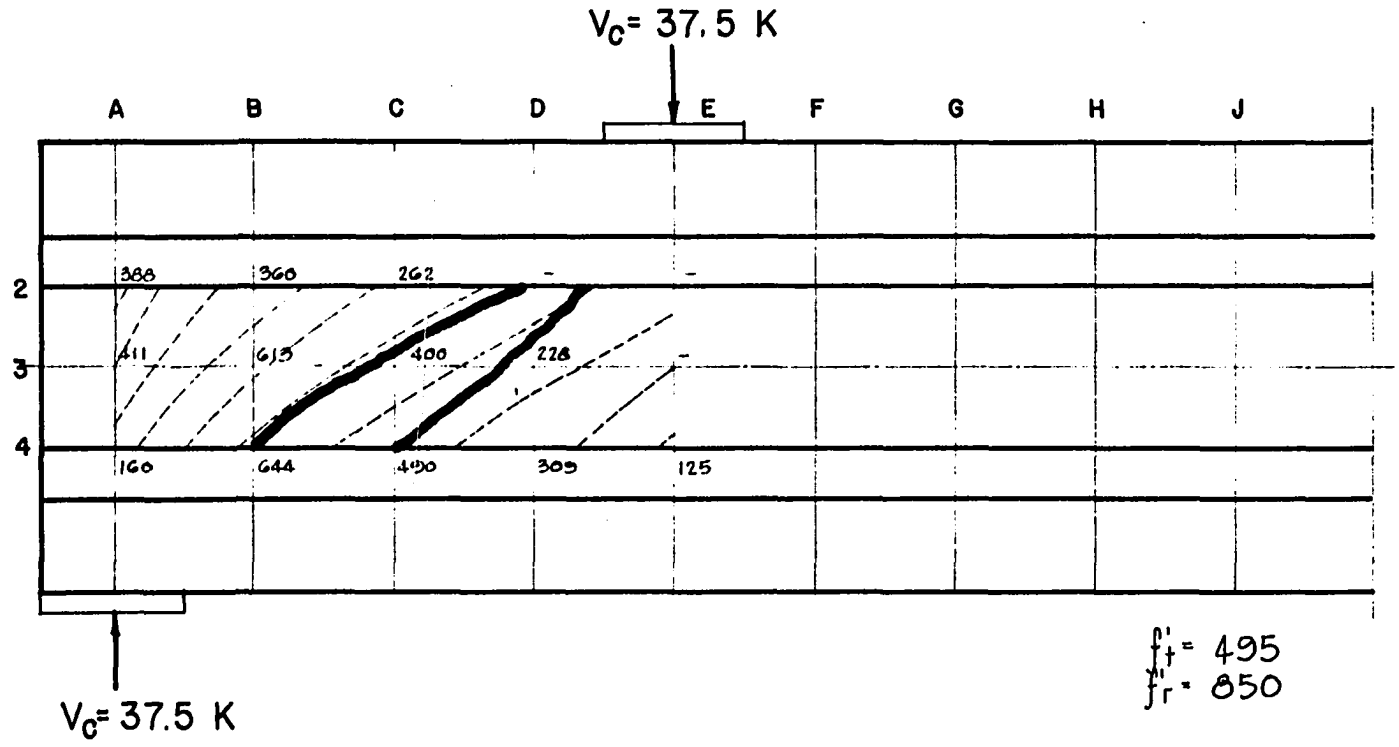

FIGURE 35. STRESS TRAJECTORIES, CRACK PATTERN, AND PRINCIPAL TENSILE STRESSES. BEAM 20

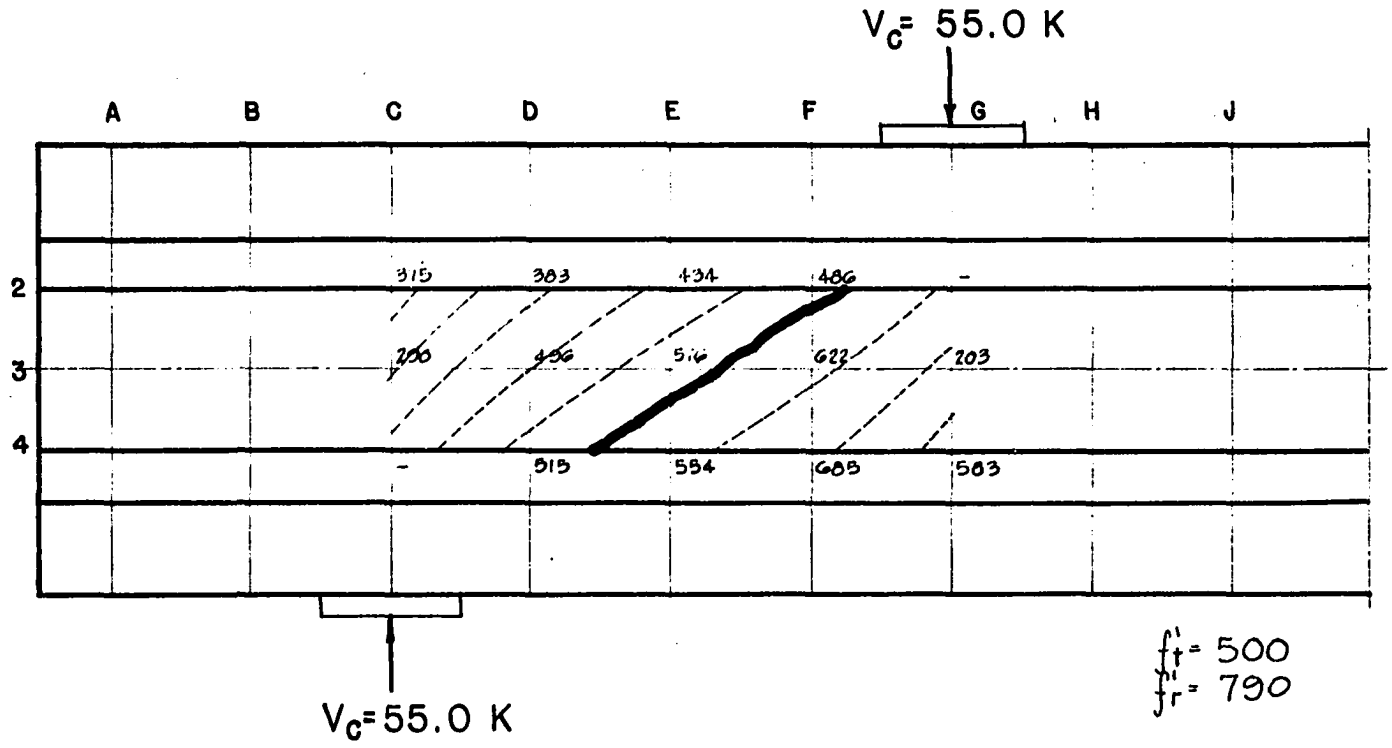

FIGURE 36. STRESS TRAJECTORIES, CRACK PATTERN, AND PRINCIPAL TENSILE STRESSES. BEAM 21

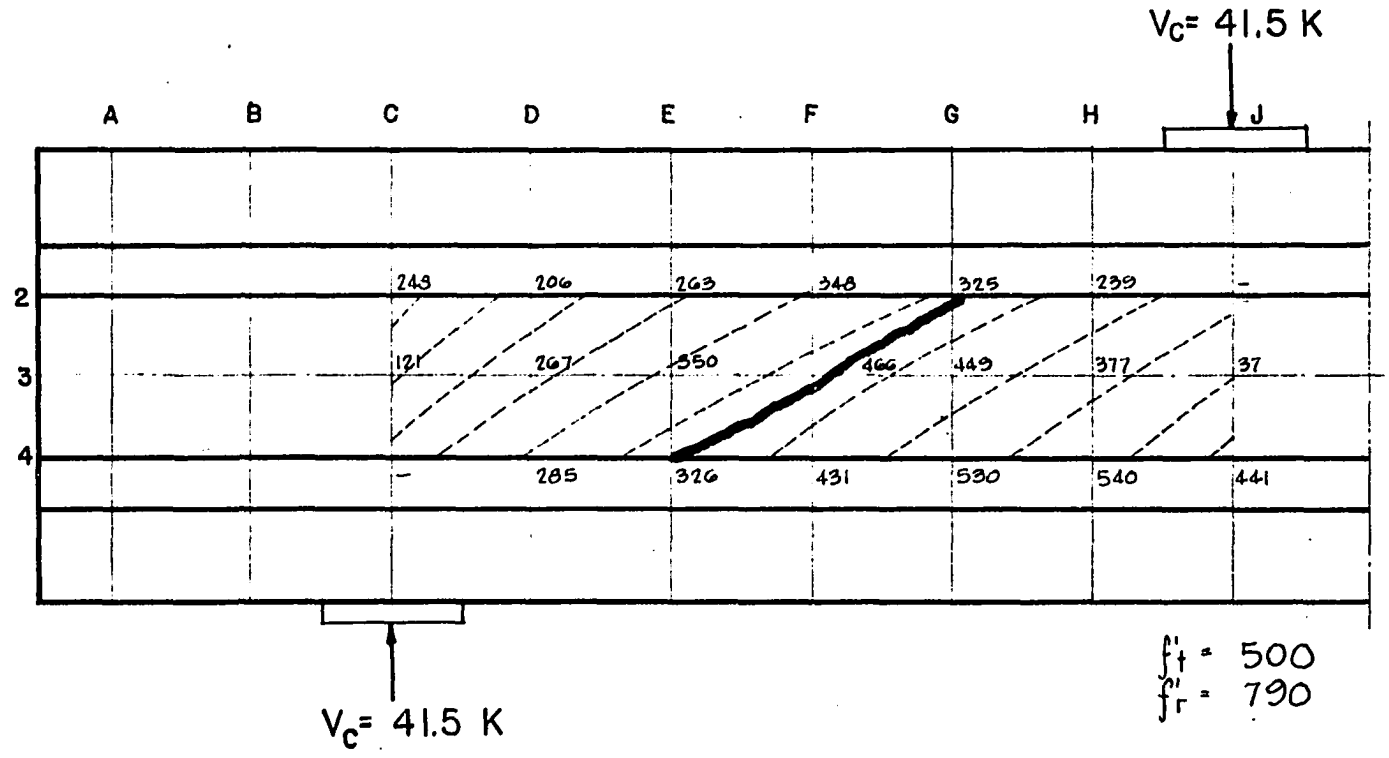

FIGURE 37. STRESS TRAJECTORIES, CRACK PATTERN, AND PRINCIPAL TENSILE STRESSES. BEAM 22

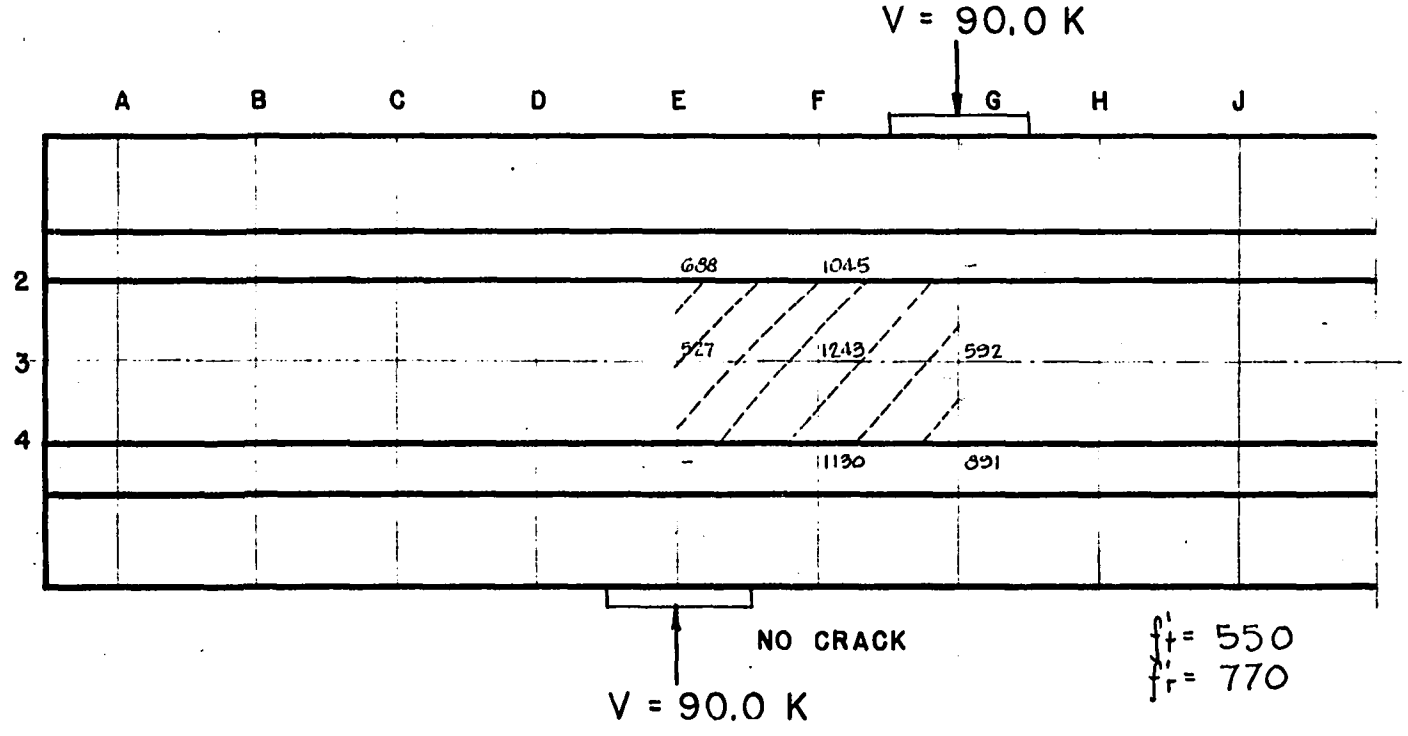

FIGURE 38. STRESS TRAJECTORIES, CRACK PATTERN, AND PRINCIPAL TENSILE STRESSES. BEAM 23

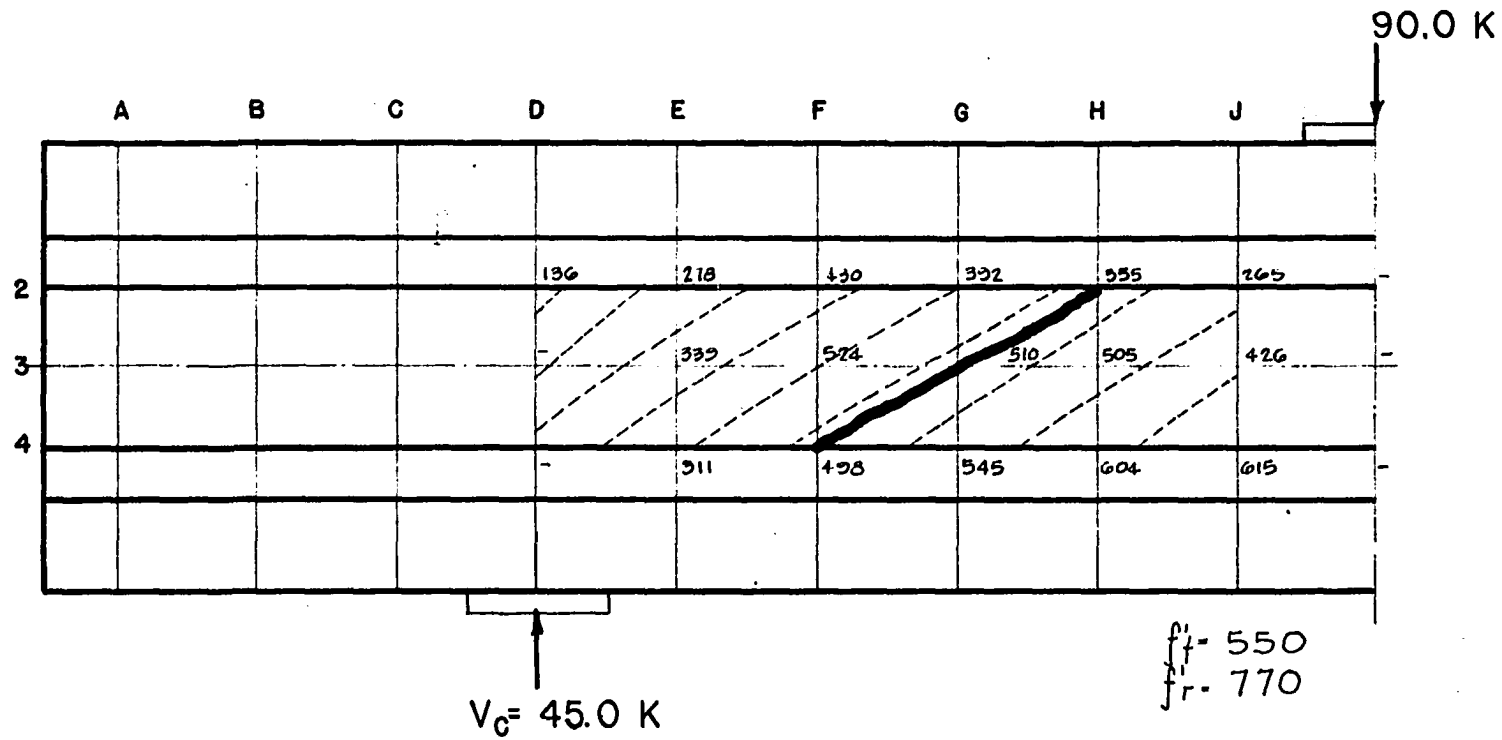

FIGURE 39. STRESS TRAJECTORIES, CRACK PATTERN, AND PRINCIPAL TENSILE STRESSES. BEAM 24

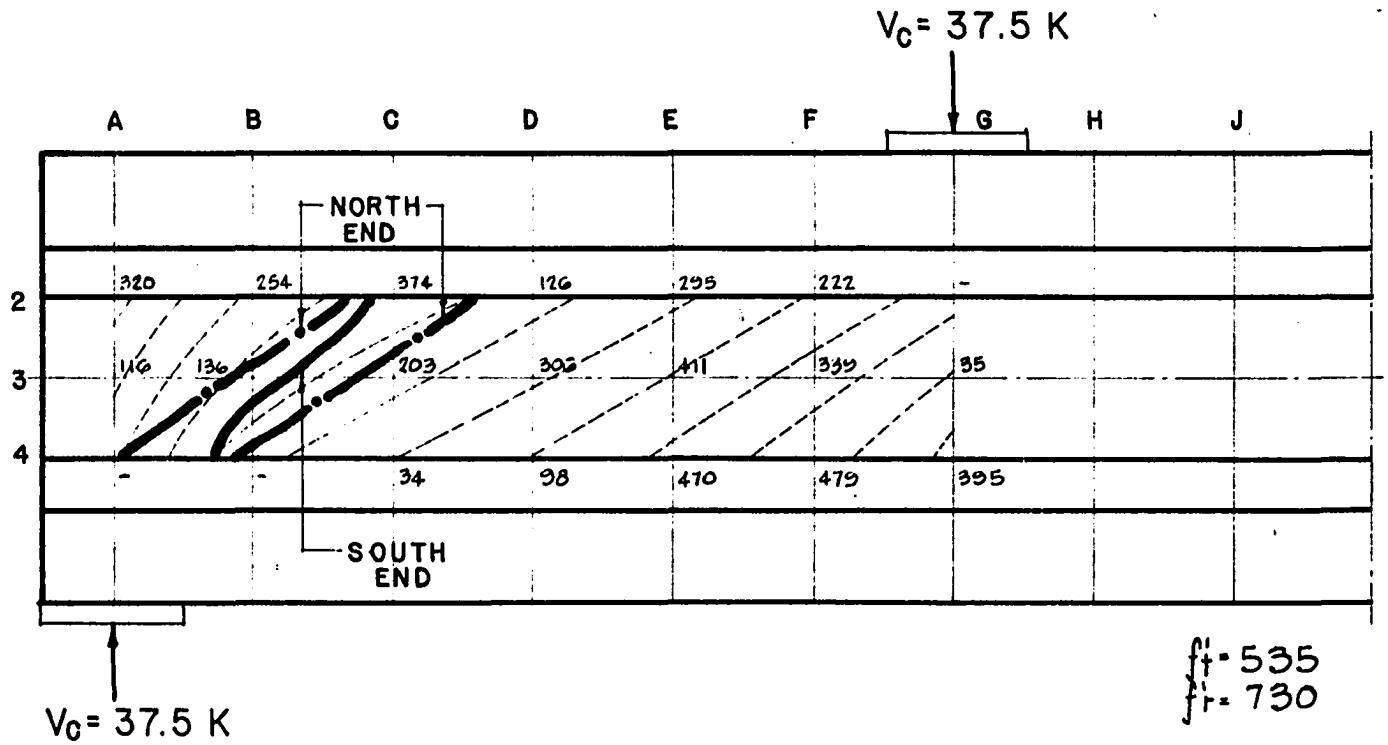

FIGURE 40. STRESS TRAJECTORIES, CRACK PATTERN, AND PRINCIPAL TENSILE STRESSES. BEAM 25

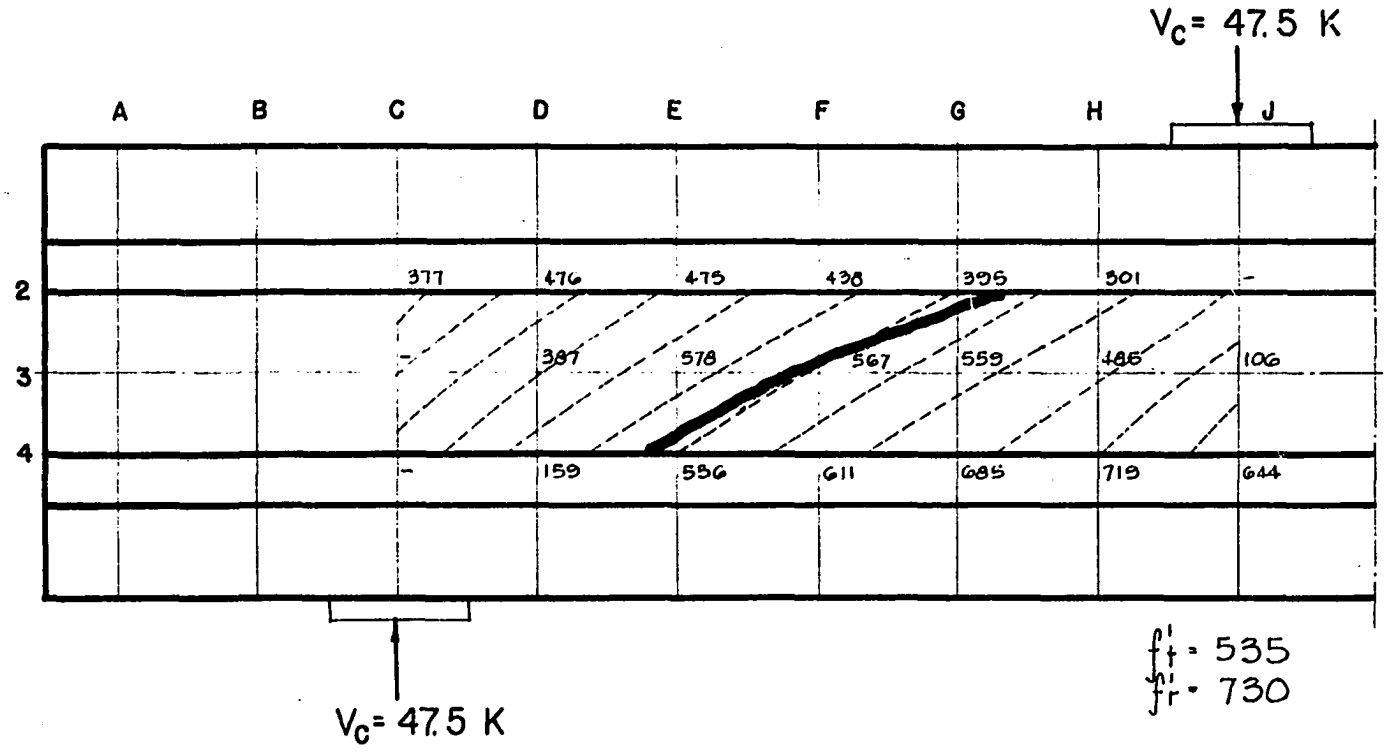

FIGURE 41. STRESS TRAJECTORIES, CRACK PATTERN, AND PRINCIPAL TENSILE STRESSES. BEAM 26

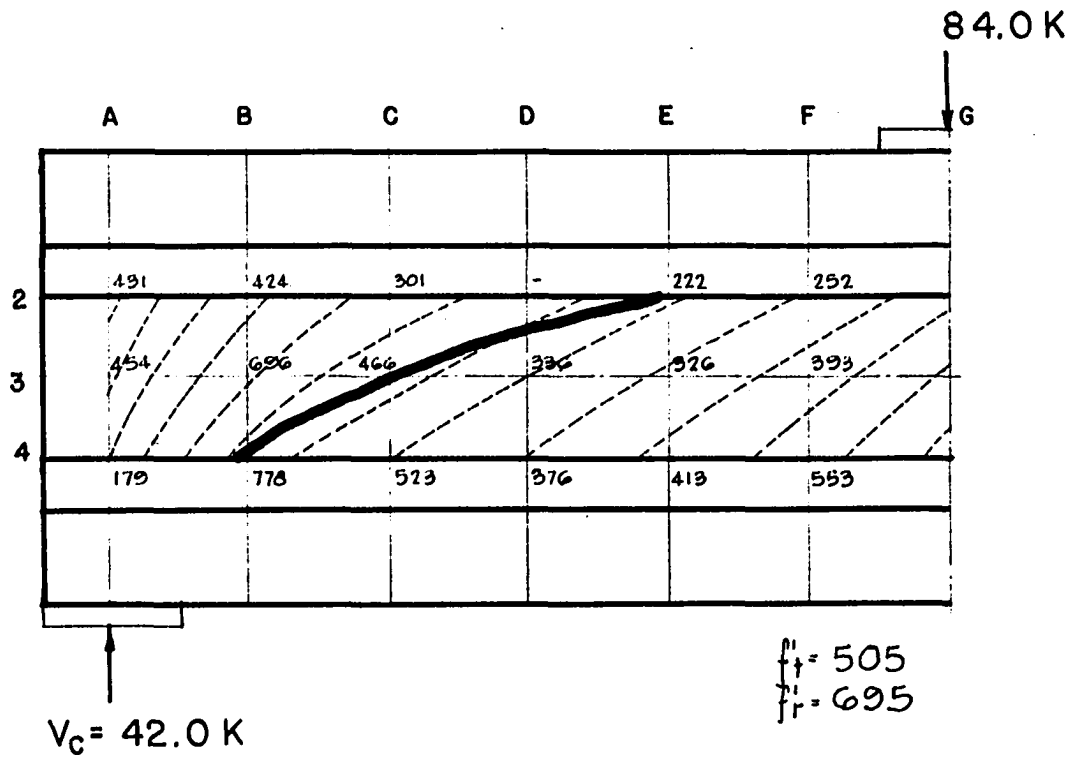

FIGURE 42. STRESS TRAJECTORIES, CRACK PATTERN, AND PRINCIPAL TENSILE STRESSES. BEAM 27

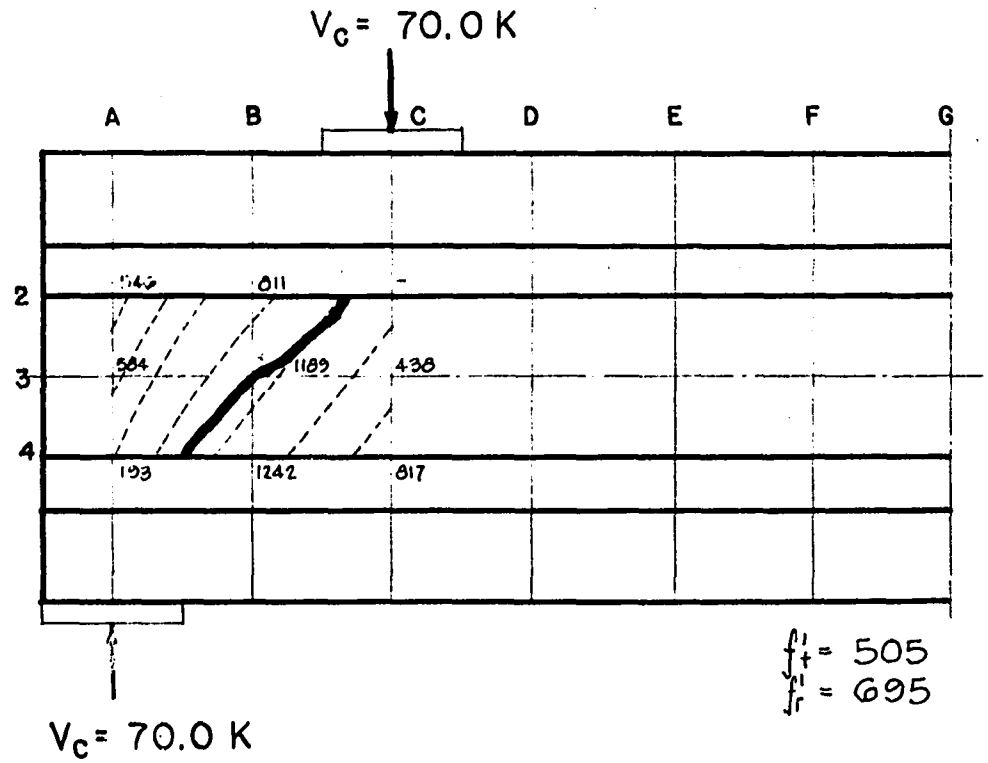

FIGURE 43. STRESS TRAJECTORIES, CRACK PATTERN, AND PRINCIPAL TENSILE STRESSES. BEAM 28

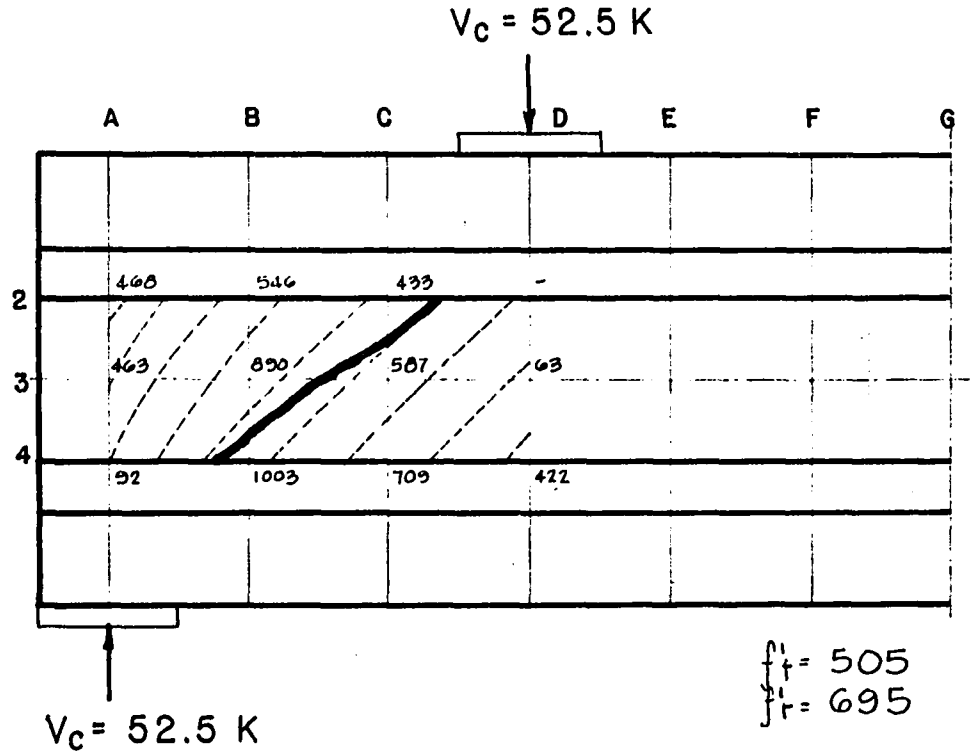

FIGURE 44. STRESS TRAJECTORIES, CRACK PATTERN, AND PRINCIPAL TENSILE STRESSES. BEAM 29

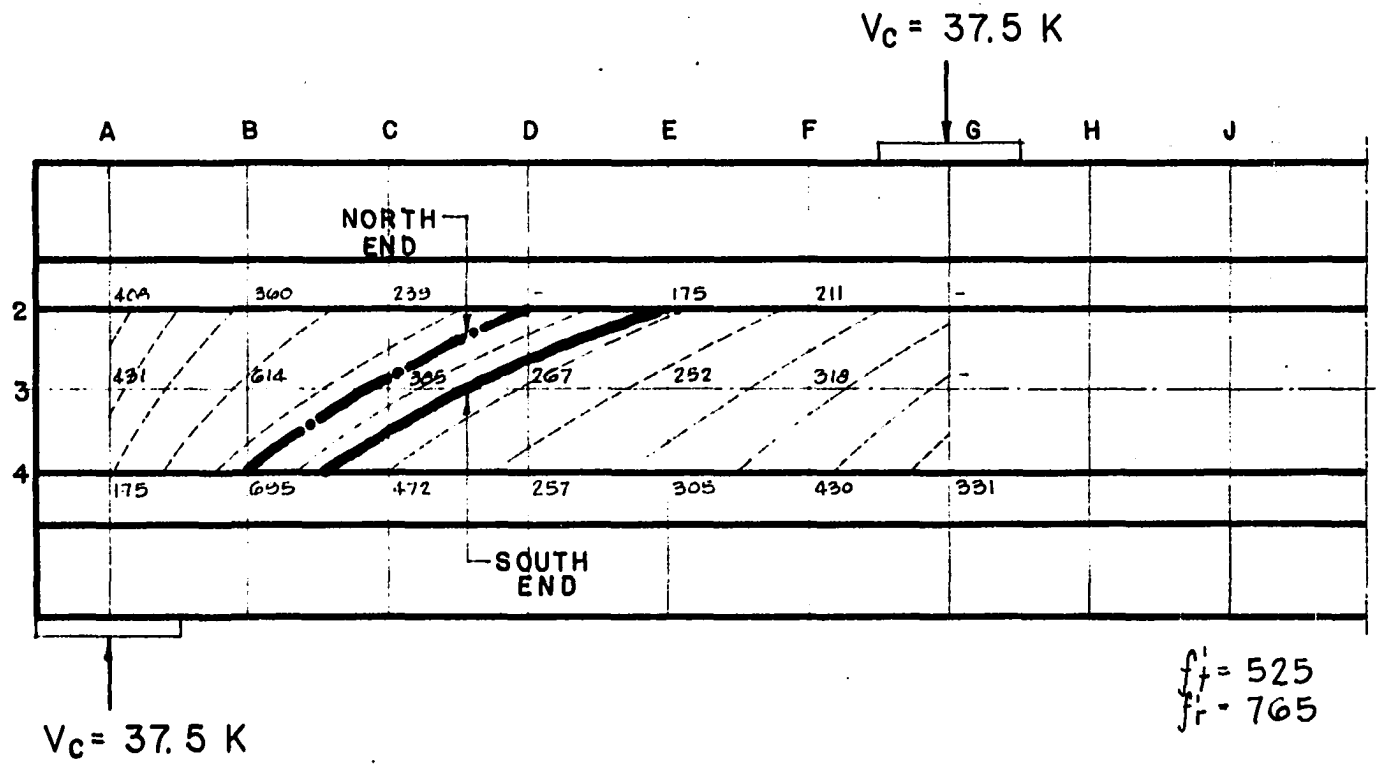

FIGURE 45. STRESS TRAJECTORIES, CRACK PATTERN, AND PRINCIPAL TENSILE STRESSES. BEAM 30

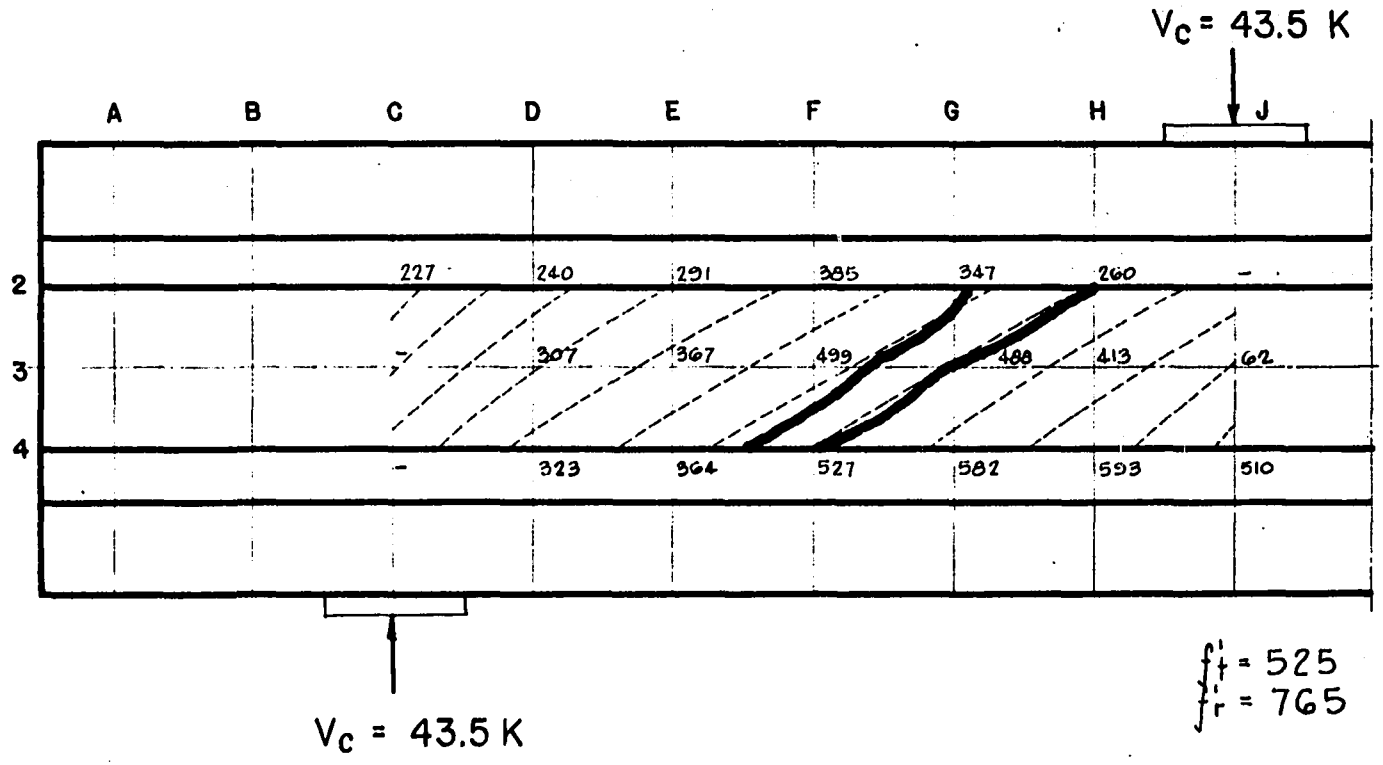

FIGURE 46. STRESS TRAJECTORIES, CRACK PATTERN, AND PRINCIPAL TENSILE STRESSES. BEAM 31

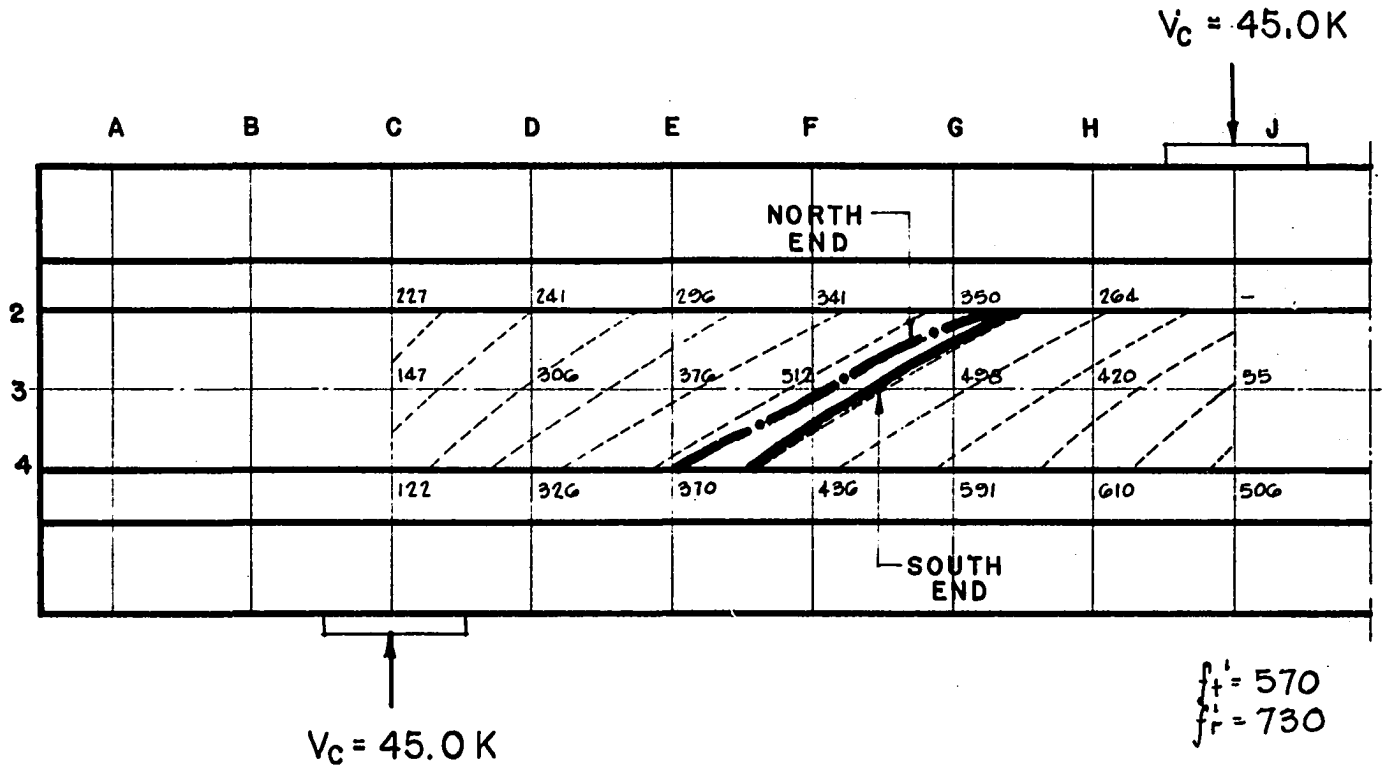

FIGURE 47. STRESS TRAJECTORIES, CRACK PATTERN, AND PRINCIPAL TENSILE STRESSES. BEAM 32

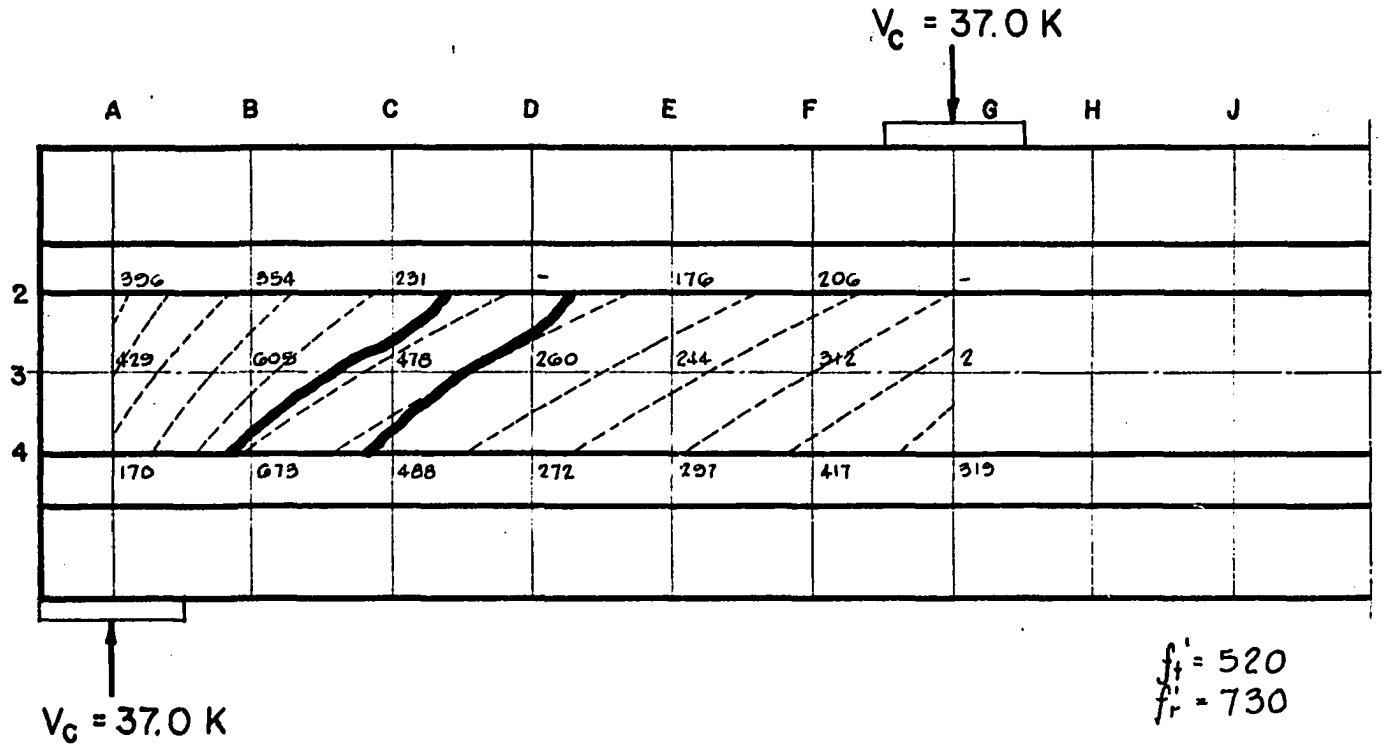

FIGURE 48. STRESS TRAJECTORIES, CRACK PATTERN, AND PRINCIPAL TENSILE STRESSES. BEAM 33

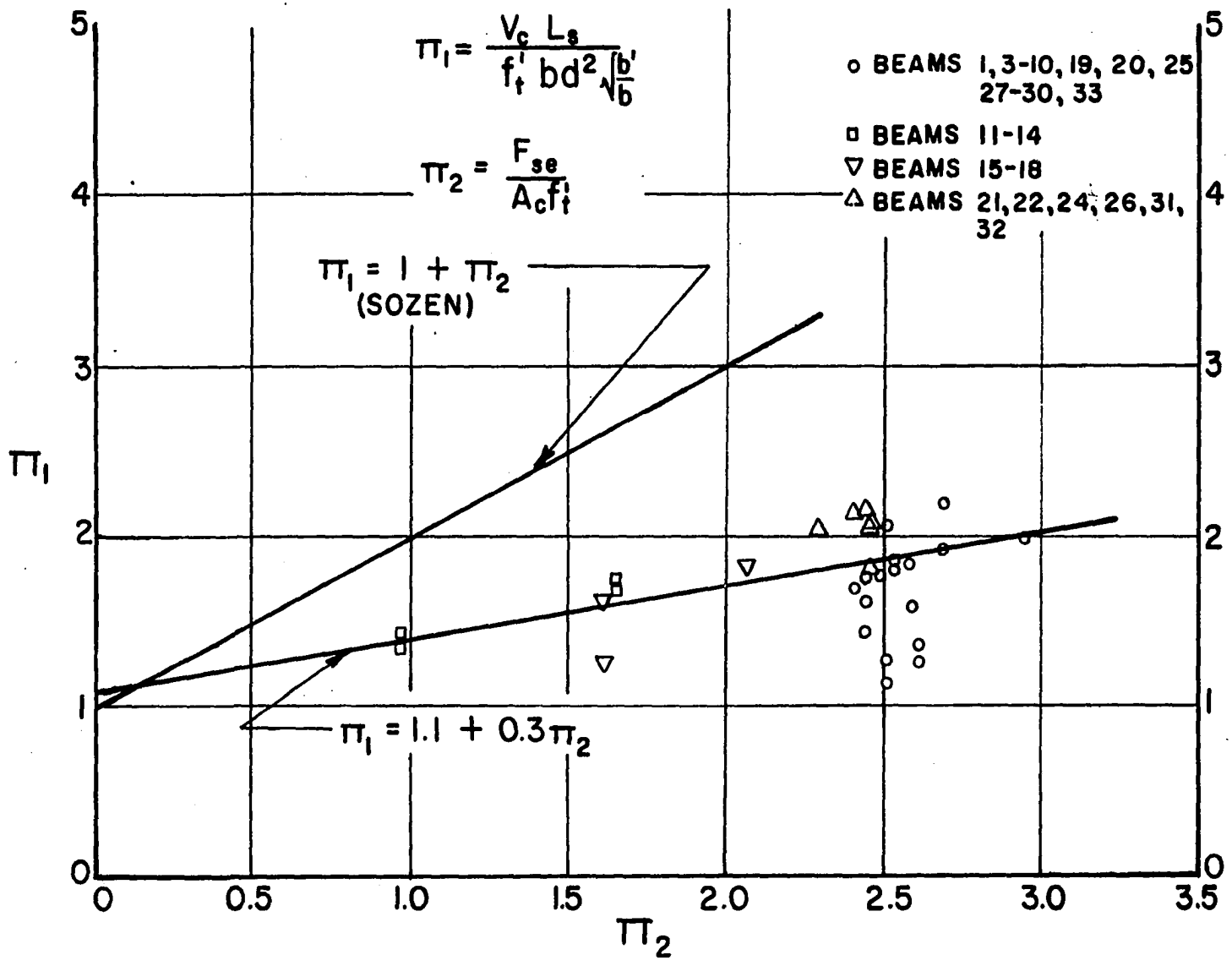

FIGURE 49. RELATIONSHIP BETWEEN π_1 AND π_2

Table 5. Test results from compression cylinders

Beams	f'_c	Avg. f'_c	Age days	Beams	f'_c	Avg. f'_c	Age days
1-2	5480			11-12	5860		
	5450				5950		
	5520	5480	7		6020		
	7150				6290	6030	7
	6460				6950		
	6560				6280		
	7510				7100		
	6850	6910	130		6710	6760	169
3-4	6145			13-14	5200		
	5680				5950		
	5210	5680	7		5320		
	7500				5400	5480	6
	7230				7550		
	6610				7420		
	6380				7650		
	6760	6900	130		7620	7560	179
5-6	5125			15-16	4960		
	5320				5360		
	4900	5120	7		4900		
	6320				4780	5000	7
	6670				7940		
	6940				7900		
	6915	6720	215		7040		
					7940	7700	219
7-8	5180						
	4875			17-18	5710		
	4900	4980	7		5440		
	7640				5730		
	7690				5410	5580	7
	7580				7880		
	7090				7800		
	7870				8010		
	8120	7670	240		8100	7960	211
9-10	5850			19-20	5590		
	5600				5780		
	5660	5700	8		6090	5820	7
	7940				6550		
	7400				6550		
	7420				7100		
	6790				6400	6660	256
	7390	7380	231				

Table 5. (Continued)

Beams	f'_c	Avg. f'_c	Age days	Beams	f'_c	Avg. f'_c	Age days
21-22	5920			27-28-29	6800		
	5830				6250		
	7060				6160		
	5350	6050	7		6010	6300	7
	7400				8900		
	8000				9250		
	7900				9120		
	7800	7780	242		9350	9150	128
23-24	5340			30-31	3030		
	5780				2830		
	5690				3090	2980	2
	5670	5620	7		7480		
	8200				7680		
	8500				6400		
	8100				7620	7300	116
	8200	8250	109				
				32-33	3760		
25-26	5150				3920		
	5240				4250	3900	3
	5300				6600		
	5210	5230	6		6710		
	7980				7200		
	7460				6480	6750	109
	7900						
	7200	7650	136				

Table 6. Test results from flexure specimens

Beams	f'_r	Avg. f'_r	f_{PL}	Avg. f_{PL}	Age days	Beams	f'_r	Avg. f'_r	f_{PL}	Avg. f_{PL}	Age days
1-2	700		420			17-18	900		335		
	695		350				905		350		
	670	690	350	370	130		880	895	320	335	211
3-4	750		335			19-20	860		335		
	775		350				855		315		
	710	745	335	340	130		835	850	320	325	256
5-6	730		370			21-22	835		265		
	695		330				730		265		
	730	720	400	370	215		805	790	310	280	242
7-8	860		400			23-24	710		310		
	805		300				765		280		
	815	825	300	330	240		830	770	280	290	109
9-10	880		300			25-26	730		280		
	870		300				765		265		
	785	845	300	300	231		695	730	310	285	136
11-12	800		250			27-28-29	620		280		
	900		350				695		265		
	800	835	350	315	169		765	695	280	275	128
13-14	835		270			30-31	765		325		
	695		350				765		325		
	785	770	300	310	179		770	765	315	320	116
15-16	915		280			32-33	760		300		
	890		310				720		265		
	895	900	310	300	219		715	730	290	285	109

Table 7. Test results from tension specimens

Beams	f'_t	Avg. f'_t	Age days	Beams	f'_t	Avg. f'_t	Age days
1-2	500			17-18	595		
	440				560		
	450				570		
	470	465	130		625	590	211
3-4	470			19-20	495		
	505				525		
	480				470		
	490	490	130		485	495	256
5-6	520			21-22	410		
	475				525		
	490				550		
	550	510	215		535	500	242
7-8	485			23-24	530		
	540				545		
	560				580		
	500	520	240		545	550	109
9-10	555			25-26	545		
	545				540		
	500				500		
	580	545	231		560	535	136
11-12	560			27-28-29	500		
	545				525		
	530				505		
	540	545	169		500	505	128
13-14	580			30-31	570		
	565				515		
	520				500		
	570	560	179		510	525	116
15-16	530			32-33	530		
	560				490		
	610				505		
	580	570	219		550	520	109

Discussion

Beam failures prior to load tests

The need for stirrups in the anchorage zone of pre-tensioned beams was emphasized by the performance of test beam 2. In this beam, in which no stirrups were used, the lifting hooks were omitted, leaving beam 2 with no web reinforcement of any kind. After release of the prestressing force, the beam was removed from the stress bed, and within minutes, a longitudinal crack at about mid-depth had begun to form at one end. Over a period of about one minute, the crack extended for nearly two-thirds of the length of the beam. A view of beam 2 is shown in Figure 50. The formation of the crack emphasizes the importance of stirrups at the time of release. The other test beams were inspected for similar cracks which might have been present but limited in size by web reinforcement. Such cracks were noticed only in beams 4, 6, 8, and 10 in which the lifting hooks constituted the only web reinforcement. The cracks were tiny and were visible only upon close inspection. The length of these cracks never exceeded two inches. Later, in the load tests, it was noticed that these cracks closed upon application of the load, due to the compressive effect of the end reaction. Hence, the presence of the longitudinal cracks did not affect the load carrying capacity. But, the fact remains that the absence of web reinforcement was responsible for the failure of beam 2 before it could be loaded.

In beams 17 and 18, the theoretical initial prestress stress at the top of the beam was -685 psi. The values of f'_t and f'_r were 590 and 895 psi respectively. When the prestress force was released, cracks formed

Figure 50. Beam 2 after release of prestress force

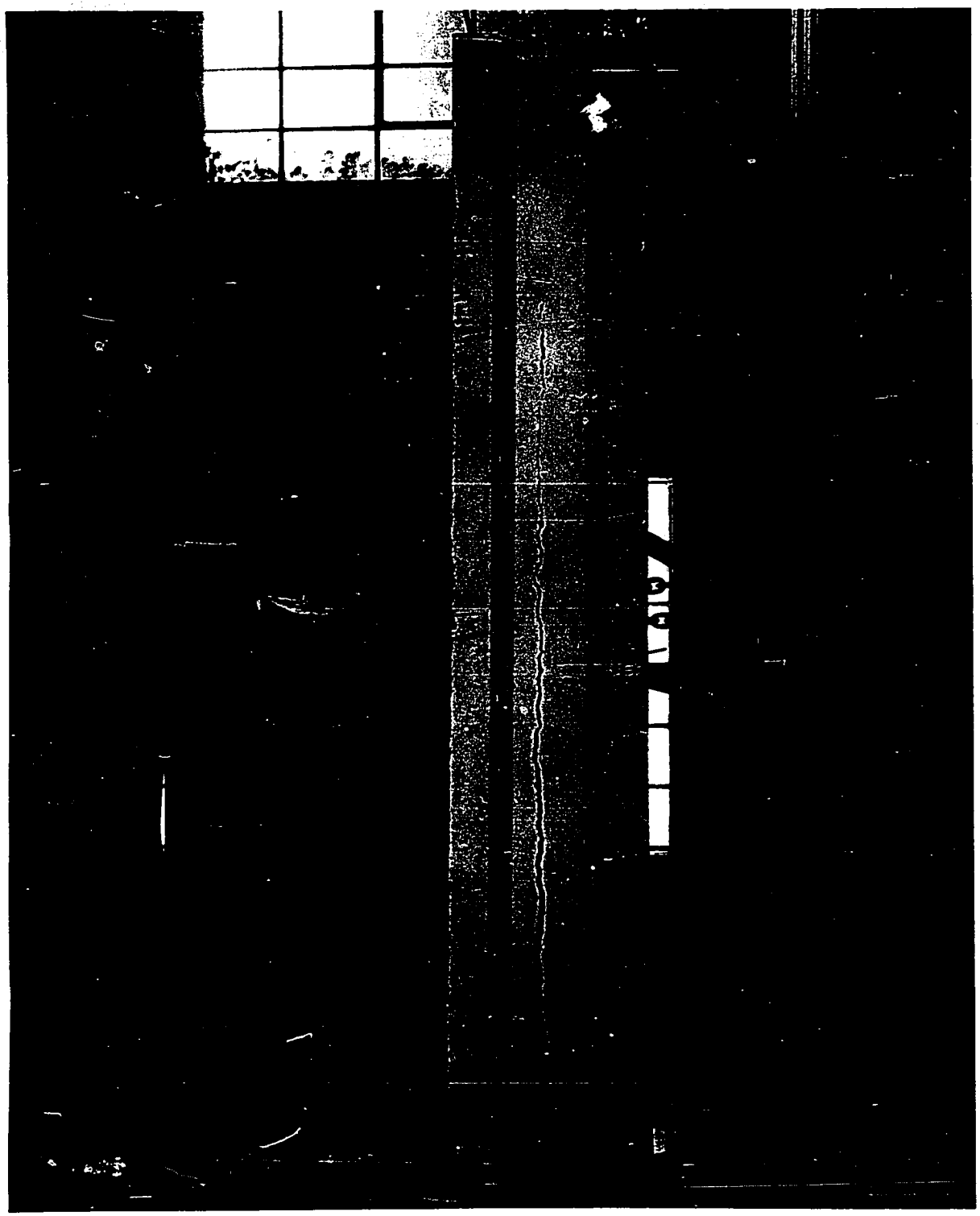

at the top of both beams. The cracks appeared at about 24-inch intervals along the beams and extended downward into the web. Therefore, theoretical analyses could not be prepared for these two beams. However, the beams were loaded to failure in the same manner as were the other test beams. With reference to Figure 49, the points representing the two beams are near the experimental curve shown.

Load tests

With one exception, the value of V_c was not difficult to obtain. In the load test of beam 23, for which L_s = 12 inches and L_o = 27 inches, the load was applied until the magnitude of the shearing force reached 90 kips. At that point, an inclined tension crack had not formed but the load beam had begun to deflect excessively and the test was stopped. The theoretical analysis was completed considering V_c to be 90 kips. In the other test beams, the formation of the inclined crack was definite.

Values of the ultimate shearing force, V_u, are given in Table 4. Observations of the ultimate failures were as follows:

1. For all of the beams with no web reinforcement, $V_u = V_c$. For the beams with web reinforcement, $V_u \geq V_c$.
2. For the beams with L_o = three inches, the ultimate load was controlled by the bond between the strands and the concrete. After the formation of the inclined tension crack, the applied load could be increased until the strands began to pull into the beam at the ends. When the strands began to slip, the beam would support no more load.

3. For the beams with L_o greater than three inches, the ultimate load, as compared to the cracking load, was increased measurably. For these beams, the ultimate load was sometimes controlled by the crushing of the concrete at the top of the beam at the end of the inclined tension crack, but no attempt was made to catalog the type of ultimate failure for each of the beams.

Results of the load tests and theoretical analyses

In all of the test beams, agreement between the direction of the inclined tension crack and the computed stress trajectories was excellent. In 22 of the 30 beams for which theoretical analyses were completed, the inclined tension crack passes through or very near to the grid point at which the maximum principal stress was computed. The 22 beams were numbers 1, 3-16, 19, 20, 27-30, and 33. For beams 21, 22, 24, 26, 31, and 32, the principal tensile stresses near the location of the inclined crack were less than the stresses computed at two or three of the other grid points. In each case, the locations of the grid points having the higher principal stress values were located along grid line 4 beneath the load point. Flexural cracks which initially formed at the bottom of the beam had progressed into the web at these points of maximum stress, and it should be emphasized that the formation of these cracks would not constitute a shear failure. In beam 25, which had strand pattern VI, an inclined crack formed where the computed principal tensile stresses were very low. Since the crack occurred in the anchorage zone, possibly the assumptions regarding build-up stresses were inaccurate. This seems

more probable than would the assumption that the construction procedure was poor or that the material was of poor quality. As mentioned before, no shear crack formed in beam 23.

As can be seen in Figures 19-48, the maximum principal tensile stresses along the location of the inclined tension crack fall between the values of f_t' and f_r'. Four of the beams, numbers 23, 25, 28, and 29, did not conform to this observation. Beam 25 has been discussed. Beams 23, 28, and 29 all had values of $L_s \leq 18$ inches, and the maximum principal stresses were much higher than the f_r' values. The complexity of the problem of considering the local effects of concentrated loads is increased when the effects overlap, as was the case for these beams.

In Figure 49, a straight line was used to represent the data from beams in this study. Another straight line, developed by Sozen (20), is also shown. It is emphasized that the data shown represents a number of beams in which the failure occurred in the end portions. In contrast, the beams represented by Sozen's line were constructed with end blocks and prestressed stirrups which forced the failures to occur in areas away from the ends of the beam. A comparison of the lines indicates that lower values of V_c are responsible for shear failures when the failures occur in the end portions. It appears then, that in pre-tensioned beams having no end blocks and no prestressed stirrups, the shear strength is critical in the end portions.

Theories of failure

As stated previously, Grassam (7) suggests that concrete might be expected to fail when the computed principal tensile stress reaches a

value of $(1.2)(f_t')$. However, the results of this study do not justify the use of the factor 1.2 because, in a number of the beams, the inclined tension crack formed when the maximum principal tensile stress was nearer the value of f_t' than $(1.2)(f_t')$.

The use of the internal-friction theories is very cumbersome due to the work involved in development of the limiting curve and to the problem of application of the theory to members in which a number of locations might be critically stressed. It has already been stated that the maximum-shearing-stress and the maximum-normal-strain theory do not accurately represent the failures of concrete.

Variables introduced in the test beams

In considering the variables introduced in the study, it was found that:

1. The amount of web reinforcement had no apparent effect upon formation of the inclined tension cracks, but the ultimate load was increased measurably over the cracking load for beams having stirrups. The stirrups greatly reduce or eliminate the possibility of a horizontal failure at time of release. During the load tests of beams 1 and 3-10, the load was reduced slightly after formation of the inclined tension crack. For beams having no stirrups, the cracks remained open when the load was reduced. However, the cracks closed partially when the load was reduced on beams having stirrups. The degree of closure varied with the amount of web reinforcement.

As the amount increased, closure of the cracks was more complete.

2. The variation of prestress stress distribution did not affect the evaluation of the shear strength by the combined stress method, but there was a change in the magnitudes of V_c.
3. The length of shear span had no effect on the use of a combined stress theory except when $L_s \leqq D$. And, since the possibility of a shear failure would be increased if $L_s > D$, the loading of beams for which $L_s \leqq D$ would not constitute a critical condition for a shear failure.
4. As the length of overhang was increased, the magnitudes of V_c and V_u were greater for a given L_s.
5. The strength of the concrete at time of release had no measurable effect on either the use of the combined stress theory or the values of V_c.

CONCLUSIONS AND RECOMMENDATIONS

The following conclusions and recommendations are presented.

1. The combined stress method can be used satisfactorily to evaluate the shear strength of pre-tensioned I-beams having no end blocks. The method gave consistent results for all beams except those in which $L_s < D$. Therefore, it is recommended that the method be used when $L_s > D$. This is not a serious limitation, however, since smaller values of V_c were obtained as L_s was increased, indicating that the critical condition for a shear failure occurred when $L_s > D$.
2. The results indicate that the maximum-normal-tensile-stress theory is a satisfactory theory of failure for concrete, in evaluating shear strength of prestressed beams. It is recommended that the limiting tensile stress be taken as f'_t.
3. The possibility of a shear-type failure is greater in the end portions than in the center portion of pre-tensioned I-beams having no end blocks.

The importance of the previous research concerning build-up of the prestress stresses must be emphasized. It is obvious that knowledge of the development of these stresses is a necessity in using the combined stress method. Much more research is needed in this area before the shear strength of all types of prestressed beams can be accurately evaluated.

Load tests of other types of prestressed beams should be made to

further justify the use of the combined stress method.

Another important factor which merits consideration in future research is the effect of fatigue, since all research to date concerning shear strength has been based on static tests.

It is also recommended that research be devoted to justification of the assumptions regarding local effects of concentrated loads, even though the assumptions used in this study gave consistent results.

REFERENCES

1. Bresler, B. and Pister, K. S. Failure of concrete under combined stresses. Transactions of American Society of Civil Engineers. 122: 1049-1059. 1957.

2. Clark, Arthur P. Diagonal tension in reinforced concrete beams. Journal of the American Concrete Institute. 23: 145-156. 1951.

3. Cowan, H. J. and Armstrong, S. Reinforced concrete in combined bending and torsion. Fourth Congress of International Association for Bridge and Structural Engineering, Cambridge and London, 1952. Preliminary publication: 861-870. 1952.

4. Evans, R. H. and Wilson, G. Influence of prestressing reinforced concrete beams on their resistance to shear. Journal of the Institution of Structural Engineers. 20: 109-122. 1942.

5. Ferguson, P. M. Some implications of recent diagonal tension tests. Journal of the American Concrete Institute. 28: 157-172. 1956.

6. _____ and Thompson, J. N. Diagonal tension in T-beams without stirrups. Journal of the American Concrete Institute. 24: 665-675. 1953.

7. Grassam, N. S. J. and Fisher, D. Experiments on concrete under combined bending and torsion. Proceedings of the Institution of Civil Engineers. Part I. 5, No. 2: 159-165. 1956.

8. Guyon, Y. Prestressed concrete. John Wiley and Sons, Inc., N.Y. 1953.

9. Irelan, Wayne C. Anchorage length for strands in prestressed concrete. Unpublished M.S. Thesis. Library, Iowa State University of Science and Technology, Ames, Iowa. 1959.

10. Johnson, James W. Relationship between strength and elasticity of concrete in tension and compression. Iowa State College. Engineering Experiment Station Bulletin 90. 1928.

11. Kesler, C. E. and Seiss, C. P. Static and fatigue strength--significance of tests and properties of concrete and concrete aggregates. American Society for Testing Materials Special Technical Publication 169: 81-93. 1955.

12. Laupa, A., Seiss, C. P., and Newmark, N. M. Strength in shear of reinforced concrete beams. University of Illinois Engineering Experiment Station Bulletin 428. 1955.

13. Magnel, Gustave. Prestressed concrete. 3rd ed. McGraw-Hill Book Co., Inc., N.Y. 1954.

14. Monson, E. M. Stress distribution in the anchorage zone of a prestressed concrete I-beam. Unpublished M.S. Thesis. Library, Iowa State University of Science and Technology, Ames, Iowa. 1957.

15. Moody, K. G. and Viest, I. M. Shear strength of reinforced concrete beams. Journal of the American Concrete Institute. 26: 698-730. 1955.

16. Moretto, O. An investigation of the strength of welded stirrups in reinforced concrete beams. Journal of the American Concrete Institute. 17: 141-164. 1945.

17. Richart, F. E., Brandtzaeg, A., and Brown, R. L. A study of the failure of concrete under combined compressive stresses. University of Illinois Engineering Experiment Bulletin 185. 1928.

18. Seiss, C. P. Review of research on ultimate strength of reinforced concrete members. Journal of the American Concrete Institute. 23: 833-859. 1952.

19. Smith, G. M. Failure of concrete under combined tensile and compressive stresses. Journal of the American Concrete Institute. 25: 137-140. 1953.

20. Sozen, M. A., Zwoyer, E. M., and Seiss, C. P. Strength in shear of beams without web reinforcement. University of Illinois Engineering Experiment Station Bulletin 452. 1959.

21. Timoshenko, S. and Goodier, J. N. Theory of elasticity. 2nd ed. McGraw-Hill Book Co., Inc., N.Y. 1951.

22. U. S. Department of the Interior, Bureau of Reclamation. Shearing strength of concrete under high triaxial stress--computation of Mohr's envelope as a curve. Structural Research Laboratory Report SP-23. 1949.

ACKNOWLEDGMENTS

The writer wishes to express sincere appreciation to Dr. C. L. Hulsbos, Professor of Civil Engineering, for his guidance and help in carrying out this project, and for his encouragement throughout the writer's entire graduate program.

During the course of the research work, a number of undergraduate students, in addition to several staff members, helped with the construction and testing of the test beams and concrete specimens. The efforts of these people were greatly appreciated.

Acknowledgment is due the Iowa Highway Research Board for providing the funds required to perform the research work, and the members of the Engineering Experiment Station staff for administering the funds and providing many services from beginning to end of the project.